

Miscellaneous Publication 155

CONCENTRATIONS AND SOURCE MODELING OF SELECTED CRUSTAL
ELEMENTS AT A RURAL SITE NEAR BONDVILLE ILLINOIS

BY

WILLIAM OCCHIOGROSSO

B.S., Purdue University, 1991
B.S., S.U.N.Y. at Cortland, 1983

THESIS

Submitted in partial fulfillment of the requirements
for the degree of Master of Science in
Environmental Engineering in Civil Engineering
in the Graduate College of the
University of Illinois at Urbana-Champaign, 1994

Urbana, Illinois

Illinois State Water Survey
Atmospheric Sciences Division
A Division of the Illinois Department of Energy and Natural Resources

CONCENTRATIONS AND SOURCE MODELING OF SELECTED CRUSTAL
ELEMENTS AT A RURAL SITE NEAR BONDVILLE ILLINOIS

BY

WILLIAM OCCHIOGROSSO

B.S., Purdue University, 1991
B.S., S.U.N.Y. at Cortland, 1983

THESIS

Submitted in partial fulfillment of the requirements
for the degree of Master of Science in
Environmental Engineering in Civil Engineering
in the Graduate College of the
University of Illinois at Urbana-Champaign, 1994

Urbana, Illinois

ACKNOWLEDGMENTS

I would like to acknowledge the special collaboration I've enjoyed with my research advisor, Dr. Gary Stensland, Head of the Atmospheric Sciences Division at the Illinois State Water Survey in Champaign, Illinois. Dr. Stensland's gratuitous support, encouragement and expertise propelled me along the rigorous path of a Master's thesis to the edge of the rainbow you see before you, this report. His many contributions to my educational experience here at the University of Illinois has helped me to think and reason in new and wondrous ways.

Assistance with this project's efforts also came from several associates within the Illinois State Water Survey (ISWS). Sherman Bauer provided FORTRAN knowledge and support in the task of completing the adaptation of the AIR.FOR code to the PC environment. Dr. Allen Williams offered specific advise on several challenging problems. Linda Jo Hascall and Dave Cox of the Office of Publications created Figures 1.1 and 2.1 in this report. In addition, appreciation goes out to the many other ISWS associates who helped make my experience here rewarding.

Kudos are given to my academic advisor, Dr. Mark Rood, Associate Professor with the Department of Environmental Engineering at the University of Illinois, whose timely review of this report made possible my compliance with the Graduate College's deposit deadline. Dr. Rood's advise throughout this project was of great assistance. His guidance, along with the entire Air Research Group's input, both past (particular Mark Rhodes) and present members , influenced this project's undertakings and outcome.

Finally, I would like to acknowledge the support of my family and friends. To my Mom whose outlook in life is so positive and motivating. She has given me the most wonderful gift of all, love. To my sister, whose acceptance and encouragement are truly appreciated and to my niece and nephew who were not happy that Uncle Bill's academic pursuits took him far away from them, but nevertheless did not let that stop them from making their Uncle's visits, special times. To my friends back east, who needed to take out the atlas to understand where the Urbana-Champaign area is and then exclaim in surprise, "so that's where Indiana is", even though I no longer lived there. And to the friends I've made during my Master's study who shared in the enjoyment of this unique community.

TABLE OF CONTENTS

LIST OF TABLES.....vi

LIST OF FIGURES.....vii

CHAPTER

1 Introduction.....1

 1.1 Background.....1

 1.2 The Bondville Study.....4

 1.3 Site Characteristics.....5

 1.4 References.....7

2 Methodology.....9

 2.1 Introduction.....9

 2.2 Filter Sampling.....9

 2.21 Filter Sampling Efficiency.....11

 2.3 Filter Processing.....11

 2.4 Calibration to Determine Sampled Air Volumes.....17

 2.4.1 Calibration of the Intermediate Standard for Volume Determinations.....17

 2.4.2 Rotameter Calibration Procedure.....19

 2.4.3 Related Calibration Efforts.....25

 2.4.3.1 Time Shifts and Calibration Method.....25

 2.4.3.2 Clean versus Dirty Rotameter Calibrations.....27

 2.4.3.3 Calibration of Bondville Pump's Pressure Gauges.....29

 2.5 Calculating Ion's Ambient Air Concentrations.....30

 2.5.1 Program Description.....30

 2.5.2 Program Modifications.....36

 2.5.2.1 Determination of Ambient Air Pressure.....36

 2.5.2.2 Determination of Rotameter Air Temperature.....37

 2.5.2.3 Miscellaneous Program Modifications.....38

 2.5.3 Filter Data Screening.....39

 2.5.3.1 Sample Protocol Screening.....39

 2.5.3.2 Data Quality Screening.....40

 2.6 Source Attribution Model.....47

 2.6.1 Soluble Versus Total Elemental Source Signatures.....51

 2.6.2 Daily Aerosol Levels of Calcium and Potassium.....54

 2.6.3 Equations of the CMB Model.....54

 2.6.4 Output from the model.....55

 2.7 References.....56

3 Results and Discussion.....59

 3.1 Introduction.....59

 3.2 Modeling Results.....59

 3.3 Patterns in Monthly Ion's Ambient Concentrations.....69

 3.4 References.....80

4 Summary, Conclusions and Recommendations.....81

 4.1 Summary.....81

 4.2 Conclusions.....82

 4.3 Recommendations.....83

Appendix A.....85

LIST OF TABLES

1.1	Mean total elemental composition (in percent) of unpaved road samples listed in Table II of Barnard et al., 1986.	3
2.1	Results of rotameter calibration efforts.	23
2.2	Calibration comparison of 1980's effort versus this study's final effort (percent error calculated at 30 L/min. @ stp).	24
2.3	Comparison of calibration methods and reproducibility over time.	27
2.4	Comparison of unclean versus solvent clean rotameter calibrations.	28
2.5	Calibration of the Gelman pumps' vacuum gauges using a manometer.	29
2.6	Summary of parameters used to established ion estimated standard deviations in the AIR.FOR program.	43
2.7	Descriptive statistics for twice iterated outside hung field filter blank values (mg/L) for the June, 1983 to May, 1988 period.	43
2.8	Descriptive statistics used to determine the air volume's standard deviation multiplier.	44
2.9	Descriptive statistics for June, 1983 to May, 1988 filter samples whose error is less than or equal to 50% (ion concentration units are ug/m ³).	45
2.10	Descriptive statistics for June, 1983 to May, 1988 filter samples whose error is less than or equal to 250% (ion concentration units are ug/m ³).	46
2.11	Student t test results using the two data quality screening criteria.	46
2.12	An example of AERMOD quantitative source model's output.	52
3.1	Number of screened daily filters used to calculate the source apportionment means by month.	60
3.2	Percentage comparison of alkaline aerosol fluxes from Gillette et al., 1992's modeling effort and this study's Bondville CMB model results (in parentheses).	69
3.3	Descriptive statistics for Bondville ion's ambient concentrations extractable levels.	71
A.1	Central tendency and variability of blank values measured in the Bondville aerosol project.	85
A.1	(continued) Central tendency and variability of blank values measured in the Bondville aerosol project.	86
A.1	(continued) Central tendency and variability of blank values measured in the Bondville aerosol project.	87
A.1	(continued) Central tendency and variability of blank values measured in the Bondville aerosol project.	88
A.2	Calibration of the Gelman pump's vacuum gauges using a manometer.	89

LIST OF FIGURES

1.1 Map of Bondville, IL sampling site.....6
2.1 Bondville ambient aerosol filter sample collection and processing diagram.....12
2.1 (continued) Bondville ambient aerosol filter sample collection and.....13
processing diagram.
2.2 Calibration runs for pump 0110's rotameter.....22
2.3 Reproducibility of solvent cleaned 0013 rotameter's calibration overtime.....26
2.4 TEST.DAT example input file for the AIR.EXE program.....31
2.5 AERCON example output file for the AIR.EXE program.....34
2.6 AERION example output file for the AIR.EXE program.....35
2.7 Scatter diagram of magnesium versus calcium.....48
2.8 Scatter diagram of potassium versus calcium.....49
2.9 Scatter diagram of potassium versus magnesium.....50
3.1 Source apportionment of calcium on Bondville aerosol filters from.....61
unpaved road source.
3.2 Source apportionment of calcium on Bondville aerosol filters from soil source.....62
3.3 Source apportionment of potassium on Bondville aerosol filters from.....63
unpaved road source.
3.4 Source apportionment of potassium on Bondville aerosol filters from soil source.....64
3.5 Modeled dust concentrations by month from the unpaved road source.....66
3.6 Modeled dust concentrations by month from the soil source.....67
3.7 Mean ambient aerosol concentrations by month for calcium for the Bondville site.....72
June 1983 through June 1988.
3.8 Mean ion's ambient concentrations by month for magnesium for the Bondville site.....73
June 1983 through June 1988.
3.9 Mean ion's ambient concentrations by month for potassium for the Bondville site.....74
June 1983 through June 1988.
3.10 Mean ion's ambient concentrations by month for sodium for the Bondville site.....75
June 1983 through June 1988.
3.11 Mean ion's ambient concentrations by month for sulfate for the Bondville site.....76
June 1983 through June 1988.

Chapter 1

Introduction

1.1 Background

Earth's atmosphere contains a mixture of gases and particles known as aerosols. An aerosol is a suspension of solid or liquid particles in a gas that exhibits stability over some relevant time period. Some aerosols generate significant interest in the field of air pollution because they produce profound environmental effects. These effects motivate scientists to quantify the mass concentrations, physical characteristics and chemical composition of aerosols found in ambient air. Mass concentration is the mass of particulate matter in a unit volume of aerosol (Hinds, 1982).

One of the preferred units of mass concentration measurements in atmospheric sampling studies is micrograms per cubic meter ($\mu\text{g}/\text{m}^3$) of air. Air is a fluid that can expand or compress in volume, contingent on the temperature and pressure of the air parcel. Therefore, to give meaning to the volume measurement in mass concentration, a standard definition defines the m^3 term. This standard definition is termed standard conditions or standard temperature and pressure (stp). Standard temperature and pressure in air pollution research is commonly defined as 25° Celsius or 298.15 Kelvin and 1 atmosphere, 101,325 Pascal or 29.921 inches of mercury measured using a barometric device (Wilson et al., 1983). This stp definition is the one used throughout this report.

Previous studies have shown the usefulness of simultaneously measuring the chemical composition of atmospheric aerosols and precipitation (Stensland and Bowersox, 1987). These efforts can assist in understanding the precipitation scavenging of trace constituents in the atmosphere. Precipitation scavenging occurs within and below clouds and is a primary mechanism to remove aerosols from the atmosphere. This scavenging process describes the ability of raindrops to absorb aerosol constituents. These constituents can influence the overall precipitation chemistry which in turn effects the pH of the precipitation.

Aerosols that have the potential to strongly influence precipitation pH include airborne dusts produced from soils and unpaved roadway surfaces. These dusts are generated from the parent material by mechanical action. Such mechanical action can occur naturally, e.g., wind erosion or be

anthropogenic in nature, e.g., automotive traffic passing over non-indigenous unpaved roadway surfaces (roadways surfaced with imported material) and agricultural equipment used for crop production. Therefore, soils and unpaved roadway surfaces can contribute alkaline and alkaline earth elements to the atmosphere (Gatz et al., 1985). Upon subsequent capture by precipitation, a certain percentage of these elements will either go into solution as ions (anions and cations) or remain insoluble. This insoluble fraction does not effect precipitation pH and thus is of secondary interest for the Bondville aerosol study. This particular study's elements of interest are calcium, magnesium and potassium.

Using 1980's U. S. Environmental Protection Agency emission estimates, Gatz, et al. calculated that 94% of the calcium, 83% of the magnesium and 84% of the potassium open source emissions (sources too large to be controlled by an enclosure or ducting) for 31 eastern states (those eastward of a line drawn from Minnesota to Louisiana) are due to wind erosion, agricultural activities and unpaved roads. The authors' estimation that the open source emission level is 19.2 times higher than conventional sources (e.g., fuel combustion, industrial, transportation and solid waste disposal) demonstrates the dominance on average of open sources and is the basis for not considering conventional sources in this report (Gatz, et al., 1985).

In Gillette et al., open source emission estimates for particles less than 10 μm indicate that in the contiguous United States the dominant producer of dust mass to the atmosphere is wind erosion (winds associated with regional and convective activity) and dust devils. Unpaved roads are less important on a mass basis. The size range of less than 10 μm is considered because measurements made during major dust storms showed that approximately 90% of the particle mass was in this size range and felt to be available for long distance transport.

Dust devils are intense local convective circulations that transport large quantities of dust high into the atmosphere, making the dust available for long range transport. The devils generate large dust concentrations high in the southwestern United States' atmosphere, where strong southwesterly winds imply long range transport of dust in a northeasterly direction, towards the Bondville, Illinois field site. The dust devil particles considered were those smaller than 25 μm , instead of 10 μm , so dust devil emissions are overestimated compared to the other sources (Gillette et al., 1992).

As previously discussed, road traffic, particularly that which traverses unpaved roadbeds, and soils are common sources of dust. Wind erosion, dust devils and agricultural activities make soils, on a mass basis, the major dust source. However, unpaved roads are the major source for alkaline dust because of their surface material's enriched nature relative to the elemental makeup of soils undergoing wind erosion and soil surfaced roads. Calcium is estimated to make up about 66% of this alkaline dust

(Gillette et al., 1992). Common source materials on unpaved roads are mechanically crushed limestone, gravel from glacial deposits or native soil. Barnard et al., 1986, estimated that at least 80% of the unpaved roads are surfaced with crushed limestone or gravel with the remaining 20% being native soil. This agrees with a locally oriented inventory performed by Gatz et al., 1981, where approximately 80% of the unpaved roads within a 5 kilometer radius of the Bondville site had crushed limestone surface material.

Table 1.1 lists the elemental composition of common unpaved road surfaces. These values are the mean percentages of the element by mass calculated from Table II in Barnard et al., 1986. Count (n) is the number of samples used in calculating the mean. The presentation of these values illustrates the typical difference that can occur between the elemental abundance (elemental composition) in each of the categories of unpaved road surfacing material.

Table 1.1. Mean total elemental composition of unpaved road samples listed in Table II of Barnard et al., 1986.

unpaved road surfaces	calcium abundance (%)	magnesium abundance(%)	potassium abundance(%)	count (n)
soils	1.56	0.71	2.22	4
gravel	7.56	2.42	1.38	9
crushed limestone	24.53	2.99	0.74	7

Barnard et al.'s calculation of a state by state elemental flux indicated that unpaved roads are a major contributor of more than 90% of all open source calcium and magnesium emissions in 37 and 33 of the 48 contiguous states, respectively. Also noted was wind erosion's significant mass contribution from 15% for Idaho to 82% for North Dakota in the central and high plains states. This resulted in soils contributing a significant amount from 11% for New Mexico to 45% for North Dakota of the calcium and magnesium fluxes. In addition, soils were the dominant contributor from 47% for New Mexico to 97% for North Dakota of airborne potassium (Barnard et al., 1986).

The U. S. National Acid Precipitation Assessment Program's 1991 report (NAPAP, 1991) presents summary statistics drawn mainly from a work published later by Gillette et al., 1992. This Gillette et al's paper utilized modified results from an earlier Illinois State Water Survey effort on unpaved road dust fluxes (Barnard et al., 1986). Road dust and agricultural activity were found to be the dominant dust producers by mass, east of the 95° W longitude, which runs approximately through the state of Minnesota, south to Louisiana. In comparison, the mainland U. S. overall average for road dust

and agricultural activity is 44.2%. The report states that almost 70% of mainland open source calcium is due to unpaved roads. Over 60% of the magnesium emissions are from unpaved roads and agricultural activity. Sixty-nine percent of potassium emissions and 67% of sodium emissions are from wind erosion and dust devils. It was also found that wind erosion strongly influences the western United States potassium fluxes (Irving, 1991)

1.2 The Bondville Study

The Atmospheric Sciences Division of the Illinois State Water Survey (ISWS) started precipitation chemistry and aerosol measurements in May, 1977 at Willard Airport in Savoy, Illinois. Relocation of these efforts occurred in June, 1978, to avoid potential influences from anthropogenic sources associated with airport activities. The new rural site location, used continuously since June, 1978, is about 8.0 kilometers (5 miles) west of the airport and about 6.4 kilometers (4 miles) south of the small town of Bondville, Illinois. This site is referred to as the "Bondville site". Collection of daily aerosol filters at Bondville complimented the numerous precipitation chemistry studies undertaken at or near Bondville. This daily filter sampling effort continued until February, 1989. Financial considerations then caused filter collection to be adjusted to a weekly basis. This weekly effort should continue well into the future.

Nuclepore™ polycarbonate filters were used at the Bondville site from June, 1978 until February, 1983. At that time, the filter media was changed to teflon type filters. This report focuses on the data generated from the collection of daily teflon filter samples during June 1, 1983 to May 31, 1988 in order to exclude any complications resulting from a change in filter media.

There are three distinct characteristics that makes the Bondville aerosol sampling study unique. First, the data set consists of daily samples collected during a long period from June, 1978 to January, 1989. Most aerosol data sets are not of such long duration and usually sample every sixth day. Second, both the Bondville and Willard Airport sites are rural settings unlike most sampling efforts which are conducted in urban settings. Third, analysis of the Bondville filters was for their soluble (as opposed to total) ionic composition using an extraction solution and method designed to simulate the dissolution of aerosol particles by acidic precipitation.

The daily aerosol study measured four crustal elements (calcium, magnesium, potassium and sodium) that are almost always measured in precipitation chemical network studies. Most aerosol studies report total element concentrations determined by multi-element analysis techniques which are

not sensitive for all four of the crustal elements measured in precipitation chemical studies. The focus in such studies is usually the measurement of airborne heavy metal concentrations to support human health effect studies (Stensland, 1987).

This report will concentrate on the analysis of the measured calcium, magnesium and potassium average monthly levels. Sulfate and sodium will be reported for completeness of data presentation, but their results will not be emphasized. The present study does not attempt to explain day to day variations but rather uses monthly averages to characterize temporal patterns which may be related to emission sources' temporal patterns. These monthly aerosol patterns will also be useful for future comparisons to precipitation chemistry data.

One notable feature of this study is the inclusion of a precision estimate of the error incurred when calculating ion's ambient concentrations from several performed measurements (section 2.5.3). The final database generated includes these precision estimates for every calculated ambient concentration. The data screening process described in section 2.5.3.2 uses these precision estimates to form the data subset appropriate for the interpretive processes presented in Chapter 3.

Additionally, this study's modeling effort in section 2.6 expands on a previous effort by Gatz et al., 1981, to understand the sources of alkaline dust at the Bondville site. Gatz et al., 1981 collected samples only during the summer and fall of 1978. The authors' chemical element model indicated that for this period unpaved roads were an important source of airborne alkaline materials, contributing 86% of the airborne calcium. Section 3.2 presents a discussion of this present study's modeling results where the analysis of its five year data set allows the observation of annual trends that the sources might exhibit.

1.3 Site Characteristics

Figure 1.1 depicts the Bondville sampling site. It is 12.8 kilometers (km) west-southwest of Champaign, IL. Linear distance using roadway paths from central Champaign is 10.8 km west on Illinois Route 10 and 6.9 km south of Bondville traveling on County Highway 19. The latitude and longitude of the site are 40° 03' 12" N and 88° 22' 19" W, respectively.

The site is located in a rural setting. The actual sampling points are on a 30 meter square area (inside a 2.5 hecter fescue grass cover plot) which is part of a 101 hecter farm owned by the University of Illinois. Agricultural activities consisting of soybean and com cultivation dominate the surrounding

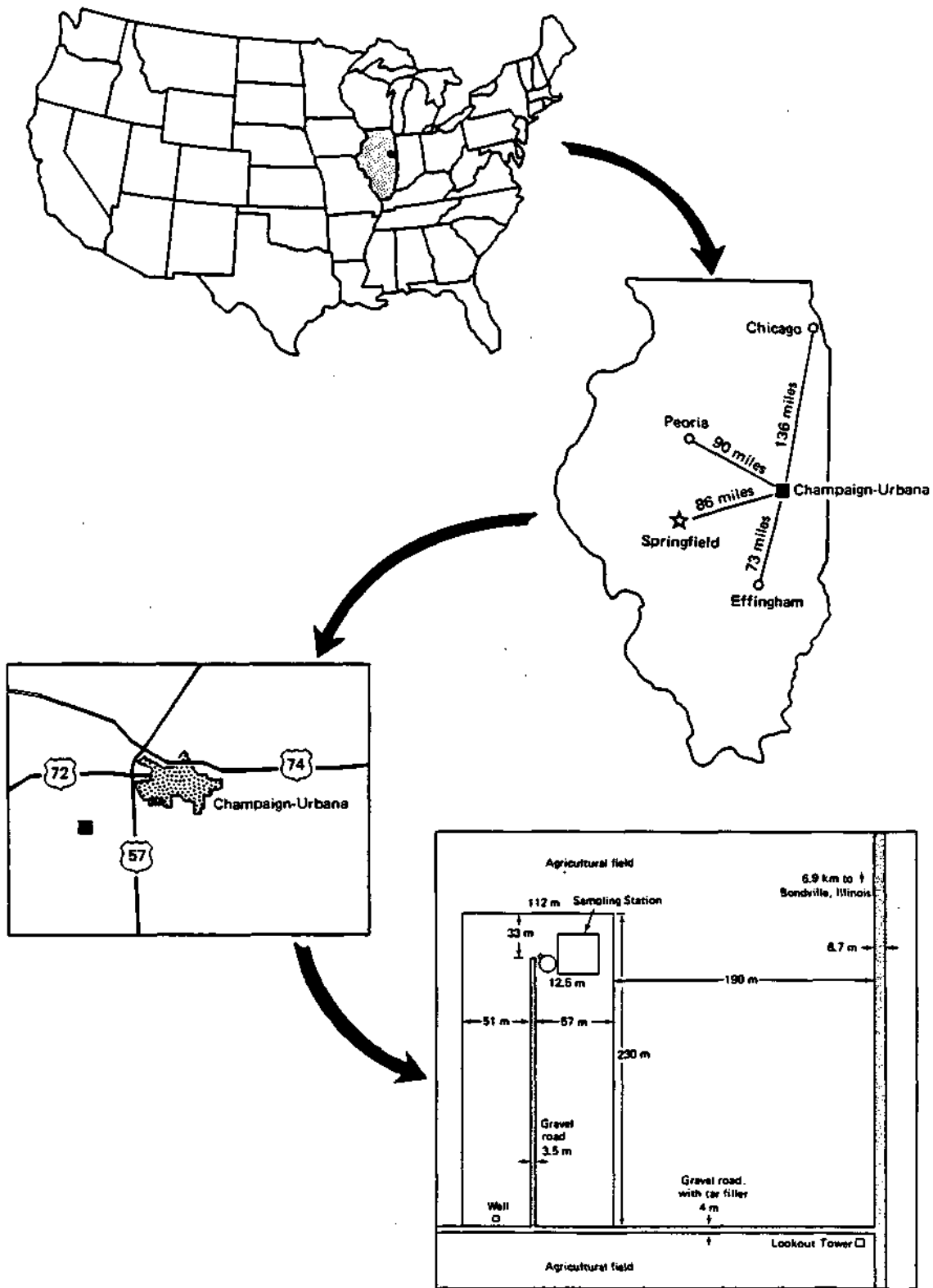


Figure 1.1. Map of Bondville, IL sampling site.

lands.

The closest significantly developed region is the Champaign-Urbana community. Bondville is a small community processing a population of about 440, whereas, the Champaign-Urbana twin city community has a population of about 95,000.

The remote location of the Bondville sampling site has facilitated its use for measurement of background ambient aerosol and precipitation chemistry concentration levels. The coordination of measurement activities at Bondville has been carried out by the Atmospheric Sciences Division of the Illinois State Water Survey since the fall of 1977. In February, 1979, Bondville became one of over 200 nationwide acid rain monitoring stations for the National Atmospheric Deposition Program (Dossett, 1987).

1.4 References

Barnard, William R., Gary J. Stensland, and Donald F. Gatz, 1986: Alkaline materials flux from unpaved roads: source strength, chemistry and potential for acid rain neutralization, *Water, Air and Soil Pollution*, vol. 30, p. 285-293.

Dossett, S.R., 1987: An annotated description of the atmospheric chemistry sampling station at Bondville, Illinois, *In Study of Atmospheric Pollution Scavenging by R. G. Semonin et al.*, COO-1199-65, 21th Progress Report to the U. S. Department of Energy, Office of Health and Environmental Research, Contract DE-AC02-76EV01199, p. 329-340.

Gatz, Donald F., Gary J. Stensland, Michael V. Miller and Alistair C. D. Leslie, 1981: Sources of airborne calcium in rural central Illinois, *American Chemical Society, Society Symposium Series, No. 167*, Report No. 17, p. 303-308.

Gatz, Donald F., William R. Barnard and Gary J. Stensland, 1985: Dust from unpaved roads as a source of cations in precipitation, *78th Annual Meeting of the Air Pollution Control Association*, Report No. 85-6B.6, Detroit, Michigan, June 16-21.

Gillette, Dale A., Gary J. Stensland, Allen L Williams, William R. Barnard, Donald F. Gatz, Peter C. Sinclair and Tezz C. Johnson, 1992: Emissions of alkaline elements calcium, magnesium, potassium

Chapter 1: Introduction

and sodium from open sources in the contiguous United States, *Global Biochemical Cycles*, vol. 6, no. 4, p. 437-457.

Hinds, William C, 1982: Aerosol technology, properties, behavior, and measurement of airborne particles, John Wiley and Sons, New York, NY, p. 6-9.

Irving, Patricia M. Ed., 1991: Acidic deposition: state of science and technology, *In The U. S. National Acid Assessment Program*, Government Printing Office, Washington, D.C., vol. 1, p 102-109.

Stensland, Gary J., 1987: Preliminary data for daily ambient aerosol measurements at the Bondville research site, *In Study of Atmospheric Pollution Scavenging by R. G. Semonin et al.*, COO-1199-65, 21th Progress Report to the U. S. Department of Energy, Office of Health and Environmental Research, Contract DE-AC02-76EV01199, p. 329-340.

Stensland, Gary J. and Van C. Bowersox, 1987: Ratios of ion concentrations in precipitation to aerosols at the Bondville site, *In Study of Atmospheric Pollution Scavenging by R. G. Semonin et al.*, COO-1199-65, 21th Progress Report to the U. S. Department of Energy, Office of Health and Environmental Research, Contract DE-AC02-76EV01199, p. 251-259.

Wilson, M. L, D. F. Elias and R. C. Jordan, 1983: Student manual second edition, *APTI Course 435 Atmospheric Sampling*, EPA 450/2-80-004, United States Environmental Protection Agency, Office of Air Quality Planning and Standards, Contract 68-02-3573, p. 2-15-2-23.

Chapter 2

Methodology

2.1 Introduction

This chapter describes the methods and procedures completed to calculate the soluble ions' concentrations sampled at Bondville. Filter sampling efforts and the extraction and analysis of those filters are discussed. In addition, a model quantifying source apportionment is presented.

2.2 Filter Sampling

Four identical filter sampling trains were operated at the Bondville site from June, 1978 to February, 1989. A train consisted of a Gelman™ air sampling kit, timer, rubber vacuum tubing and filter holder support structure. The sampling train systems operated automatically using timers to switch on one train every morning (approximately at 10 o'clock) to sample for a 24 hour period. The system was able to operate, collecting a total of four daily filter samples, automatically over a four day period. The timers controlled air sampling using half-hour periods, cycling on and then off, over the 24 hour period. This 24 hour composite sample (consisting of approximately a 12 hour sampling period) was collected on a circular Zefluor™ teflon filter. The 37 millimeter diameter, 1.0 micrometer (μm) pore sized filter was mounted in a Millipore™ Field Monitor plastic filter holder. A historical note; Nuclepore™ 0.8 μm pore size polycarbonate filters were used from June, 1978 till February, 1983. The current sampling effort at this writing involves one 7 day composite filter sampled for ten minutes every hour using the described sampling train.

The aforementioned Gelman™ air sampling kit is an oil-less Gast™ piston vacuum pump mounted in a covered steel rectangular container. An electric motor drives this piston pump. Attached to the outside of the container is a Dwyer™ rotameter and vacuum gauge. The rotameter consists of a vertically graduated Plexiglas tube, rotating spherical steel ball float and knurled adjusting knob. The tapered tube diameter increases as the demarcated scale indicates increasing flow. The tube graduations indicate flow from 10 to 72 Liters per minute (L/min). The float (the flow indicator) moves up when air passes it, to a level where the ball's downward force is equal to the flow's viscous force up.

Chapter 2: Methodology

The pump is capable, under no load conditions, of producing a maximum air flow rate of approximately 70 L/min at stp. To convert rotameter scale flow readings to stp flow values, a vacuum gauge provides the pressure drop reading near the entrance to the rotameter (GelmanTM, 1970).

The filter support structure is located outside in the ambient air. The support structure holds the MilliporeTM filter holders face down, approximately 1.5 meters above the fescue grass surface, inside inverted 30 centimeters (cm) diameter polyethylene funnels. The funnels act as rain shields. They are attached to the short side of u-shaped poles. A center support anchors the four poles and the inverted funnels radiate out, 90 degrees apart from each other. The filter's surface is about 2 cm above the bottom edge of the inverted funnel. An identical sole funnel setup, located one meter away, holds the "outside hung field filter blank" discussed in section 2.3.

The GelmanTM pumps operate in an underground room, nicknamed "The Cave". The Cave is a 10 meter diameter circular room whose roof is level with the ground surface. The filter holder sampling structure is mounted outside on the ground. Its base is level to The Cave's roof. The pump delivers vacuum to the filter holders using approximately 10 meters of 1.27 cm internal diameter thick rubber tubing.

A technician would visit the site and complete field sheets and field log sheets. The field sheets are a descriptive account of the observed daily conditions at the field site, e.g., notation of nearby agricultural activities generation visible dust plumes. The field log sheets provide information about the pump's sampling cycle, specifically rotameter flow rates and pressure drops at the beginning and end of the sampling cycle. Readings were recorded after the pumps underwent a 2 minute warm up period (Stensland and Bartlett, 1979).

RockwellTM dry gas meters, the type commonly found measuring residential natural gas usage, were used from April 1983 till November 1992. The air volume measured by the gas meters was compared to the volume calculated using the average of the rotameter flow rates. Subsequently, the RockwellTM air volume data has been found to be questionable so this check was not used for this study. Experiments indicated that the RockwellTM meters were unable to maintain calibration at the pressure drops and varying flows experienced at Bondville.

2.2.1 Filter Sampling Efficiency

The filter funnel setup's collection efficiency was never evaluated. Therefore, it is unknown to what extent larger sized particles are being collected. Pattenden and Wiffen, 1977 conducted a study on particle size dependence for an aerosol sampler. The Bondville filter funnel setup was similar to the setup in their study. Their setup possessed an inlet duct of 1.25 cm in diameter, 3.1 cm in length, leading to a 6 cm diameter Whatman 40 paper element, backed by polypropylene gauze. Bondville's filtering setup possesses no inlet duct. Instead, the Nuclepore filter's face (3.7 cm in diameter) captured particles directly. The authors sampled at 6 L/min, Bondville at approximately 27 L/min (stp). Nevertheless, Pattenden and Wiffen, 1977's results indicate that particles of less than about 6 μm aerodynamic diameter are sampled with greater than 60% efficiency in wind tunnel test in 4 m/sec winds. The restrictive turn the particles needed to maneuver to reach the filter's surface makes the authors' sample setup less efficient than Bondville's easier turning setup. Therefore, it can be safely concluded that Bondville's setup should be collecting particles that are slightly larger than 6 μm with at least 60% efficiency.

Gatz, 1981 compared the collection efficiency of the Bondville funnel setup and a specially constructed quasi-isokinetic sampler. This sampler processed a vane so its vertically rotating entrance constantly faced the wind. The sampler contained an expanded collection tube so the average wind speed (3.0 m/sec) would slow and approach the filter media at about the same speed as the face velocity across the filter's surface. This approach increases the collection of large particles not sampled by the funnel setup. This is due to the particles' inertia which prevents them from making the 90 degree bend from their horizontal trajectory up to the inverted filter. Gatz found that the vane sampler collected from 20 to 35% greater mass over the funnel setup. Future studies will compare the Bondville sampling setup to dichotomous samplers in order to understand the ability of the current sampling method to capture particles.

2.3 Filter Processing

Filter processing involves two main undertakings; filter extraction (briefly discussed in section 1.1) and chemical constituent analysis. Figure 2.1 summarizes the Bondville aerosol filters' handling process and related quality control/quality assurance (QC/QA) procedures.

Procedures were standardized for the steps involved in determining the mass and chemical constituents on the filters. Tweezers were used to handle boxed new filters. An electronic balance,

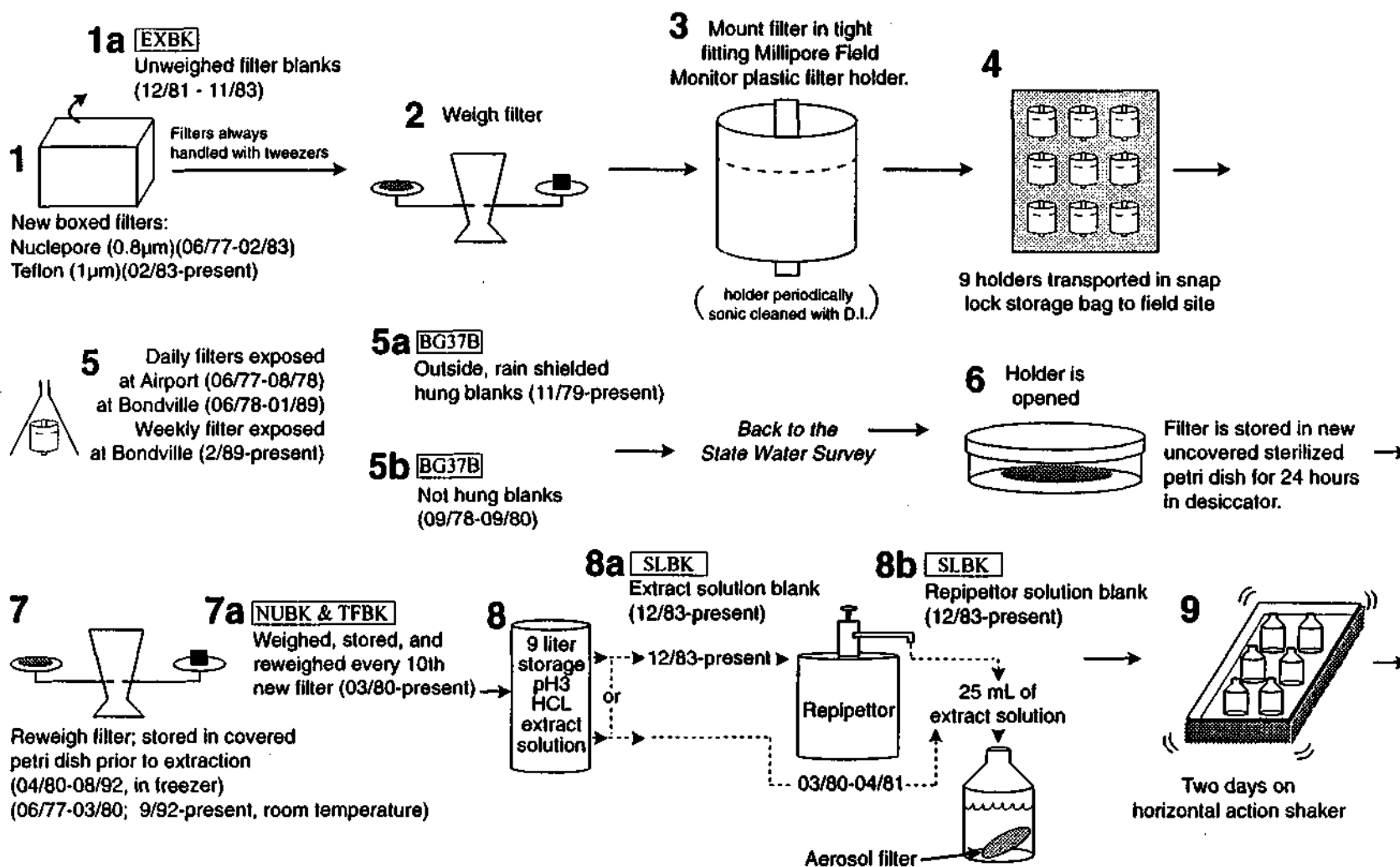


Figure 2.1. Bondville ambient aerosol filter sample collection and processing diagram.

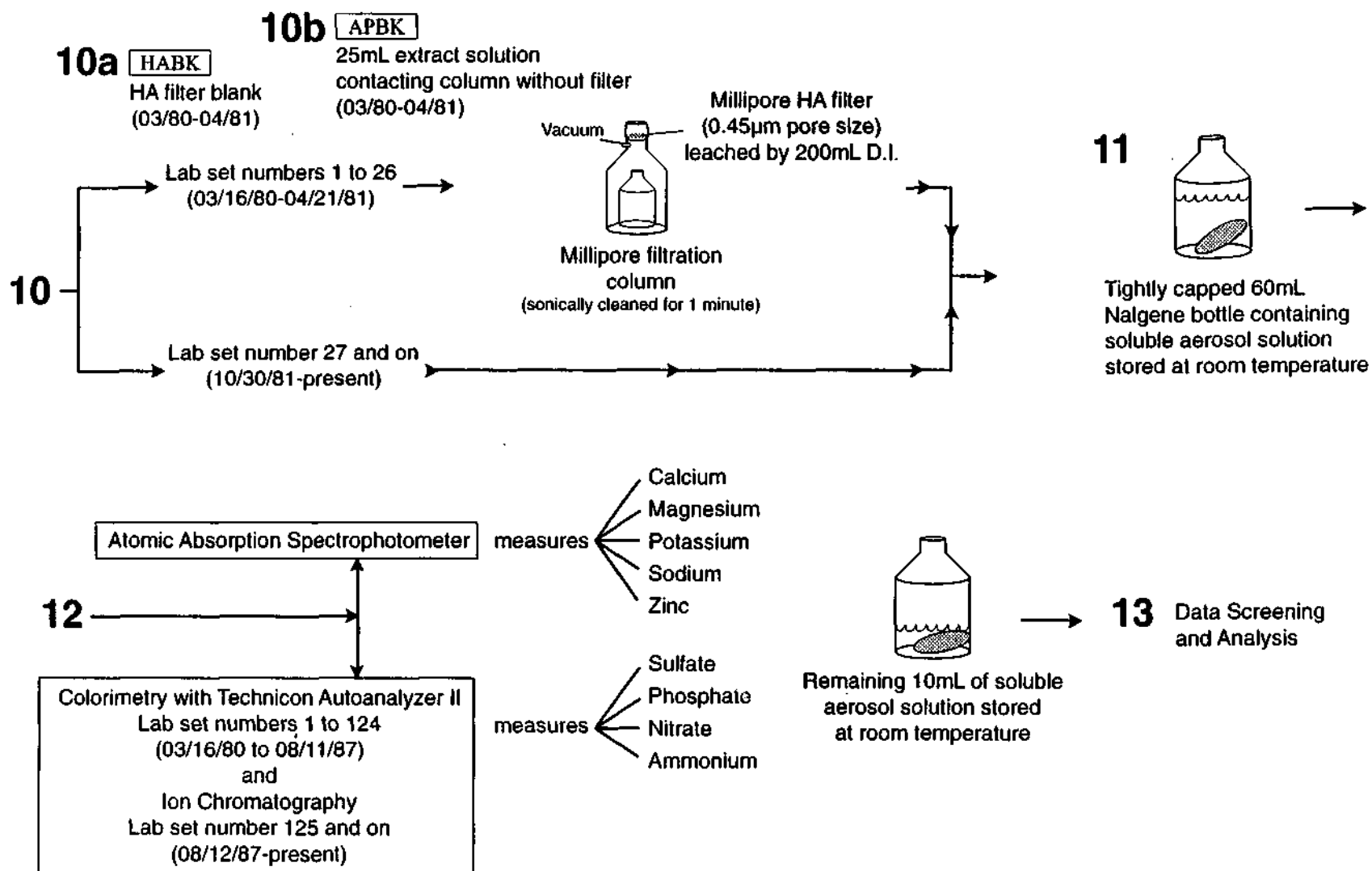


Figure 2.1 (continued) Bondville ambient aerosol filter sample collection and processing diagram.

Chapter 2: Methodology

whose tray was lined with fresh parafilm to avoid contamination, weighed the new filter. Next, the filter was loaded into a matched snug fitting Millipore™ Field Monitor plastic filter holder. The holder was cellophane adhesive taped together to prevent separation during transport to the field site. Each filter received a referenced lab number and its holder was labeled with this same number. Nine assembled units were snap closed in a plastic bag, ready for transport to Bondville.

The filter holders were returned to the Illinois State Water Survey (ISWS) labs where they were opened. The filters were then transferred to a sterilized petri dish. The open dishes were stored in a desiccator for at least 24 hours before reweighing. This served to minimize weight gain due to the collected particles' hydroscopicity. After reweighing, the filters were then stored in a freezer or in another clean and secure area before the extraction procedure.

The extraction procedure involved reacting 25 milliliters (mL) of the extraction solution and the filter in a new Nalgene™ linear polyethylene 60 mL bottle. These bottles and their screw top lids were tripled rinsed with deionized water before using in order to limit possibly contamination. Next, a shaker tray at room temperature agitated a "lab set" of bottled filters (approximately 27 filters) for 48 hours. Please note that deionized water is used to indicate a very clean water supply. In the beginning of the Bondville project it was often tap water that was distilled at least twice and later in the study this distilled supply was additionally treated by a reverse osmosis/ultrafiltration unit.

Initially for the 1977 to 1978 filters collected at Willard Airport, extraction of the filter's collected particles used room temperature deionized water ($\text{pH} \cong 5.6$) as the extraction solution. The filter and solution was shaken for 20 minutes. A primary goal of the aerosol sampling and analysis at Bondville was to relate the aerosol data to the soluble chemical constituents found in precipitation. Therefore, Bartlett and Stensland reevaluated the extraction process and suggested that both acidity and extraction time should be increased. They reasoned that this would better simulate the conditions experienced by the atmospheric aerosol particles which are scavenged by rainfall samples collected in the National Atmospheric Deposition Program/National Trends Network (NADP/NTN).

The fraction of soil dust minerals that solubilize, (become soluble ions), typically increases as the extraction solution becomes more acidic and as the filter and its dust particles reside longer in the extraction solution. Some of the soluble base cations in precipitation originate from ion exchange whereby base cations absorbed on organic or clay soil aerosols are displaced by hydronium ions (H^+) in acid rain. Again, as the acidity increases (the amount of H^+), more base cations go into solution as indicated by the equation (2.1) (Bartlett and Stensland, 1980).

Chapter 2: Methodology



The Bondville site has experienced precipitation events where a minimum pH value of 3.0 has been measured. Therefore, Bartlett and Stensland recommended that the extraction solution's pH should be 3. This pH value represents the upper limit of acid rain's acidity seen by atmospheric particles. On the issue of extraction time, Bartlett and Stensland recognized that a few hours is too short since many rain samples collected by NADP/NTN are at least 1 to 2 days old before they are particle are filtered out of the samples. The filtering process stops the further solubilization of dust particles. Weekly precipitation chemistry samples are shipped to the Illinois State Water Survey central lab before filtering. Therefore, rain samples can contain dust particles two or more weeks before the termination of the solubilization process.

The soil particles may come close to equilibrium with the extraction solution after a few days but not after a couple hours so a reasonable extraction procedure suggested by Bartlett and Stensland was to choose a longer shake time on the order of two days (Bartlett and Stensland, 1980). Note on steps 9 and 10 in Figure 2.1 the first Bondville aerosol filters, lab sets 1 to 26, were shaken for 2 days and then filtered with HA filters which stopped the further solubilization of dust particles. However, for lab set 27 and on, samples were not filtered with the HA filters, so the dust particles could continue to solubilize up to the time of analysis (step 12). This is not a concern since it is felt that the pH 3 solution solubilizes all available ions from the filter very quickly.

Extracted ion solutions were stored at room temperature for about a month and sometimes longer before analysis. Peden and Skowron, 1978 demonstrated that filtered precipitation extracts maintained steady ion concentration values over a six week period. This study's extracts are similar to the aforementioned precipitation study. Therefore, these extracted ion concentrations are felt to be stable during experienced storage period (Stensland and Bartlett, 1979).

The extraction solution was analyzed by the Illinois State Water Survey Atmospheric Chemistry Laboratory. The analytical method for sulfate concentrations was methylthymol blue automated on the Technicon™ Autoanalyzer II. This analysis was switched to ion chromatography in January, 1986. Other anions (phosphate, nitrate and ammonium) were analyzed at the beginning of the Bondville project by automated Technicon™ methods, but were not analyzed during the present study's period. Calcium, magnesium, potassium and sodium concentrations were evaluated using flame atomic absorption on an Instrumentation Laboratory™ Atomic Absorption Emission Spectrophotometer 353. A very

Chapter 2: Methodology

comprehensive QA/QC program was in place for the analytical chemistry measurements since the same methods, equipment and staff were being used for precipitation chemistry samples submitted to the laboratory in its role as The Central Analytical Laboratory (CAL) for NADP/NTN (Stensland and Bartlett, 1980).

Strict attention was paid to quality control throughout the filter sampling and processing steps. Measured ion concentrations should reflect only sampled aerosols, so nine different blanks were collected in order to quantify any introduced contamination. Blank correction values would then ensure that the calculated ions' concentrations would represent concentrations sampled at the Bondville site. The nine blanks each represent different portions of the filter sampling and handling process on Figure 2.1. Blanks collected have their lab reference abbreviations in upper case lettering surrounded by a text box and followed by a short descriptor. Noting step 1a on Figure 2.1, new unweighed filters from the manufacturer were analyzed for the studied ions (EXBK). Additional blank filters were weighed, mounted in a holder, transported to and from the field site and reweighed (step 5b: BG37B). Blank filters were also hung in the ambient air at Bondville (see section 2.2), to quantify the effect the whole sampling and analysis process had on the ions' ambient air concentrations (step 5a: BG37B). Blanks representing the weighing, storage in a petri dish and reweighing steps were analyzed (step 7a: NUBK & TFBK). Extract solutions were passed through clean filtration columns (step 10b: APBK) and also through ones with an installed HA filter (step 10a: HABK) to see if this step presented contamination. After December 1983 (this study period's filters) the stored extraction solution (step 8a: SLBK) and the extraction solution dispenser (Repipet®) (step 8b: RPBK) were checked for contamination. The total number of blank samples taken in addition to this study's sampling effort was about 32% of the actual number of daily filter samples.

Table A.1 in Appendix A shows the arithmetic mean, standard deviation and median as calculated by Microsoft® EXCEL version 4.0 software for all of the field and lab blanks. Count is the actual number of blank filter samples used in the derivation of these statistics. Standard deviation is an estimate of the standard deviation of a population based on a sample and measures how widely values disperse from the mean. This calculation used the non bias or "N-1" denominator method, where N is equal to the number of blanks analyzed (Microsoft® EXCEL). Note, with the exception of the FORTRAN program AIR.FOR (section 2.5.1), this report's mathematical calculations (calibrations performed and statistical analyses) was performed with EXCEL software.

Table 2.7 in section 2.5.3 provides central tendency statistics on the outside hung blanks for this study's period. The outside hung field blanks contain some of the highest mean values for this study's period. Therefore, this study's outside hung field blank mean values were subtracted from the daily

Chapter 2: Methodology

sample values to provide the blank corrected Bondville filter ion concentrations (section 2.5.1). This is reasonable since these blanks best represent the entire sampling and handling process.

This study's calcium, sodium and sulfate means for outside hung blanks are statistically different from the previous period, June 1978, to May 1983. The statistical test used to prove this difference was the "student t test difference of the means" method. It was expected that the outside hung field blank values should remain relatively constant over time. Future efforts addressing occurrence of traceable filter contamination should be considered as part of the blank correction procedure.

2.4 Calibration to Determine Sampled Air Volumes

Several pump calibration efforts were undertaken before calculating the daily Bondville ambient air concentrations for the analysis presented in Chapter 3. Beginning in 1978, on many separate occasions the rotameters on the pumps used at Bondville were calibrated by different ISWS staff members. In some cases special tests were conducted which raised questions that lead to changes in calibration or sampling procedure.

In the early 1990's researchers were beginning to present time trend results for precipitation chemistry measurements which covered a 10 to 15 year period that began in the late 1970's. Some sites reported a statistically significant trend for sulfate and the crustal ions including calcium, magnesium and potassium (Stensland, 1993). Therefore, the Bondville aerosol record took on additional importance in addressing issues related to acid rain trends. Thus an important objective of the present study was to very carefully calibrate the rotameters associated with the Bondville pumps and to do sensitivity tests to investigate the uncertainty of the air volumes calculated for each daily aerosol sample.

2.4.1 Calibration of the Intermediate Standard for Volume Determinations

A Singer™ Dry Test Meter, model number 115 (DTM-115) was used to measure air volumes during the rotameter calibration efforts. The DTM-115 is an intermediate standard with a more accurate indexing system (readout) than the common dry gas meter (a secondary standard) used to meter retail gas supplies. The DTM-115 requires calibration with a primary standard to ascertain its accuracy (Wilson et al., 1983). A mini-Buck™ Calibrator served this purpose. The mini-Buck™ is an electronic flow indicator that uses the classic soap bubble principle (a primary standard). The manufacturer rates

Chapter 2: Methodology

the Calibrator to be 0.5% accurate at any display reading (from 0 to 30 L/min, its flow capacity) under steady flow conditions (Buck, 1985). The Calibrator was considered to be the true flow rate indicator.

During all calibration procedures, the author was able to use an electronic stopwatch with a readout to the hundred of a second to obtain time intervals with a precision of ± 0.10 second and to read the DTM-115 dial with a precision of ± 0.05 L. Fifty liter and 100 L volumes were indicated by the DTM-115 and the smallest time measured was approximately two minutes. Calculations indicate that the worst case measurement error involving the smallest volume and time period measured contribute an insignificant error in all the study's calibration efforts.

Ambient air pressure and temperature conditions were measured for the calibration runs. Conversion to stp (defined in section 1.1) allowed comparison of the mini-Buck™ and DTM-115 paired air volumes. The conversion to stp was done with the ideal gas law equation:

$$PV = nRT \tag{2.2}$$

where P is the absolute pressure, V is the volume, n is the number of moles and T is the absolute temperature of the gas. R is the universal gas constant.

Solving equation 2.2 for "n" and using the conservation of mass concept, we relate an air parcel at ambient conditions (indicated by subscript a) with the same air parcel at stp conditions (indicated by subscript s) with the equation:

$$\frac{P_a V_a}{T_a} = \frac{P_s V_s}{T_s} \tag{2.3}$$

We used the stp definition of 29.92 in. of Hg for P_s and 298.15 K for T_s calculate stp volumes (V_s).

The DTM-115 was calibrated using four separate calibration runs conducted over a range of flows (from approximately 5 to 25 L/min in increments of 5) to generate 5 data points per run for a total of 20 paired data points. One pair was discarded because it was clearly an outlier when compared to the other pairs. The percent errors of the DTM-115 compared to the mini-Buck™ air volumes at stp were computed. Percent error is equal to the DTM-115's stp value and minus the mini-Buck™ stp value, divided by the mini-Buck™ stp value. This resultant is multiplied by 100.

The mean of these 19 percent error values was 1.539% $\pm 0.326\%$ where the 0.326% is twice the standard error of the mean. Standard error is the standard deviation divided by the square root of the

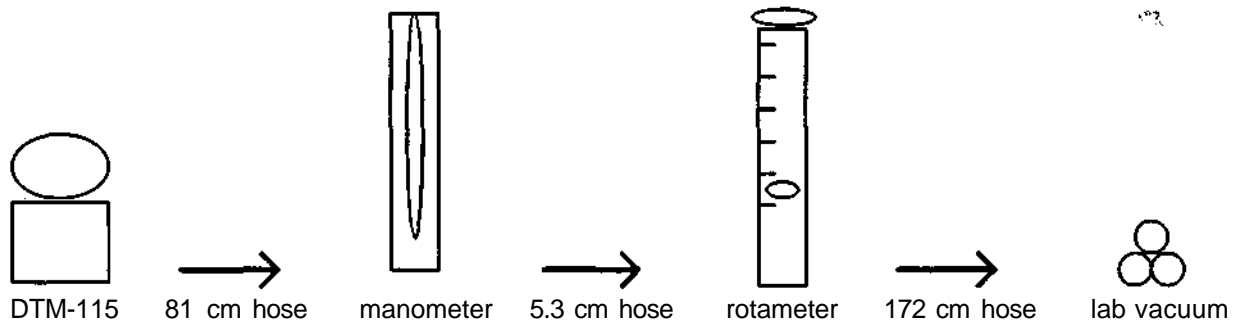
Chapter 2: Methodology

number of observations (Lapin, 1990). For the 19 percent error values, the ratio of twice the standard error to the mean indicates that we can say at about the 95% confidence level that the DTM-115 calibration value is accurate to $\pm 0.326\%$.

2.4.2 Rotameter Calibration Procedure

Three separate calibration runs were completed for each of the ten rotameters used at Bondville. These three runs were used to calculate the rotameter calibration curve. Only ten of the twelve rotameters used throughout the Bondville project were available for calibration, two are missing. Fortunately, these two rotameters were not used during this study's period.

Rotameter calibration runs involved the following setup depicted in the schematic below. Ambient conditions were measured using a thermometer on the DTM-115 and an aneroid barometer to get the DTM-115's air temperature in degrees Celsius and atmospheric pressure in inches of mercury, respectively. A laboratory vacuum supply drew this ambient air through the DTM-115. The DTM-115 indicated Liters of air, while the electronic stopwatch (discussed in section 2.4.1) measured the time for a fixed air volume (100 L) to pass through the DTM-115.



The flow continued through 81 cm of 10 mm internal diameter vacuum hose and passed through a plastic tee connected to the rotameter's base by a short piece of vacuum hose, 5.3 cm in length. The plastic tee's open end allowed a Dywer u-tube 91 cm open ended mercury manometer to measure the flow's pressure drop at this point. This pressure drop (gauge pressure) was subtracted from the ambient pressure to compute the absolute pressure seen by the rotameter float. The flow then entered the bottom of the rotameter, traveled past the float and out the top and continued through a 172 cm vacuum hose connected to the laboratory vacuum source.

Chapter 2: Methodology

The adjusting knob on the top of the rotameter was used to vary the flow rate. The knob was adjusted to obtain flow rates from 20 to 60 L/min, at 10 L intervals. Recorded for each of the five flow rates were the manometer's pressure drop reading, the rotameter flow rate and the time for the DTM-115 to indicate an air volume of 100 L.

When adjusting the flow, good technique for sighting the rotameter float was found to be critical in obtaining precise results, so that the three separate calibration runs closely reproduced each other. The circular steel ball appears elliptical when viewed through the rotameter's Plexiglas body. This noticeable shape distortion was used to finely adjust the flow rates. This method was superior to the usual method of determining the location of the ball's center.

The length of the float when viewed is slightly over 12 L on the rotameter scale. Coarse positioning of the float involved placing one's eye level with the desired flow rate mark. Then observing the bottom and top positions of the float, fine adjustment of the ball placed these ball positions equidistance from the desired flow rate.

Early Fall, 1992 calibration attempts of the Bondville pump rotameters used an in-line needle valve to adjust the flow instead of the flow adjusting knobs on top of the rotameter. This needle valve was placed after the rotameter and before the lab vacuum source.

The later calibration runs are the ones used for this study. This calibration method is depicted in the above flow diagram where the needle valve is not used to vary the flow. Instead, the flow is varied by the rotameter adjusting knob located on top of the rotameter. A comparison of these two calibration methods is discussed in section 2.4.3 with results presented on Table 2.3.

The rotameters had never been cleaned so a buildup of foreign material in the rotameters was believed to be causing the calibration drift experienced during previous calibration attempts. This concern led to the cleaning of pump 0013's rotameter. This solvent cleaning occurred before the decision was made to recalibrate the rotameters using the no needle valve method described above and depicted by the schematic. Therefore, the only unclean rotameter calibration available for 0013 is the needle valve method. Table 2.4 presented in section 2.4.3 compares calibration results of unclean versus clean rotameters.

The conversion of the DTM-115 measured air volumes into stp used equation 2.3. However, the ideal gas law does not define rotameter conversions to stp. We use equation 2.4 to convert rotameter conditions to stp (Wilson et al., 1983):

$$Q_s = Q_r \sqrt{\frac{T_s P_r}{T_r P_s}} \quad (2.4)$$

where subscript r stands for rotameter conditions and subscript s stands for stp conditions. Q is the flow, T is the temperature and P is the pressure of the gas. A temperature measuring experiment (see section 2.5.2) found no significant temperature change occurred as the ambient air traveled to the rotameter, so in this equation T_r is equal to the measured ambient temperature.

The paired stp flows were hand plotted to illustrate if the pump's three separate calibration runs reproduced each other. This effort produced figures resembling Figure 2.2, a rotameter calibration curve. The ordinate is the DTM-115 flow (considered the true flow) and the abscissa is pump 0110 rotameter flow, both at stp.

The "method of least squares equation fitting" in EXCEL was used to generate the straight line equations listed next to the run dates. This best line fit produces a slope and intercept for the curve fit. The straight line equation with y as the ordinate and x as the abscissa is of the form:

$$y = mx + b \quad (2.5)$$

where m is the least squares derived slope and b, the y axis intercept.

The three separate calibration runs need to reproduce each others findings in order to be considered valid. Therefore, it is useful to quantify the difference among the three runs. We chose to compare the three lines at a single rotameter flow rate, namely the typical Bondville project's flow rate (\cong 30 L/min stp). Using Figure 2.2, the possible flow value for run one is gotten by inputting the 30 L/min stp rotameter flow into the calibration equation and getting a true flow value (y) of 26.71 L/min stp. Run two's equation gives 26.47 L/min stp and run three gives 26.75 L/min stp.

Table 2.1 summarizes the final results of the calibration effort for the Bondville rotameters. It lists the pump number, date of calibration, "method of least squares" slope and intercept, and maximum percent error. It uses the same approach as the Figure 2.2 example to get three possible true flow values. A description of the maximum percent error can be illustrated using Figure 2.2's three separate calibration runs. The maximum percent error at 30 L/min for the three calibration equations in Figure 2.2 is the difference between the highest true flow value (26.75) and the lowest true flow value (26.47) divided by the lowest value (26.47) and multiplied by 100 which gives 1.058%. The maximum in maximum percent error indicates that this approach gives the highest percent error value. Note, the difference calculation disregarded the middle y value (26.71) and instead used the highest and lowest

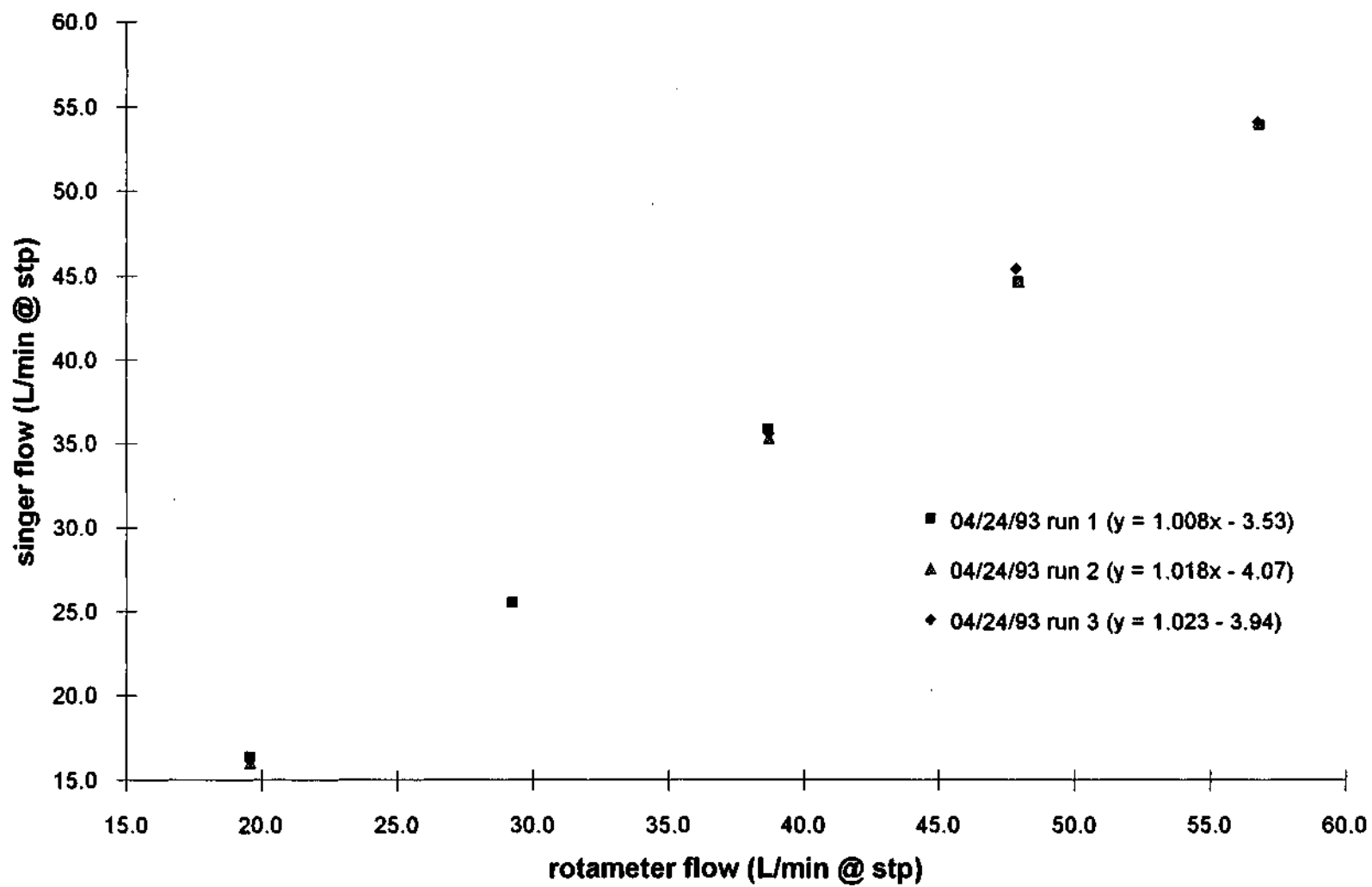


Figure 2.2. Calibration runs for pump 0110's rotameter.

Table 2.1. Results of rotameter calibration efforts.

pump number	new effort run date	run	best-fit calibration line		maximum percent error (30 L/min @ stp)
			slope	intercept	
0013	Dec '92	1	1.001	-2.54	0.292
		2	1.006	-2.77	
		3	1.018	-3.05	
0017	Mar '93	1	1.002	-2.88	0.518
		2	0.995	-2.81	
		3	0.992	-2.59	
0030	Feb '93	1	1.025	-1.20	0.817
		2	1.017	-0.88	
		3	0.996	-0.49	
0062	Jan '93	1	1.010	0.39	1.187
		2	1.020	0.02	
		3	1.010	0.03	
0110	Apr '93	1	1.008	-3.53	1.058
		2	1.018	-4.07	
		3	1.023	-3.94	
0111	Nov '92	1	1.059	-5.65	0.810
		2	1.070	-6.19	
		3	1.061	-5.82	
274B	Dec '92	1	0.993	0.81	0.526
		2	1.002	0.45	
		3	1.008	0.20	
0457	Apr '93	1	1.010	-7.10	1.754
		2	1.016	-7.43	
		3	1.021	-7.83	
0462	Oct'92	1	0.996	-3.87	1.602
		2	0.999	-4.08	
		3	1.002	-4.46	
0591	Oct'92	1	1.063	-4.84	0.334
		2	1.075	-5.24	
		3	1.081	-5.47	

values to arrive at a maximum difference between the three possible calibrations and then divided by the lesser value, thereby arriving at the greatest calculated resultant (note all are less than 2%). Pump numbers 0013, 0017, 0110 and 0457 were used during this study's sampling period.

Chapter 2: Methodology

Table 2.2 compares a past 1980 rotameter calibration effort with this study's 1993 effort. The 1980's and 1993's effort used the method of least square curve fitting on all the data points from the three separate runs to calculate Table 2.2's slopes and intercepts. This study used the 1993 values in order to calculate the volume of air sampled through the collected Bondville aerosol filters. A single slope and intercept was obtained by lumping all the data points from the three runs together before doing least squares analysis.

Table 2.2. Calibration comparison of 1980's effort versus this study's final effort (percent error calculated at 30 L/min @ stp).

pump number	past effort (1980's)		new effort (1993)		percent error (%)
	slope	intercept	slope	intercept	
0013	0.923	-1.663	1.008	-2.786	-5.24
0017	0.890	-2.95	0.996	-2.761	-12.47
0030	0.984	-2.993	1.012	-0.850	-10.16
0062	0.488	-0.495	1.013	0.146	-53.70
0110	0.818	-1.124	1.016	-3.846	-12.13
0111	0.818	-1.124	1.063	-5.884	-9.98
274A	1.02	-6.23	**	**	**
274B	0.865	-2.83	1.001	0.486	-24.24
0457	0.856	-4.962	1.015	-7.453	-9.96
0462	0.854	-3.21	0.999	-4.137	-13.24
0591	0.89	-2.046	1.073	-5.183	-8.73
0855	0.977	-3.833	**	**	**
**rotameter is missing, but not used during this study's sampling period					

The percent error column in Table 2.2 compares the true flow y values using an x valve of 30 L/min @ stp. The percent error is the 1980 effort's true flow value minus this study's true flow value divided by this study's true flow value, then multiplied by 100. This study's new effort is assumed to be the true value in this relative error approach. Note , that previous air volumes calculated using the 1980's effort calibrations underestimated air volumes from 5 to 54% when compared to this study's calibrations.

The 1980's calibration efforts did not develop precise reproducible calibration curves on the order of 1993's effort, despite several attempts by different Illinois State Water Survey personnel. This imprecisness was probably caused by the placement of a needle valve before the rotameter with the idea

that this best simulated the equipment configuration used at the Bondville field site. This placement caused the rotameter to see a pressure drop, as a function of restricted flow, of 25 cm to 38 cm of mercury. A pressure drop of this magnitude will cause inaccuracies when using the rotameter conversion formula, equation (2.4), (Wilson et al., 1983). This pressure drop was probably responsible for the 5 to 10% variability experienced during the previous individual calibration runs and from calibration attempt to attempt.

2.4.3 Related Calibration Efforts

Several issues arose as a result of the calibration effort. They included such concerns as the effects that might be introduced due to the calibrations being conducted after the study's actual sampling period and the changing conditions of the rotameters throughout the project.

2.4.3.1 Time Shifts and Calibration Method

One question of concern was, "Do rotameter calibrations change depending on when the calibration is performed?" Pump 0013's rotameter was disassembled and solvent cleaned using a hexane and ethanol mixture. The rotameter parts soaked for two days in this unmeasured mixture. They were then wiped cleaned using Kim™ wipes. In March 1993, the rotameter was cleaned, reassembled and calibrated using the rotameter's adjusting knob to vary the flow as described in section 2.4.2. Then after one month of storage (no use) the rotameter was recalibrated using the same method. The maximum percent error for the sets of three separate calibration runs were 0.650% for March and 0.337% for April. Figure 2.3 shows the best fit curves for these two calibration set runs. The best fit curves were calculated using the least squares equation fitting method on all three runs' data points. Then, the approximate rotameter flow values used during calibration were substituted into these best fit curves in order to generate the data points and curves. Clearly the two calibration curves are shifted with respect to each other so, there is a time shift when comparing the identical March and April calibration efforts. A substitution into March's calibration of 30 L/min stp becomes a true flow of 26.2408 L/min and April's is 26.7332 L/min. Over a typical 11 hour sampling period at Bondville the difference in air volume sampled would be 0.325 m³. This is 1.88% of the lower air volume sampled using March's calibration (17.32 m³). This was the only evaluation completed. Therefore, these results alone do not adequately quantify the magnitude of imprecision or bias due to time shifts.

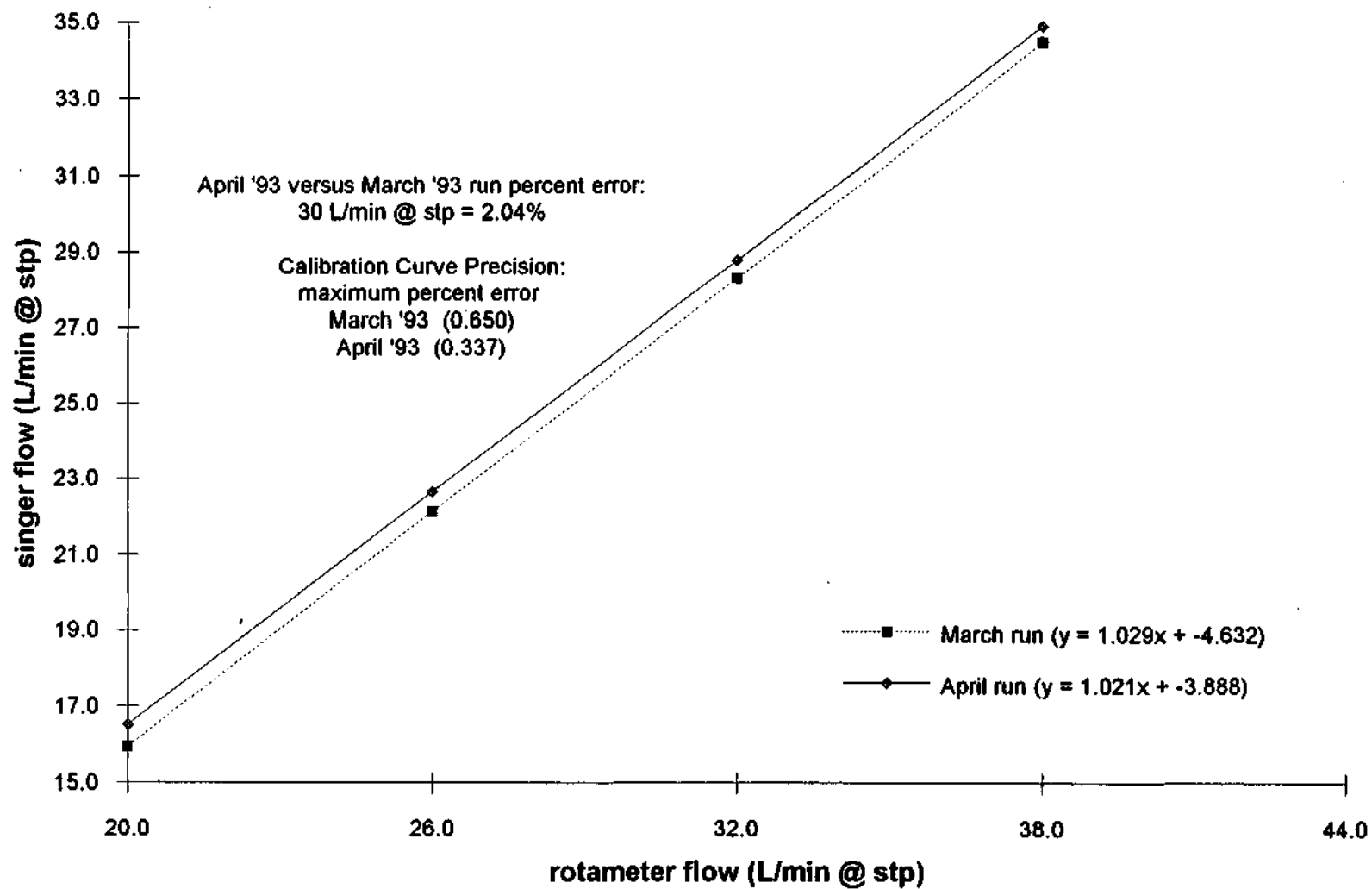


Figure 2.3. Reproducibility of solvent cleaned 0013 rotameter's calibration over time.

Chapter 2: Methodology

Table 2.3 compares this study's early calibration attempts using the needle valve and sealed rotameters with the latter attempts using the rotameter adjusting knob method. Presented is the date, slope, intercept and percent error calculated at 30 L/min for rotameters 0017, 0110 and 0457. The percent error column's values do not vary greatly when compared to 0013's discussed time shift calibration. It is interesting that 0457's percent error for difference in method plus a time shift is less than the percent error for 0013's time shift calibration.

Table 2.3. Comparison of calibration methods and reproducibility over time.

pump no.	needle-valve method (1992's past effort)			rotameter's adjust knob method (1993's recent effort)			percent error (%)
	date	slope	intercept	date	slope	intercept	
0017	Oct 1992	0.972	-0.823	Mar 1993	0.996	-2.761	4.40
0110	Oct 1992	1.023	-2.888	April 1993	1.016	-3.846	4.30
0457	Oct 1992	1.019	-7.165	April 1993	1.019	-7.165	1.72

2.4.3.2 Clean versus dirty rotameter calibrations

Another concern was, "does the rotameter's physical condition effect their calibration?". Filter samples for this study were collected over a five year period, using pumps 0013, 0017, 0110 and 0457. During this period, particles and gases collected on the rotameter's tapered tube and float. It was of interest to examine if these deposits would effect rotameter calibration.

To test the extreme effect deposits might have on calibrations, five rotameters were cleaned and recalibrated according to the previously described methods. Results of the recalibration of these rotameters appear in Table 2.4. The dates pertain to the calibration effort. The unclean versus clean maximum percent error are calculated as described in section 2.4.2. The maximum percent error is maximized by taking the difference of the two y value flows (both a clean and unclean states) at 30 L/min stp and dividing by the smaller flow.

These maximum percent error values are derived by finding the difference between the unclean rotameter flow rate and the clean rotameter flow rate and dividing this difference by the lower valued calibration curve. Note, the maximum percent errors are below 1%, with the exception of 0013's. This rotameter, as discussed, was cleaned before the 1993 efforts to redo the 1992 needle valve calibrations.

Chapter 2: Methodology

Therefore, this comparison is not only for unclean versus clean physical condition, but for calibration method as well. The solvent cleaned rotameters' maximum percent errors are of same magnitude compared to the unclean rotameters' maximum percent error values.

It was concluded that a clean versus dirty rotameter state did not significantly affect the calculation of air volumes, so current calibrations are satisfactory to calculate air volumes for this study. To illustrate this point, ignore pump 0013's outlier maximum percent error value for unclean versus clean, which is a product of calibration method and rotameter condition. Using the highest percent error under the value of one, we note for pump 0062, its stp air volume at 30 L/min would be for the unclean state 30.536 L/min and the clean, 30.774 Umin. The difference in air volume sampled would be 0.157 m³ over a typical Bondville 11 hour sampling period. This is only 0.78% of the lessor's (unclean state) air volume (20.15 m³).

Table 2.4. Comparison of unclean versus solvent clean rotameter calibrations.

pump no.	unclean rotameters				solvent cleaned rotameters				maximum percent error (%)
	date	slope	intercept	max % error	ate	slope	intercept	max % error	
0013	Dec 1992*	1.008	-2.786	0.292	Mar 1993	1.029	-4.632	0.650	4.680
0017	Mar 1993	0.996	-2.761	0.518	April 1993	0.994	-2.511	0.625	0.689
0062	Jan 1993	1.013	0.146	1.19	Feb 1993	1.021	0.144	0.946	0.701
0110	April 1993	1.016	-3.846	1.06	May 1993	0.995	-3.253	1.55	0.216
0457	April 1993	1.015	-7.453	1.75	April 1993	1.016	-7.529	0.656	0.318

*pump 0013's unclean calibration used the needle valve method

Also supporting the use of Table 2.1 1993's calibrations for this study's air volume calculations is that since the early 1970's, other projects used the Bondville pumps. Throughout this period, the rotameters were not solvent cleaned, so the assumed condition of the rotameters at Bondville throughout the project is a dirty state.

2.4.3.3 Calibration of Bondville Pump's Pressure Gauges

The final related calibration effort concerned the accuracy of the vacuum gauges supplied with the Gelman™ pump kits. Lab measurements compared the vacuum gauges with a 91 cm u-tube open end mercury manometer. An experiment schematic, the results and some calculations are shown on Table A.2 in Appendix A. A flow was vacuumed through a restricting needle valve to create a pressure drop. The flow continued through 81 cm of vacuum hose to a plastic tee that allowed the manometer to read the pressure drop. A short 5.3 cm hose connected the flow to the vacuum gauge inlet. The gauge's outlet had a 172 cm hose connecting it to the vacuum supply (Bondville pump number 0062).

Recorded were vacuum gauge and manometer readings for three rotameter flow rates common during Bondville sampling: 35, 40 and 45 L/min. Subtracted from the vacuum gauge readings was the added pressure drop caused by the plumbing of a half of the plastic tee and the 5.3 cm hose. A previous experiment established this pressure drop to be 0.33 cm of mercury.

Each flow rate had a percent error calculated. This percent error is the relative error between the manometer and vacuum gauge with the manometer considered the true value. The difference between the vacuum gauge reading and the manometer's reading is divided by the manometer's reading. This resultant is multiplied by 100. The mean percent errors of the three flow rates for the locatable and operational vacuum gauges are presented in Table 2.5.

Table 2.5. Calibration of the Gelman pumps' vacuum gauges using a manometer.

pump number	mean percent error (%)
0013	-0.857
0017	-0.659
0030	-2.695
0062	-5.552
0110	0.322
0111	-4.772
274A	pump missing
274B	vacuum gauge broken
0457	-4.578
0462	vacuum gauge broken
0591	-5.345
0855	pump missing

The negative values indicate the vacuum gauge under read the pressure drop relative to the manometer. A method to correct this gauge bias was constructed and implemented in the AIR.FOR program.

2.5 Calculating Ions' Ambient Air Concentrations

Data concerning the daily filter samples collected at Bondville and the laboratory analyses of those filters were entered in field positioned ASCII files. A FORTRAN program called AIR.FOR uses these files as input to generate output, e.g., calculated ions' ambient air concentrations, data quality screening and pump operating conditions. Several efforts modifying the AiR.FOR program resulted in improved performance.

2.5.1 Program Description

The "AIR.FOR" program was built using FORTRAN code originally written for the mainframe environment. Code modifications allow the program to compile on a personal computer using the software, Microsoft® PC FORTRAN. The program accepts a field specific ASCII input file containing Bondville aerosol filter data. These input files supply information on filters numbers, dates of samples, pump sampling conditions and laboratory established ion concentrations (mg/L), for one sampling year (June 1 to May 31) or less. Figure 2.4, the TEST.DAT" file, shows an example of 8 days worth of data collected in the fall of 1983. Line numbers list the input fields. Each filter is described by three lines of data. The first line of data is information recorded by the field technician except the calculated gray meter total volume (which is hand-calculated). The second line lists the fraction of pump running time, information about the filter extraction process and laboratory measured anion concentrations. The third line gives the laboratory measured cation concentrations.

"AIR.EXE", the compiled version of AIR.FOR, begins operation by prompting for an input file's name and opening that input file and two output files, one called "AERION" and the other, "AERCON". These files accept AIR.EXE's output. The code then reads in all the raw data from the user designated input file and stores it in arrays, one filter at a time. The program processes one filter at a time until it reaches the last filter entry in the input file.

The first step in this processing is the establishment of the "elapsed sampling time" which is the variable name assigned to the amount of time the filter is sampled. The code compares the technician's

Chapter 2: Methodology

TEST.DAT

```
BG37W270 T3988 0017 092783 1000 12.0 44.0 092883 1000 12.6 46.0 0032BAD 10.7 910.3 11.2 973.2 62.9
BG37W270 .50 1150 1.00 25.0 .84 2
BG37W270 .08 .010 .056 .019 3
BG37W271 T3989 0457 092883 1000 13.2 50.0 092983 1000 13.2 49.0 1037 11.6 369.5 11.8 133.0 763.5
BG37W271 .50 130 1.00 25.0 12.06 2
BG37W271 1.50 .225 .091 .153 3
BG37W272 T3991 0110 092983 1000 11.4 41.0 093083 1000 11.5 40.0 1040 10.2 24.2 10.4 978.4 954.2
BG37W272 .50 320 1.00 25.0 15.84 2
BG37W272 1.61 .289 .089 .160 3
BG37W273 T3992 0013 093083 1000 13.3 38.0 100183 1000 13.6 37.0 1033 11.7 603.4 11.9 658.8 1055.4
BG37W273 .50 1260 1.00 25.0 6.81 2
BG37W273 2.05 .409 .082 .212 3
BG37W274 T3993 0017 100183 1000 14.1 44.0 100283 1000 14.2 43.0 1040 12.9 973.2 12.9 109.4 1136.2
BG37W274 .50 210 1.00 25.0 13.32 2
BG37W274 1.47 .241 .085 .202 3
BG37W275 T3994 0457 100283 1000 13.1 49.0 100383 1000 13.3 48.0 1040 11.6 133.0 11.8 249.3 1116.3
BG37W275 .50 1270 1.00 25.0 10.36 2
BG37W275 .85 .158 .116 .238 3
BG37W276 T3995 0110 100383 1000 12.0 40.0 100483 1000 12.0 39.0 1038 10.8 978.4 10.6 973.9 995.5
BG37W276 .50 1440 1.00 25.0 9.37 2
BG37W276 1.00 .172 .165 .283 3
BG37W277 T3997 0013 100483 1030 13.9 38.0 100583 1000 14.0 46.0 1105BAD 12.4 658.8 12.5 754:6 1095.8
BG37W277 .50 1720 1.00 25.0 6.58 2
BG37W277 .83 .133 .067 .136 3
```

INPUT FIELDS ARE:

FIRST LINE

Field filter number, Lab filter number, Pump number, Date on, Time on, Pressure drop on (in. of Hg), Flow rate on (L/min), Date off, Time off, Pressure drop off (in. of Hg), Flow rate off (L/min), Elapsed sampling time (hours), Protocol filter screening symbol, Data line identification number (number one is missing), Grey meter pressure drop on (in. of Hg), Grey meter dial reading on (cu. ft.), Grey meter pressure drop off (in. of Hg), Grey meter dial reading off (cu. ft.), Grey meter air volume measurement (cu. ft.)

SECOND LINE

Field filter number, Pump running fraction, Net filter mass (ug), Filter analysis fraction, Lab's extraction volume (mL), S04 measurement (mg/L), Data line identification number (lab analysis sheet 2)

THIRD LINE

Field filter number, Ca measurement (mg/L), Hg measurement (mg/L), Na measurement (mg/L), K measurement (mg/L), Data line identification number (lab analysis sheet 3)

Figure 2.4. TEST.DAT example input file for the AIR.EXE program.

Chapter 2: Methodology

"reported" filter sampling time against the "calculated" sampling time. The reported time is derived from the sampling train's alarm clock that is connected to each timer. The clock ran whenever the timer supplied power to the pump for sampling, thus recording the actual run time. The calculated time is computed by AIR.FOR using the reported on/off dates and times. If the technician's reported time exceeds the calculated time, then the elapsed sampling time's output is flagged. In addition, if the technician did not report a sampling time, then the calculated time multiplied by the pump running fraction (0.5 since half hour on, half hour off during this study's period) becomes the elapsed sampling time.

Next, the on and off vacuum gauge readings are corrected using the results summarized in previous listed Table 2.5 in section 2.4.3.3. The readings are multiplied by the correction factor assigned to that filter's pump number. These products are added to the vacuum readings and the corrected on/off readings are stored. Vacuum gauge readings from pump kits whose gauge has no correction factor are not altered.

The month of sampling is read from the on filter date and the climatic mean monthly temperature is obtained from a data table. The on date is used because the sampling time begins at 10:00 a.m. More of the actual sampling time is on the first day than on the next day (7 hours versus 5). The calculation of the air volume uses this mean temperature. Section 2.5.2 discusses this further.

The program then calculates the air volume sampled. A modified version of equation 2.4, as shown below by equation (2.6), performs this calculation. It uses the average of the rotameters flows with each flow converted to stp.

$$V_{\text{air}} = \frac{3}{100} \times t_s \times \left[\left(m \times Q_{\text{on}} \sqrt{\frac{(P_a - \delta P_{\text{on}}) \times T_{\text{stp}}}{P_{\text{stp}} \times T_a} + b} \right) + \left(m \times Q_{\text{off}} \sqrt{\frac{(P_a - \delta P_{\text{off}}) \times T_{\text{stp}}}{P_{\text{stp}} \times T_a} + b} \right) \right] \quad (2.6)$$

where v_{air} is the air volume sampled, the fraction $\frac{3}{100}$ is a unit conversion constant multiplied by $\frac{1}{2}$ to get the average flow, t_s is the elapsed sampling time, m is the slope of the rotameter's calibration curve and b is its intercept. The rotameter flow at the beginning and end of the filter sampling cycle is Q_{on} and Q_{off} , respectively. P_a is the ambient pressure and δP_{on} and δP_{off} are the vacuum gauge corrected pressure drops at the beginning and end of the filter sampling cycle, respectively. T_a is the monthly mean ambient air temperature, T_{stp} is the standard temperature and P_{stp} is the standard pressure. The units of measurements used are for sampling time (hours), rotameter's slope and intercept (L/min stp), rotameter flows (L/min), all pressures and pressure drops (inches of mercury) and

Chapter 2: Methodology

temperatures (Kelvin). This combined with the unit conversion constant gives cubic meters for the air volume sampled.

Referencing Figure 2.4, we use the filter sampled on 09/28/83, field number BG37W271, to present an example calculation. The elapsed sampling time (t_s) converted to hours is 10.61667. Referring to Table 2.2 (section 2.4.2), the 1993 new effort calibration equation for pump 0457 is $y = 1.015x + -7.453$, where the slope (m) is 1.015 and the y intercept (b) is -7.453 L/min stp. The rotameter flow on (Q_{on}) is 50 L/min and the flow off (Q_{off}) is 49 L/min. The ambient pressure (P_a), discussed in section 2.5.2, for Bondville is assumed constant at 29.18 inches of Hg. On (δP_{on}) and off (δP_{off}) vacuum gauge readings are 13.2 inches of mercury. Both gauge readings require correction. This procedure uses Table 2.5 for pump number 0457. The program multiplies 13.2 by the correction factor (0.04578). These products are added to 13.2 attaining corrected readings of 13.804.

Sampling occurs in the ninth month so referencing Table 2.6, the monthly mean ambient air temperature (T_a) is 310.43 Kelvin. The standard pressure (P_{stp}) used is 29.92 inches of mercury. The standard temperature (T_{stp}) used is 298.15 Kelvin. We now have:

$$V_{air} = \frac{3}{100} \times 10.617 \times \left[\left(1.015 \times 50 \sqrt{\frac{(29.18 - 13.8)}{29.92} \times \frac{298.15}{310.43}} + (-7.453) \right) + \left(1.015 \times 49 \sqrt{\frac{(29.18 - 13.8)}{29.92} \times \frac{298.15}{310.43}} + (-7.453) \right) \right] \quad (2.6a)$$

which calculates the air volume sampled (v_{air}) as 17.74 m³ at stp.

Next, the individual ions' ambient air concentrations are calculated. From Figure 2.4, we note that the laboratory raw data in lines 2 and 3 are in mg/L. The ion concentrations are adjusted for contamination by the subtraction of blank values. The blank values are ion specific. Section 2.5.2.3 discusses the establishment of these blank values.

Modules constructed within the code performed the computation of each ion's ambient air concentration and the propagation of error of that calculated concentration. This propagation of error is due to the variance associated with each measurement step used to attain this concentration. The program is capable of establishing ambient air concentrations for a total of eight ions. This study period contains credible data for only five ions, calcium, magnesium, potassium, sodium and sulfate.

Arrays containing raw and calculated information are then down loaded to the two output files, AERCON (Figure 2.5) and AERION (Figure 2.6). Figure 2.5 is an abbreviated example of an AERCON output file. These results are generated by inputting the TEST.DAT file (Figure 2.4) into AIR.EXE. The first set of rows is a listing of some of the field data recorded by the technicians. The second set is the sampling time, calculated total suspended particulate measurement and some calculated ions' ambient

Chapter 2: Methodology

TEST.DAT		AERCON OUTPUT FILE														
LAB FILTER NUMBER	FIELD FILTER NUMBER	PUMP NO	DATE ON	TIME ON	PRESS DROP (in)	ON FLOW (L/m)	GRY ON (in)	GRY ON VOL (ft3)	DATE OFF	TIME OFF	PRESS DROP (in)	OFF FLOW (L/m)	GR OFF (in)	GRY OFF VOL (ft3)	GRY VOL TOTAL (ft3)	FLAG
T3988	8G37W270	0017	092783	1000	12.0	44.0	10.7	910.3	092883	1000	12.6	46.0	11.2	973.2	62.9	BAD
T3989	BG37W271	0457	092883	1000	13.2	50.0	11.6	369.5	092983	1000	13.2	49.0	11.8	133.0	763.5	
T3991	BG37W272	0110	092983	1000	11.4	41.0	10.2	24.2	093083	1000	11.5	40.0	10.4	978.4	954.2	
T3992	BG37W273	0013	093083	1000	13.3	38.0	11.7	603.4	100183	1000	13.6	37.0	11.9	658.8	1055.4	
T3993	BG37W274	0017	100183	1000	14.1	44.0	12.9	973.2	100283	1000	14.2	43.0	12.9	109.4	1136.2	
T3994	BG37W275	0457	100283	1000	13.1	49.0	11.6	133.0	100383	1000	13.3	48.0	11.8	249.3	1116.3	
T3995	BG37W276	0110	100383	1000	12.0	40.0	10.8	978.4	100483	1000	12.0	39.0	10.6	973.9	995.5	
T3997	BG37W277	0013	100483	1030	13.9	38.0	12.4	658.8	100583	1000	14.0	46.0	12.5	754.6	1095.8	BAD

FIELD FILTER NUMBER	SAMPLE TIME (hr)	TSP (ug/m3)	AIR CONC SO4 (ug/m3)	% ERROR SO4	AIR CONC Ca (ug/m3)	% ERROR Ca	AIR CONC NH4 (ug/m3)	% ERROR NH4	AIR CONC NO3 (ug/m3)	% ERROR NO3
BG37W270	.5333	*****	19.179	16.8	1.503	39.0	-9.999	-9.999		
BG37W271	10.6167	7.33	16.858	5.2	2.083	5.2	-9.999	-9.999		
BG37W272	10.6667	18.36	22.580	5.1	2.278	5.2	-9.999	-9.999		
BG37W273	10.5500	83.02	11.053	5.4	3.340	5.1	-9.999	-9.999		
BG37W274	10.6667	11.89	18.710	5.1	2.049	5.2	-9.999	-9.999		
BG37W275	10.6667	72.04	14.549	5.2	1.174	5.5	-9.999	-9.999		
BG37W276	10.6333	85.66	13.786	5.2	1.454	5.4	-9.999	-9.999		
BG37W277	11.0833	95.63	9.007	5.4	1.123	5.5	-9.999	-9.999		

FIELD FILTER NUMBER	AIR VOLUME (m3)	TSP (ug/m3)	AIR CONC Mg (ug/m3)	% ERROR Mg	AIR CONC Na (ug/m3)	% ERROR Na	AIR CONC K (ug/m3)	% ERROR K	AIR CONC Zn (ug/m3)	% ERROR Zn
SG37W270	.9646	*****	.181	91.5	.881	49.9	.337	48.3	-9.999	
BG37W271	17.7367	7.33	.313	5.4	.097	26.7	.207	11.0	-9.999	
BG37W272	17.4268	18.36	.410	5.3	.096	27.3	.221	10.9	-9.999	
BG37W273	15.1775	83.02	.669	5.2	.099	30.0	.339	10.6	-9.999	
BG37W274	17.6639	11.89	.337	5.4	.089	28.8	.277	10.6	-9.999	
BG37W275	17.6299	72.04	.220	5.7	.133	21.0	.329	10.5	-9.999	
BG37W276	16.8100	85.66	.251	5.6	.213	16.1	.412	10.4	-9.999	
BG37W277	17.9868	95.63	.181	6.0	.063	38.6	.181	11.2	-9.999	

FIELD FILTER NUMBER	SO4 ION	SO4 BLK	SO4 VOL	Ca ION	Ca BLK	Ca VOL	Mg ION	Mg BLK	Mg VOL	Na ION	Na BLK	Na VOL	K ION	K BLK	K VOL
BG37W270	.114	.885	.001	.499	.499	.000	.609	.390	.000	.109	.890	.000	.366	.633	.000
BG37W271	.953	.035	.010	.946	.043	.010	.879	.111	.009	.244	.755	.000	.901	.096	.002
BG37W272	.968	.021	.010	.952	.037	.010	.919	.070	.010	.236	.763	.000	.908	.088	.002
BG37W273	.885	.104	.009	.966	.023	.010	.953	.036	.010	.208	.791	.000	.945	.052	.002
BG37W274	.959	.029	.010	.945	.044	.010	.892	.098	.009	.220	.779	.000	.940	.057	.002
BG37W275	.941	.048	.010	.867	.123	.009	.789	.202	.008	.344	.655	.000	.955	.042	.002
BG37W276	.931	.058	.010	.898	.092	.009	.815	.176	.008	.514	.484	.001	.967	.030	.002
BG37W277	.879	.111	.009	.862	.128	.009	.728	.263	.007	.149	.850	.000	.879	.118	.002

FIELD FILTER NUMBER	Zn ION	Zn BLK	Zn VOL	NO3 ION	NO3 BLK	NO3 VOL	NH4 ION	NH4 BLK	NH4 VOL
BG37W270	MMM	MMM	MMM	MMM	MMM	MMM	MMM	MMM	MMM
BG37W271	MMM	MMM	MMM	MMM	MMM	MMM	MMM	MMM	MMM
BG37W272	MMM	MMM	MMM	MMM	MMM	MMM	MMM	MMM	MMM
BG37W273	MMM	MMM	MMM	MMM	MMM	MMM	MMM	MMM	MMM
BG37W274	MMM	MMM	MMM	MMM	MMM	MMM	MMM	MMM	MMM
BG37W275	MMM	MMM	MMM	MMM	MMM	MMM	MMM	MMM	MMM
BG37W276	MMM	MMM	MMM	MMM	MMM	MMM	MMM	MMM	MMM
BG37W277	MMM	MMM	MMM	MMM	MMM	MMM	MMM	MMM	MMM

Figure 2.5. AERCON example output file for the AIR.EXE program.

Chapter 2: Methodology

```

TEST.DAT          AERION OUTPUT FILE

FIELD FILTER;    TSP;  AIR CONC;  % ERROR; AIR CONC;  X ERROR; AIR CONC;  X ERROR; AIR CONC;  X ERROR;
NUMBER;         (ug/m3);   SO4;    SO4;    Ca;    Ca;    NH4;    NH4;    NO3;    NO3;

BG37W270;      *****;  19.179 ;  16.8;  1.503 ;  39.0;  -9.999 ;  ;  -9.999 ;  ;
BG37W271;      7.33;  16.858 ;  5.2;  2.083 ;  5.2;  -9.999 ;  ;  -9.999 ;  ;
BG37W272;      18.36;  22.580 ;  5.1;  2.278 ;  5.2;  -9.999 ;  ;  -9.999 ;  ;
BG37W273;      83.02;  11.053 ;  5.4;  3.340 ;  5.1;  -9.999 ;  ;  -9.999 ;  ;
BG37W274;      11.89;  18.710 ;  5.1;  2.049 ;  5.2;  -9.999 ;  ;  -9.999 ;  ;
BG37W275;      72.04;  14.549 ;  5.2;  1.174 ;  5.5;  -9.999 ;  ;  -9.999 ;  ;
BG37W276;      85.66;  13.786 ;  5.2;  1.454 ;  5.4;  -9.999 ;  ;  -9.999 ;  ;
BG37W277;      95.63;  9.007 ;  5.4;  1.123 ;  5.5;  -9.999 ;  ;  -9.999 ;  ;

DATE;  AIR;  SAMPLE; PUMP; FLAG; AIR CONC; X ERROR; AIR CONC; X ERROR; AIR CONC; X ERROR; AIR CONC; X ERROR;
ON;  VOLUME;  TIME;  NO;  SYM;  Mg;  Mg;  Na;  Na;  K;  K;  Zn;  Zn;

92783;  .9646;  .5333 ; 0017;  BAD;  .181 ;  91.5;  .881 ;  49.9;  .337 ;  48.3;  -9.999
92883;  17.7367;  10.6167 ; 0457;  ;  .313 ;  5.4;  .097 ;  26.7;  .207 ;  11.0;  -9.999
92983;  17.4268;  10.6667 ; 0110;  ;  .410 ;  5.3;  .096 ;  27.3;  .221 ;  10.9;  -9.999
93083;  15.1775;  10.5500 ; 0013;  ;  .669 ;  5.2;  .099 ;  30.0;  .339 ;  10.6;  -9.999
100183;  17.6639;  10.6667 ; 0017;  ;  .337 ;  5.4;  .089 ;  28.8;  .277 ;  10.6;  -9.999
100283;  17.6299;  10.6667 ; 0457;  ;  .220 ;  5.7;  .133 ;  21.0;  .329 ;  10.5;  -9.999
100383;  16.8100;  10.6333 ; 0110;  ;  .251 ;  5.6;  .213 ;  16.1;  .412 ;  10.4;  -9.999
100483;  17.9868;  11.0833 ; 0013;  BAD;  .181 ;  6.0;  .063 ;  38.6;  .181 ;  11.2;  -9.999

SO4 ERROR DUE TO;;; Ca ERROR DUE TO;;; Mg ERROR DUE TO;;; Na ERROR DUE TO;;; K ERROR-DUE TO;;;
ION;  BLK;  VOL;  ION;  BLK;  VOL;  ION;  BLK;  VOL;  ION;  BLK;  VOL;  ION;  BLK;  VOL;

.114; .885; .001; .499; .499; .000; .609; .390; .000; .109; .890; .000; .366; .633; .000;
.953; .035; .010; .946; .043; .010; .879; .111; .009; .244; .755; .000; .901; .096; .002;
.968; .021; .010; .952; .037; .010; .919; .070; .010; .236; .763; .000; .908; .088; .002;
.885; .104; .009; .966; .023; .010; .953; .036; .010; .208; .791; .000; .945; .052; .002;
.959; .029; .010; .945; .044; .010; .892; .098; .009; .220; .779; .000; .940; .057; .002;
.941; .048; .010; .867; .123; .009; .789; .202; .008; .344; .655; .000; .955; .042; .002;
.931; .058; .010; .898; .092; .009; .815; .176; .008; .514; .484; .001; .967; .030; .002;
.879; .111; .009; .862; .128; .009; .728; .263; .007; .149; .850; .000; .879; .118; .002;

Zn ERROR DUE TO;;; NO3 ERROR DUE TO;;; NH4 ERROR DUE TO
ION;  BLK;  VOL;  ION;  BLK;  VOL;  ION;  BLK;  VOL;

MMM;  MMM;  MMM;  MMM;  MMM;  MMM;  MMM;  MMM;  MMM;
MMM;  MMM;  MMM;  MMM;  MMM;  MMM;  MMM;  MMM;  MMM;
MMM;  MMM;  MMM;  MMM;  MMM;  MMM;  MMM;  MMM;  MMM;
MMM;  MMM;  MMM;  MMM;  MMM;  MMM;  MMM;  MMM;  MMM;
MMM;  MMM;  MMM;  MMM;  MMM;  MMM;  MMM;  MMM;  MMM;
MMM;  MMM;  MMM;  MMM;  MMM;  MMM;  MMM;  MMM;  MMM;
MMM;  MMM;  MMM;  MMM;  MMM;  MMM;  MMM;  MMM;  MMM;
MMM;  MMM;  MMM;  MMM;  MMM;  MMM;  MMM;  MMM;  MMM;

```

Figure 2.6. AERION example output file for the AIR.EXE program.

air concentrations and their percent error evaluations. The third set of rows is the rest of the ions' ambient air concentrations and their percent error evaluations. The fourth and fifth sets quantify the fraction of percent error awarded to each measurement step taken to calculate the ion's ambient air concentration. These fractions are due to the laboratory measured extract solution's ionic concentration, blank value and air volume sampled measurements. Section 2.5.3 explains these fractions in detail.

Figure 2.6 is the AERION output file. It is a reiteration of most of AERCON's output. The difference is AERION's output is semi-colon delimited, making this output capable of being inputted into a spreadsheet program. This file allows the movement of AIR.EXE's output into the EXCEL environment.

2.5.2 Program Modifications

As part of this study the AIR.FOR program was modified in several ways. The motivation for these efforts was to improve the results generated from the raw data. Following is a discussion of these undertakings.

2.5.2.1 Determination of Ambient Air Pressure

The calculation of the air volume sampled through the Bondville filters required a determination of an ambient air pressure at Bondville. During each filter's 24 hour sampling period the ambient pressure would vary. Therefore, the taken approach used the elevation of the Bondville site to determine a constant ambient pressure specific to the Bondville site. Haltiner and Martin, 1957, presents an equation for calculating the ambient pressure based on elevation. It is:

$$z = 44,308 \left[1 - \frac{p^{0.19023}}{1013.25} \right] \quad z \leq 10,769 \text{ meters} \tag{2.7}$$

where z is the height in meters and p is the pressure in millibars. Bondville is 212 meters above sea level (Dossett, 1987). Substituting this for z and taking the anti-log, the site pressure (p) is 590.12 millibars. Conversion gives us 29.18 inches of mercury. Temporal variability in ambient pressure was not considered

2.5.2.2 Determination of Rotameter Air Temperature

Calculation of the air volume sampled also requires the determination of ambient site temperature. For this requirement we turned to the State Water Survey's compiled statistics for temperatures in the Champaign-Urbana area. Bryan and Wendland, 1993, lists the mean monthly values in the Urbana area for the 1961 to 1990 period.

The application of these mean monthly temperatures required experiments to determine if the air temperature experienced by the rotameters during sampling differed from the ambient air temperature. Bondville operating conditions were simulated while thermocouples measured the air temperature along the sampling path. These conditions were operation of the pump kit with their metal lids on and run cycles a half hour on then a half hour off, over a twenty-four hour period.

The first set of experiments demonstrated that the temperature rise experienced at the rotameter was independent of flow rate. Flow rates from 20 to 40 L/min experienced the same rise in temperature--as time passed. Therefore, the varying flow rates recorded for the collected filters was not a parameter needing consideration.

Additional experiments demonstrated the effect of different ambient temperatures on rotameter temperature. The first one simulated the hottest temperatures experienced in the Bondville underground room, which occurs in July. The second simulated the coldest month temperatures, which occurs in January.

Both experiments indicated that a large rise in temperature occurred after the first 60 minute run cycle. Additional cycles (half-hour on, half-hour off) duplicated this rise in temperature at the end of their cycles.

The ambient air temperatures (for the experiments they were 45 °F and 75 °F) influenced the rotameter temperatures at the beginning of the second on sampling cycle. The rotameter was approximately 10.7 °C or 14.0 °C higher than the ambient air temperatures of 45 °F and 75 °F, respectively. During the on cycle of thirty minutes the temperature rose an average of 9.8 °C or 10.8 °C for the ambient air temperatures of 45 °F and 75 °F, respectively. This average rise in temperature was spread out over the half an hour on period, so it was deemed that half of this increase would adequately represent this actual increase in temperature experienced while the pump was running. This was accomplished by assuming a linear rate of rise in combination with the lack of attaining the actual half-

value increase during the first 15 minutes of run and exceeding this half-value increase during the last 15 minutes running.

Adding the half-value increase and the beginning higher than ambient air temperature, we see that for January the rotameter ran at 15.6 °C higher than ambient air and for July it ran at 19.4 °C, e.g., for January: 10.7 °C plus 4.9 (½ of 9.8) °C equals 15.6 °C. This difference of 3.82 °C (19.4-15.6) was assumed to be changing in a linear fashion over the monthly periods, so the mean monthly averages were adjusted up by some fraction of 3.82 plus the increase in temperature due to the last sampling run cycle. Illustration of this adjustment appears below for the month of April:

$$T_r = T_m + 15.56 + 3.82(n/6) \tag{2.8}$$

where T_r is the temperature at the rotameter in Kelvin (301.68 K), T_m is the mean monthly temperature supplied by Bryan and Wendland, 1993, in Kelvin (April's value is 284.21 K), 15.56 °C is the calculated half-value increase plus the beginning of the second cycle higher than ambient air temperature increase for January and 3.82 °C is the difference between the January and July rises. Multiply the 3.82 °C by a fraction of the number of months away from January (n , for April $n = 3$) provides the difference in rise. For the months July and on, n is the number of months away from January counting backwards (n , for August $n = 5$).

AIR.FOR uses these adjusted monthly mean temperatures to calculate the air volume sampled through the Bondville filters. The month of the on date determines the temperature used in this calculation.

2.5.2.3 Miscellaneous Program Modifications

Section 2.4.2 discusses the recent effort to calibrate the Bondville sampling site rotameters. Table 2.2 lists both the past and new calibration best fit slope and intercept equations. The AIR.FOR program uses Table 2.2's new effort (1993) calibration curves to calculate the air volume sampled through the filters.

Section 2.3.3 discusses the calibration of the Bondville pump kits' vacuum gauges. Comparison against a manometer quantified the gauges' bias when reading a pressure load. Table 2.5 lists the correction factors used in the AIR.FOR program.

Chapter 2: Methodology

One unique feature of this data set is the quantification of the propagation of error introduced by each measurement step taken in order to calculate the ions' ambient air concentrations. Each filter uses three measurement steps to determine the ion's ambient air concentration. The three steps are the laboratory measured extract solution's ionic concentration, air volume sampled and outside hung field blank values. Section 2.5.3 discusses this propagation of error analysis and data quality screening feature in detail.

The standard deviations used in this error analysis required quantification specific to this study's sampling period. Section 2.5.3 also discusses the establishment of these new standard deviation values.

Concluding the efforts in program modification was the statistical analysis for this study period's "outside hung field blank" values. Section 2.5.3.2's Table 2.7 lists the central tendency statistics for these blanks. A comparison of the outside hung blanks with all the collected blanks listed in Table A.1 in Appendix A noted, that for this study's period the outside hung field blanks have some of the highest mean values. The program uses these values to correct the laboratory measured ionic concentrations as discussed in section 2.5.1.

2.5.3 Filter Data Screening

Data screening procedures eliminated non-representative ambient air concentration values from the data set before Chapter 3's analysis. Review of technician recorded field data identified filters not meeting established criteria. This procedure is termed sample protocol (SP) screening. An additional screening effort quantified the error introduced by the various measurement steps taken to calculate the ion ambient air concentrations at Bondville. This is termed data quality (DQ) screening.

2.5.3.1 Sample Protocol Screening

The first step in screening the data involves a review of the gas flow rates and vacuum gauge readings recorded by the field technician on the Bondville field data log sheets. This approach is termed sample protocol (SP) screening. Descriptive flags are used to identify filters that have undesirable data that did not pass the SP screening.

Flow on rotameter readings (indicated flows after the installation of a new filter holder and filter) and flow off rotameter readings (flows after the sampling cycle was completed) were recorded after a two

minute pump warm up period. The flow on and off values were compared to ascertain if the calculations performed with these values would result in credible air volumes. If the flow off was greater than or equal to 50% and less than 75% of the flow on, then flagging the filter "QUE" indicated questionable flow rates. "QUE" is also used to indicate a flow off greater than 110% but less than or equal to 120% of a flow on. A "BAD" flag indicated the flow off was less than 50% or greater than 120% of the flow on.

The pump kit's vacuum gauge quantified the pressure drop seen by the rotameter. This SP screening used the "QUE" and "BAD" labels to indicate abnormal pressure drop differences. The "QUE" label indicated if the pressure drop on (the drop noted at the beginning of the sampling cycle: clean filter) was greater than 110% and less than or equal to 120% or if it was between 50% and 75% of the pressure drop off (the drop noted at the end of the sampling cycle: sampled filter). The "BAD" label indicated if the pressure drop on was greater than 120% or less than 50% of the pressure drop off.

Another SP screening involved looking at the ratio of the total filter sampling time over the normal sampling time. This screening used the "QUE" label to indicate filters that were 60% to less than 80% or greater than 120% to 140% of the normal sampling time. "BAD" filters were those whose ratios were less than 60% or greater than 140%. "QUE" also indicated if the filter had a time gap of greater than 2 hours during sampling. The "POU" label was used if this gap was traceable to a power outage.

Multiple flagged samples received the worst case flag. All data analyses in Chapter 3 did not include any flagged daily filter samples. The SP screening on this study's data set eliminated 84 flagged filters out of a total 1733 collected filters (Staggs, 1982).

2.5.3.2 Data Quality Screening

An additional screening method termed data quality (DQ) was also used to ensure representative data. This method quantifies the error introduced by the various measurement steps taken in order to calculate the ambient air concentrations at Bondville. The method originates from subject matter addressing probability distributions for continuous variates and is known as a propagation of error analysis.

Chapter 2: Methodology

The calculated ambient air concentrations' total variance is a function of the individual measurements' estimated standard deviations. AIR.FOR uses equation (2.9) to calculate the ions ambient air concentrations:

$$\text{ion's conc}_{\text{amb air}} = \frac{(\text{ion} - \text{blank})(\text{ext vol})}{\text{air volume}} = X(\text{ion, blank, air volume}) \quad (2.9)$$

where $\text{ion's conc}_{\text{amb air}}$ (the ion ambient air concentration calculated at the Bondville site ($\mu\text{g}/\text{m}^3$)) depends on ion (laboratory measurement of the extract solution's ionic concentration (mg/L)), blank (outside hung field blank value (mg/L)), ext vol (extraction volume (mL)), air volume (volume of air at stp sampled through the filter (m^3)) and X (a function of the three independent variables) (section 2.2). Note, the extraction volume variance was assumed to be so small that for this error analysis, the extraction volume is considered a constant instead of a variable with measurement error.

Each independently measured variable on the right hand side of equation (2.9) has a variance associated with its measurement. Of interest for this study is total variance for the ion ambient air concentration. Bajpai et al., 1978, indicates that the total variance for a quantity which is a function of three independent variables is:

$$\sigma^2 = \left(\frac{\delta X}{\delta X_1} \right)^2 \sigma_1^2 + \left(\frac{\delta X}{\delta X_2} \right)^2 \sigma_2^2 + \left(\frac{\delta X}{\delta X_3} \right)^2 \sigma_3^2 \quad (2.10)$$

where σ is a variance and X is the function of the independent variables X_1 , X_2 and X_3 . Now taking the partial derivatives for $X(\text{ion, blank, air volume})$ and substituting in the volume of the extract solution that was used to extract the sampled particles from the filter (25 mL), we get:

$$\sigma_{\text{ion's conc}_{\text{amb air}}}^2 = \left(\frac{25}{V_{\text{air}}} \right)^2 \sigma_{\text{ion}}^2 + \left(\frac{-25}{V_{\text{air}}} \right)^2 \sigma_{\text{blank}}^2 + \left(\frac{-25 C_{\text{ion}}}{V_{\text{air}}^2} + \frac{25 C_{\text{blank}}}{V_{\text{air}}^2} \right)^2 \sigma_{\text{air}}^2 \quad (2.11)$$

where $\sigma_{\text{ion's conc}_{\text{amb air}}}^2$ (the ion's ambient air concentration's calculated variance) depends on V_{air} (the volume of air sampled (m^3)), σ_{ion}^2 (variance of the laboratory measurement of the extract solution's ionic concentration (mg/L)), σ_{blank}^2 (variance of the outside hung field blank value (mg/L)), σ_{air}^2 (variance of the volume of air at stp sampled through the filter (m^3)), C_{ion} (the laboratory's measurement of the extract solution's ion concentration (mg/L)) and C_{blank} (outside hung field blank value (mg/L)). The square root of this calculated variance is the ion's ambient air concentration's estimated standard deviation.

The next step involved dividing this standard deviation by the ion's ambient air concentration. Multiplying the resultant by 100 awards each ambient air concentration a value for the error due to

measurements. This data quality screening value is termed the percent error. Figure 2.5, the AERCON printout, provides some examples of percent error values. The FORTRAN program AIR.FOR performed all of these calculations (section 2.5.1).

It should be noted that this rigorous approach to quantifying error for individual ion ambient air concentrations for each filter is exemplary. Typical aerosol studies use the approach of flagging filters having questionable sampling protocol. The Bondville effort not only uses SP flags but assigns data quality flags using the discussed percent error value. This allows the data set to quantify the precision of the calculated ion ambient air concentrations. Furthermore, the DQ screening method used could have been a simple qualitative approach using DQ flags, i.e., low, medium or high, to classify ions' ambient air concentrations. Instead the more precise propagation of error analysis was used to quantify the percent error DQ flag.

Equation (2.11)'s three standard deviations were quantified for this study's period. Established were values for the laboratory measurement of the extract solution's ionic concentration, outside hung field blanks and air volume sampled through the filter. A discussion of these three follows along with the evaluation of the DQ screening tool, the percent error.

(1) Laboratory Measurement of the Extract Solution's Ionic Concentration

Stensland concluded that the standard deviations of the laboratory measurement of the extract solution's ionic concentrations are a function of the analytical instrument's detection limit. A desirable way to quantify these standard deviations would have been to perform split sampling. This method involves calculating the standard deviation for repeat measurements of the same sample. However, split sample data collection was not performed. Therefore, good scientific practice was used to quantify these standard deviations (Stensland, 1993).

Table 2.6 outlines Stensland's approach quantifying the variance of the laboratory measured extract solution's ionic concentration used in AIR.FOR. The program chooses for each filter, ion specific multipliers based on that filter's extract solution's ionic concentrations. The chose of these multipliers is done by comparing the extract solution's ionic concentrations to "detection limit (DL) cutoff point" ranges of less than five times the DL, from five times the DL to ten times the DL and greater than ten times the DL. These multipliers times the extract solution's ionic concentration quantify the estimated standard deviation for each particular extract solution's ionic concentration measurement. Note, the multipliers increase in value as the ionic concentrations approached the instrument's detection limit. This is due to the measured value's validity becoming increasingly imprecise when concentrations are low.

Table 2.6. Summary of parameters used to established ion estimated standard deviations in the AIR.FOR program.

ion	typical detection limit (DL) (mg/L)	multipliers used based on the inputted filter's extract solution's ionic concentrations (mg/L)			
		ion _{conc} < 5 DL	5DL	ion _{conc} 10 DL	ion _{conc} > 10 DL
Ca	0.009	0.5		0.2	0.05
Mg	0.003	0.5		0.2	0.05
K	0.003	0.5		0.2	0.1
Na	0.003	0.5		0.2	0.1
SO ₄	0.03	0.5		0.2	0.05

(2) Outside Hung Field Blank Measurements

Table 2.7 lists the program's standard deviations for the outside hung field blanks collected during this study's period, June 1983 to May 1988. The final statistics reported are a product of an iteration method that served to eliminate outlier influence. This method was performed twice. First calculated were statistics for all the reported outside hung field blank concentrations. An outlier in this data set was any value greater than or equal to the mean plus three times the standard deviation. The outlier values were deleted from the data set before the calculation of the second set of statistics. Calculation of this second set's outlier value used the new mean plus three times the new standard deviation. Again, any value greater than or equal to the new outlier value was eliminated. New statistics - were generated and reported in Table 2.7 for this twice iterated data set.

Table 2.7. Descriptive statistics for twice iterated* outside hung field filter blank values (mg/L) for the June 1983 to May 1988 period.

	Ca	Mg	K	Na	SO ₄
median	0.020	0.0015	0.005	0.018	0.05
mean	0.022	0.0033	0.0063	0.0217	0.1002
standard deviation	0.016	0.0042	0.0047	0.0155	0.1174
minimum	0.005	0.001	0.0015	0.0015	0.01
maximum	0.08	0.045	0.029	0.091	0.52
count	237	240	237	242	241
* Two iterations were used to eliminate outlying values (values greater than the ion group's mean plus three times the standard deviation).					

(3) Air Volume Measurements

The process to evaluate standard deviations for the air volumes sampled required a typical air volume sampled through the filter. A year's worth of data (June 1986 to June 1987) consisting of 702 readings was used to establish medians and mean for the on/off pressure drops and rotameter flow values. These values were used to describe a typical pump flow and pressure drop condition experienced at Bondville. This description is a median flow rate of 40 L/min (mean of 40.87 L/min) and a median pressure drop of 14.1 inches of Hg (mean of 14.18 inches of Hg). Using the above median values and an average (pump lid on) mean temperature (section 2.5.2.2), the rotameter equation (section 2.4.2) produced a typical rotameter flow of 27.306 L/min (stp). This flow was substituted into the three separate calibration runs listed in Table 2.1 for the four pumps operated during this study. Each calibration equation generated a flow valve, so three possible flow values were calculated for each pump.

Table 2.8 lists the means and standard deviations of the flows obtained using the four pump calibration equations along with the mean of the mean flow rates and mean of the standard deviations. The ratio of the mean standard deviations divided by the mean of the mean flow rates is 0.00527. Each filter's calculated air volume sampled was multiplied by 0.00527 to evaluate the standard deviation of that filter's air volume sampled (Stensland, 1993).

Table 2.8. Descriptive statistics used to determine the air volume's standard deviation multiplier.

pump number	mean flow rate (L/min @ stp)	mean flow rate's standard deviation
0013	24.746	0.0467
0017	24.445	0.0752
0110	23.905	0.154
0457	20.280	0.217
mean of the mean flow rates = 23.344 L/min @ stp		
mean of the standard deviations = 0.123 L/min @ stp		

(4) The Percent Error

As discussed before, the square root of equation (2.11) which contains the three measurements' standard deviations was then divided by the ion ambient air concentration. This resultant multiplied by

Chapter 2: Methodology

100 gave the percent error term for each ion ambient air concentration.. Figure 2.5 presents examples of quantified percent errors.

The percent error criterion chosen to screen the ion ambient air concentration values was fifty percent. Ion ambient air concentrations with percent errors greater than 50% were considered to be too imprecise and therefore, questionable. All questionable values were discarded prior to this study's data analysis. Table 2.9 presents the central tendency statistics on the 1,749 daily filter samples screened using the 50% error value.

Table 2.9. Descriptive statistics for June 1983 to May 1988 filter samples whose error is less than or equal to 50% (ion concentration units are $\mu\text{g}/\text{m}^3$).

	Ca	Mg	K	Na	SO ₄
median	0.422	0.072	0.062	0.095	3.05
mean	0.568	0.099	0.079	0.133	4.58
standard error	0.015	0.003	0.002	0.004	0.12
standard deviation	0.563	0.100	0.071	0.110	4.75
minimum	0.057	0.014	0.016	0.042	0.33
maximum	10.023	1.701	1.187	0.937	59.80
count	1464	1392	1524	689	1642

The 50% error value was chosen to screen the data because it was felt that this percent error would be the maximum tolerated before the values would be considered too imprecise. It was unknown if this screening eliminated many of the low ion ambient air concentration values, resulting in clean days not being represented in the data set. Table 2.10 presents the central tendency statistics on the 1,749 daily filter samples that were screened using a much higher error value of 250%.

A comparison of Table 2.9 and 2.10 illustrates the importance in choosing the percent error screening value. The 250% screening results in a data set that processes a larger data spread as illustrated by the two tables' minimum and maximum values.

Student t tests using EXCEL's "Two Samples Assuming Unequal Variances" method were performed to see if the means of the two screening criteria (50% and 250%) were statistically different. The critical t value for 95% confidence is 1.64 for all the screening cases since the count (>120) and therefore the degrees of freedom are very large. Noting Table 2.11, with a 95% confidence level the t

Chapter 2: Methodology

test demonstrates that the 50% and 250% means are statistically different for calcium, magnesium and sodium.

Table 2.10. Descriptive statistics for June 1983 to May 1988 filter samples whose error is less than or equal to 250% (ion concentration units are ug/m³).

	Ca	Mg	K	Na	SO ₄
median	0.366	0.062	0.059	0.051	3.05
mean	0.526	0.090	0.078	0.091	4.73
standard error	0.016	0.003	0.003	0.008	0.174
standard deviation	0.649	0.119	0.131	0.280	7.24
minimum	0.012	0.003	0.004	0.009	0.12
maximum	14.362	2.849	4.644	9.795	230.64
count	1710	1674	1703	1391	1732

Table 2.11. Student t test results using the two data quality screening criteria.

ion	screening case (%)	count	mean	standard. deviation	t valu
Ca	50	1464	0.568	0.563	1.94
Ca	250	1710	0.526	0.649	
Mg	50	1392	0.099	0.100	2.27
Mg	250	1674	0.090	0.119	
Na	50	689	0.133	0.110	4.86
Na	250	1391	0.091	0.280	
K	50	1524	0.079	0.071	0.24
K	250	1703	0.078	0.131	
SO ₄	50	1642	4.58	4.75	0.72
SO ₄	250	1732	4.73	7.24	

Interpretation of Table 2.11's results can be illustrated using sodium as an example. Sodium's t value is 4.86 which is greater than the critical t value of 1.64 so as stated before the two means are statistically different. The 250% screened data set produced a lower mean value and a larger standard deviation. Therefore, concerning these three ions (calcium, magnesium and sodium) the choice of the 50% error screening value produced a data set with overall more precise measurements than the 250% data set, but eliminated some of the low ion ambient air concentrations which might indicate clean sampling days.

Chapter 2: Methodology

It is expected that the low ion ambient air concentrations eliminated by the 50% screening were clustered around certain times of the year and not evenly distributed throughout. Many of the low calcium and magnesium values might have been primarily winter month measurements. The low sodium values could be from February to May. Reasoning for this belief comes from results presented in Chapter 3 where these months are shown to possess the low monthly mean values. Nevertheless, the welcomed precision of the ion ambient air concentrations justified the choice of the 50% error DQ screening criterion.

2.6 Source Attribution Model

The construction of a chemical mass balance (CMB) model of two sources assisted in analyzing the influence of various sources on the ambient air concentrations measured at Bondville. Using the calcium and potassium ion aerosol concentrations and the elemental signatures for the sources, the relative importance of the considered sources (unpaved roads and soils) was predicted.

The scatter diagram (Figure 2.7) shows magnesium and calcium are closely related on a daily basis with a correlation coefficient of 0.814. Therefore, it is valid to assume that calcium and magnesium are coming from the same source, so it was reasoned that the inclusion of magnesium to the CMB modeling effort would provide little additional information. Figure 2.8 and Figure 2.9 show potassium versus calcium and potassium versus magnesium, respectively. Their correlation coefficients of 0.423 and 0.406, respectively, are low so it is assumed that this poor correlation on a daily basis is due to two different sources with different emission patterns.

Soil and unpaved roads were the two emission sources assumed in the model. As mentioned in section 1.1, Gatz, et al., 1985 found that wind erosion (a soil source), agricultural activity (a soil source) and unpaved road emission levels were 19.2 times higher than conventional sources (i.e., smokestacks associated with fuel combustion, industrial, transportation and solid waste disposal sources). Therefore, these conventional source contributions were considered negligible.

Bondville, a rural site, has one major conventional source located nearby. This source is a coal-fired power plant about 10 miles northeast of the site. Bondville's prevailing winds (northwesterly and southerly) take the plant's emissions away from the site, so the plant's contribution to filter mass was considered negligible (Dossett, 1987). In addition, the data set did not analyze for an emission fingerprint which could have been used to identify the power plant's mass contribution.

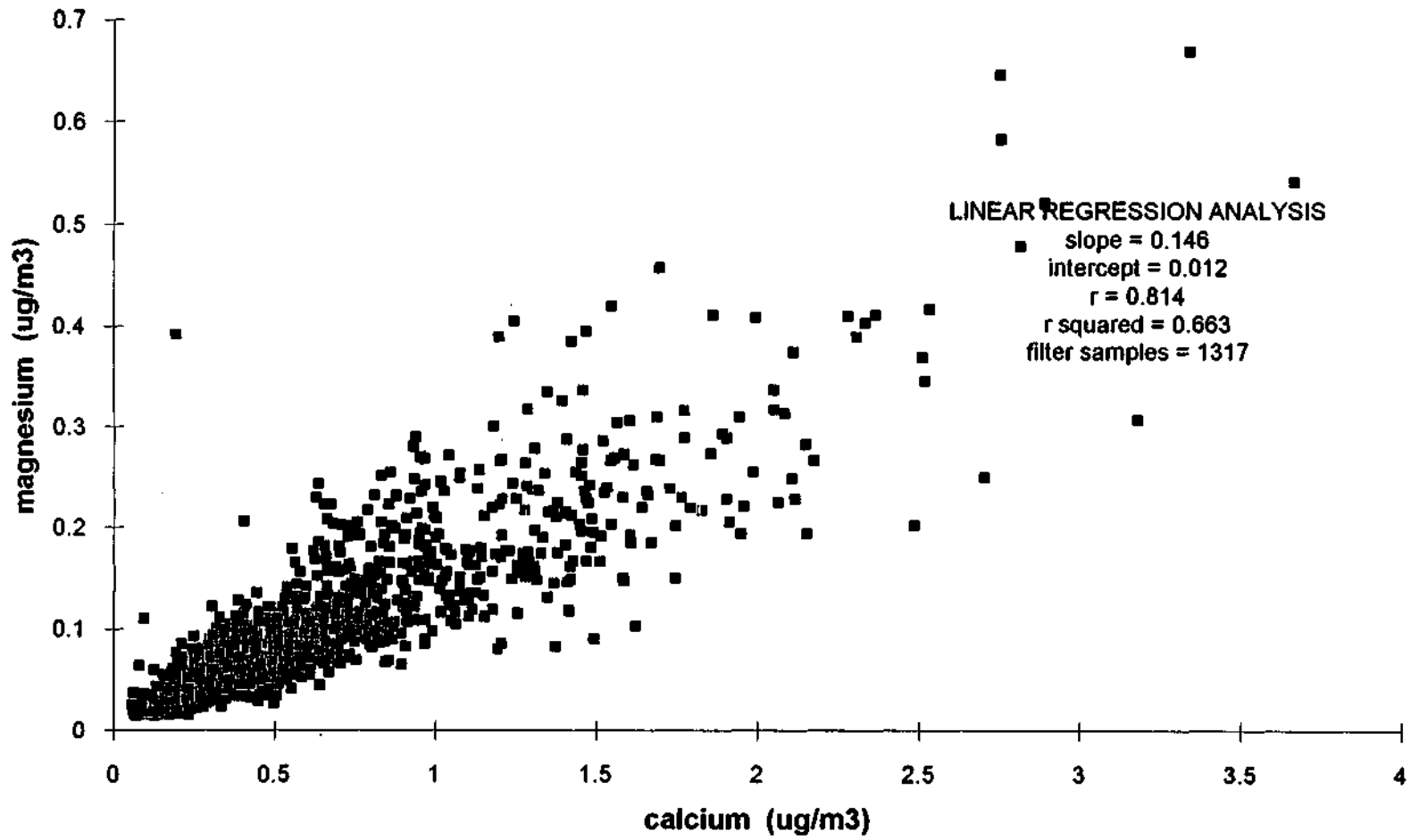


Figure 2.7 Scatter diagram of magnesium versus calcium.

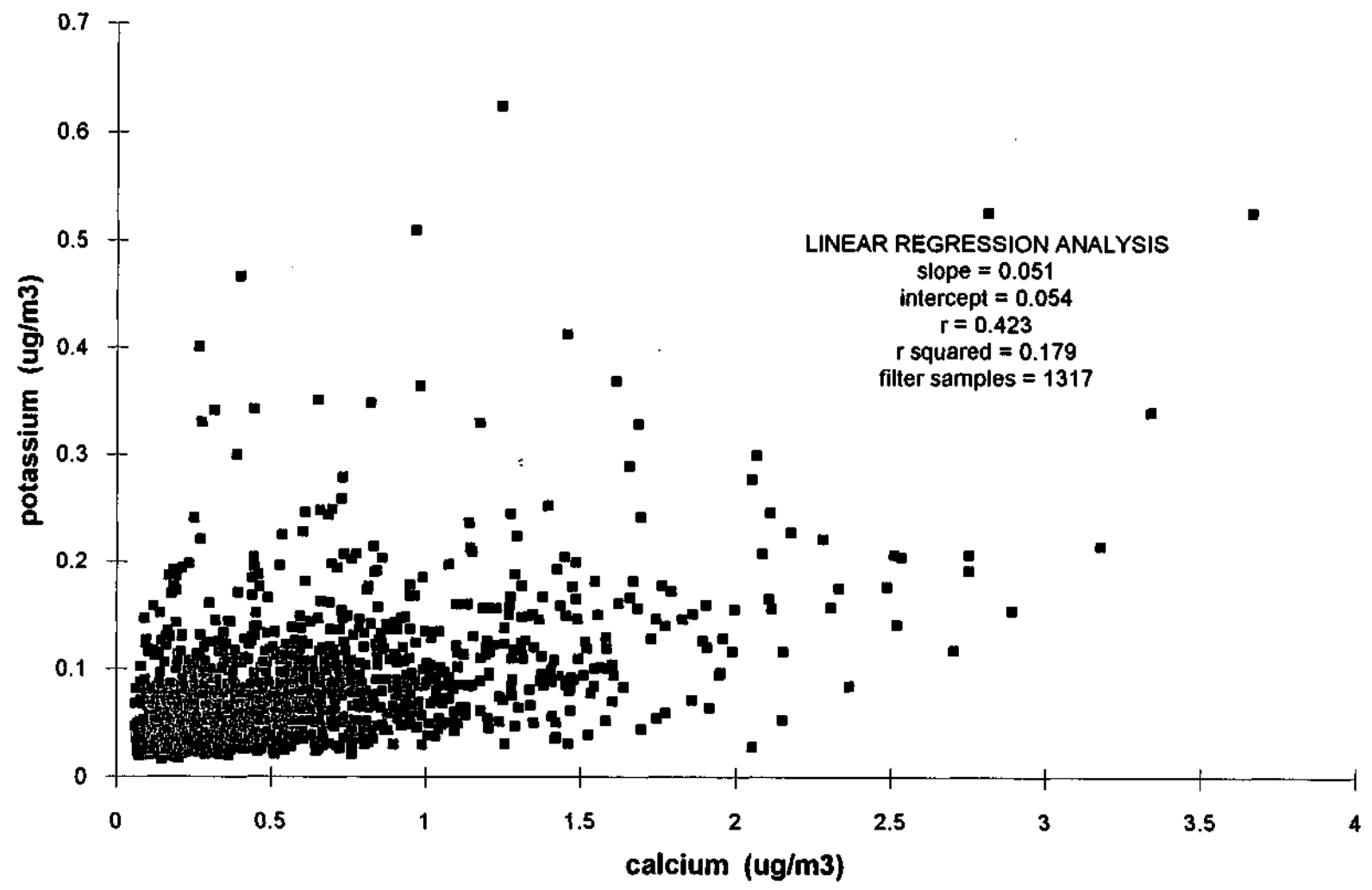


Figure 2.8 Scatter diagram of potassium versus calcium.

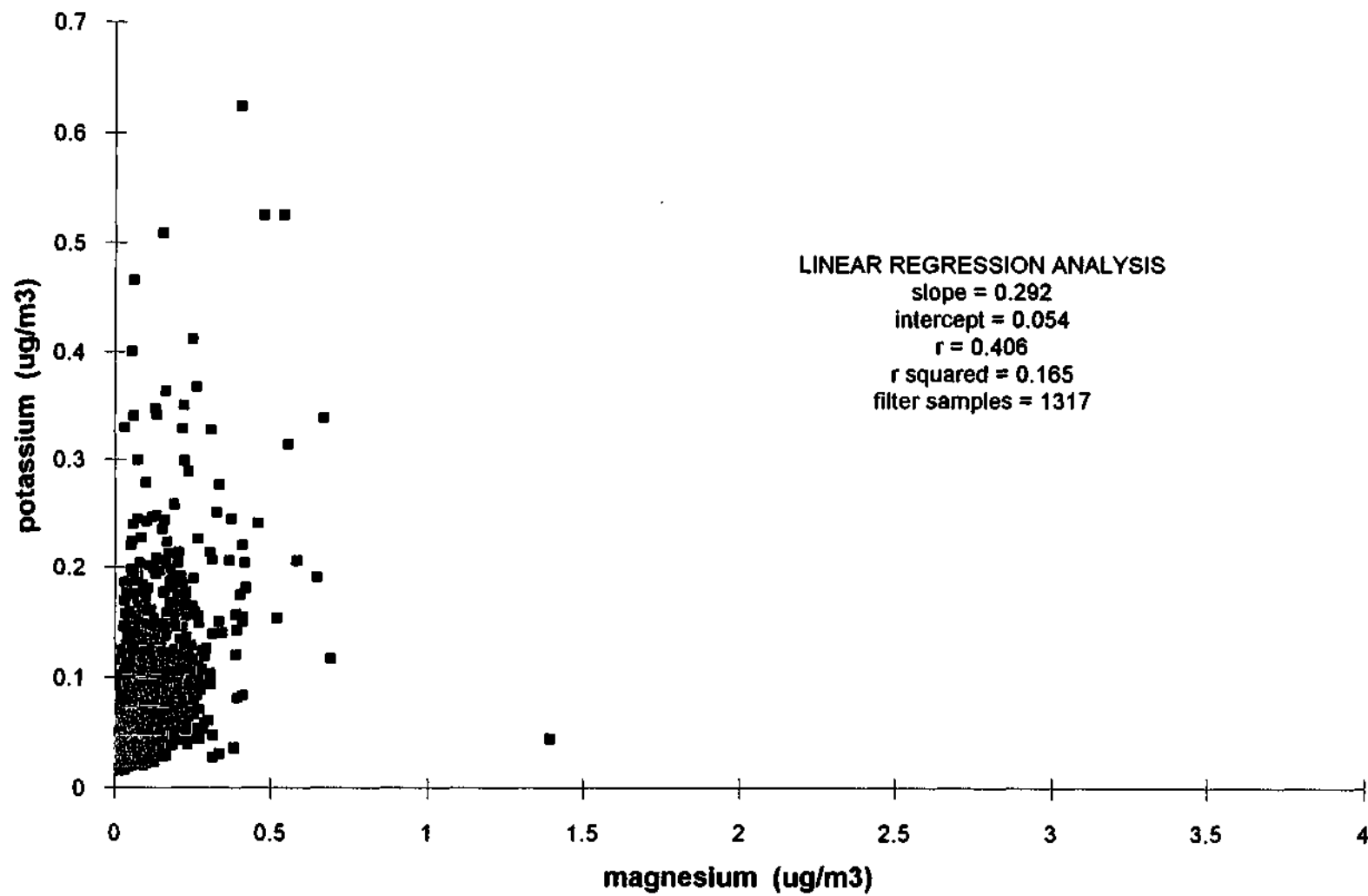


Figure 2.9 Scatter diagram of potassium versus magnesium

Chapter 2: Methodology

Figure 2.6, the AERION file, (AIR.EXE's output) serves as the model's input. Table 2.12 shows an abbreviated example of the model. This example illustrates the model for daily samples taken on June 1, 1983 to June 10, 1983. Columns A to Q contain input information and columns R to W are the source apportionments.

Data in columns A through H are from the AERION file. Column A is the field filter number. Columns B and C list the ion ambient air concentrations in $\mu\text{g}/\text{m}^3$ for calcium and potassium, respectively.

Column D lists the date the filter started its 24 hour sampling run, usually at 10:00 a.m. Column E is the AIR.FOR calculated air volume sampled through the filter in cubic meters. Column F is the amount of sampling time in hours. Column G is the pump number that supplied the vacuum for air sampling. Column H is the sample protocol (SP) flag symbol awarded to filters that had questionable sampling protocol. Sections 2.5.1 and 2.5.3.1 provide greater detailed descriptions of these columns.

2.6.1 Soluble Versus Total Elemental Source Signatures

The ion ambient air concentrations inputted in the CMB model are soluble concentrations. Most elemental source signature values are total amounts, not soluble quantities. Therefore, the ion ambient air concentrations were changed to soluble mass amounts which were converted to total mass amounts.

Referencing Table 2.12, columns I and J present the soluble ion mass (μg) captured by the Bondville sampling for calcium and potassium, respectively. These two columns were derived by taking the respective ion ambient air concentrations (columns B and C) and multiplying them by the air volume sampled (column E).

Columns K and L calculate the total mass conversion of the soluble ion mass values. Total mass of calcium (column K), is calculated by dividing the soluble calcium mass (column I) by the constant 0.88. Total mass of potassium (column L) is calculated by taking the soluble potassium mass (column J) and dividing it by the constant 0.42. These constants originate from a study by Stensland and Gatz, 1981. Twenty-four duplicate daily filter samples were collected simultaneously at the Bondville site and analyzed for total and soluble elemental concentrations. Stensland and Gatz's soluble method differs from the method to extract ions from this study's daily filters described in section 2.3, as follows. Stensland and Gatz's extraction solution was deionized water with an approximate pH of 5.6. The

Table 2.12 An example of AERMOD quantitative source model's output.

	A	B	C	D	E	F	G	H	I	J	K	L	M	N	O	P	Q
1	AERMOD QUANTITATIVE MODEL																
2	A model built to compare with Bondville sampling results.																
3	Data columns A to H were obtained from the 50% error screened AERION file output (8388.XLS) of the AIR.FOR FORTRAN program.																
4	The solubility factors (columns K & L) used in calculating the total mass of the elements were obtained from GJS 19th DOE Report May '81.																
5	Total elemental abundance values for soils (columns M & O) were obtained from Boerngen and Shacklette USGS report 81-197.																
6	Total elemental abundance values for roads (columns N & P) were obtained from Barnard, 1986, Table II crushed limestone road surfaces.																
7																	
8																	
9		Ca	K		air				Ca sol	K sol	Ca total	K total	Ca	Ca	K	K	K
10	field	soluble	soluble	filter	volume	sampling	pump	flag	filter	filter	filter	filter	in	in	in	in	in
11	filter	air conc	air conc	date	sample	time	number	symbol	mass	mass	mass	mass	soil	roads	soil	roads	roads
12	number	(ug/m3)	(ug/m3)	on	(m3)	(hours)			(ug)	(ug)	(ug)	(ug)	0.61%	26.20%	1.66%	0.56%	road
13																	
14	BG37W152	0.564	0.051	06/01/83	21.633	11.45	17		12.2	1.1	13.9	2.6	0.006	0.262	0.017	0.006	0.02
15	BG37W153	0.501	0.074	06/02/83	17.877	11.4333	457		9.0	1.3	10.2	3.1					
16	BG37W154	0.216	0.052	06/03/83	18.318	11.4167	110		4.0	1.0	4.5	2.3					
17	BG37W155			06/04/83			13	QUE									
18	BG37W156	0.486	0.133	06/05/83	18.932	11.4667	17		9.2	2.5	10.5	6.0					
19	BG37W157	1.108	0.085	06/06/83	16.202	11.4	457		18.0	1.4	20.4	3.3					
20	BG37W158	1.374	0.095	06/07/83	19.255	11.5167	110		26.5	1.8	30.1	4.4					
21	BG37W159	1.582	0.129	06/08/83	15.454	11.4167	13		24.4	2.0	27.8	4.7					
22	BG37W160	1.279	0.11	06/09/83	18.927	11.4667	17		24.2	2.1	27.5	5.0					
23	BG37W161	1.659	0.166	06/10/83	17.455	11.45	457		29.0	2.9	32.9	6.9					
24																	
25																	
26				columns	R	S	T	U	V	W							
27					road	soil											
28					mass	mass	percent	percent	percent	percent							
29					on	on	of Ca	of Ca	of K	of K							
30					filter	filter	from	from	from	from							
31					(ug)	(ug)	road (%)	soil (%)	road (%)	soil (%)							
32																	
33					49.6	141.5	93.8	6.2	10.6	89.4							
34					34.7	178.0	89.3	10.7	6.2	93.8							
35					14.1	131.9	82.1	17.9	3.5	96.5							
36																	
37					31.7	350.4	79.6	20.4	3.0	97.0							
38					73.8	172.6	94.8	5.2	12.6	87.4							
39					109.5	225.4	95.4	4.6	14.1	85.9							
40					100.2	252.1	94.5	5.5	11.8	88.2							
41					98.8	265.3	94.1	5.9	11.2	88.8							
42					116.8	376.2	93.0	7.0	9.5	90.5							

Chapter 2: Methodology

vigorous agitation of the filters in the extract solution was performed by a wrist action shaker for 20 minutes. Then the solution was filtered with the Millipore HA filters as illustrated in step 10 on Figure 2.1. Therefore, if Stensland and Gatz's extract solution was the same acidity and longer shake time as used for the Bondville study (pH = 3.0, shake time = 48 hours), then the determined calcium and potassium soluble fractions would be larger by some unknown amount. This concern is addressed in Chapter 4. The Crocker Nuclear Laboratory at the University of California-Davis performed the total elemental mass analysis using ion-excited X-ray fluorescence. Stensland and Gatz, 1981, used the quantity termed the fractional increase to report the results of the filters' elemental analysis. They report that for calcium, the median fractional increase is 0.133. Equation 2.12 presents the operation used to calculate the fractional increase of total when compared to soluble:

$$\text{fractional increase} = \frac{\text{Ca}_t - \text{Ca}_w}{\text{Ca}_w} \quad (2.12)$$

where Ca is the elemental symbol for calcium, subscript t stands for the total element measured and subscript w stands for the water soluble part of the element measured. Note equation (2.12) is the same approach used to evaluate the relative error between two values. Setting equation (2.12) equal to the median fractional increase value of 0.133 and solving for the ratio of soluble by total (Ca_w/Ca_t) gives the constant (0.88) used above. Therefore, dividing the measured soluble calcium values by 0.88 gives an estimate of the total calcium on the daily filters. Taking the same equation as (2.12) and substituting potassium for calcium, the median potassium fractional increase value of 1.362 gives a ratio of soluble by total of 0.42. This constant is used in the same way to derive column L's values of total potassium (Stensland and Gatz, 1981):

Columns M through P in Table 2.12 give the total elemental abundance of calcium and potassium in soils and limestone covered roads. The soil percentages (columns M and O) listed were obtained from a United States Geological Survey (USGS) study by Boerngen and Shacklette, 1981, for 22 soil samples taken in Illinois. The mean value for the percentage of calcium in these soils was 0.61% and of potassium was 1.66%. Gatz et al., 1981 paper, determined elemental abundances for 74 surface soil samples distributed over a one square kilometer area centered at the Bondville site. The mean values for the 74 soil samples was 0.70% for calcium and 1.75% for potassium. These means agree well with the USGS study's Illinois means.

The unpaved road total elemental abundances (columns N and P) originate from an article by Barnard et al., 1986. The article lists the elemental analysis from seven unpaved roads whose surface material was crushed limestone. The roads are in states surrounding Illinois with two each in Pennsylvania and Tennessee and one each in Indiana, Kentucky and Iowa. These unpaved roads had

mean values for calcium of 26.2% and 0.56% for potassium. Again, these values agree well with Gatz et al.'s mean elemental abundance values for eight crushed limestone surfaced unpaved roads near the Bondville site, 25% for calcium and 0.52% for potassium (Gatz et al, 1981).

2.6.2 Daily Aerosol Levels of Calcium and Potassium

This study contains five years of daily filter sampling efforts that produced a collected total of 1,833 analyzed filters. Sampling protocol (SP) screening reduced that number by 84 to 1,749 reliable filters. The data quality (DQ) screening effort reduced that number to 1,317 filters possessing ion ambient air concentrations for both calcium and potassium that passed the 50% error criterion value. These filters make up the input into the CMB model. Columns B and C in Table 2.12 show the soluble ion ambient air concentrations, in $\mu\text{g}/\text{m}^3$, for calcium and potassium, respectively.

2.6.3 Equations of the CMB Model

Several equations are used by the model to generate the desired output. These equations generate the values in columns Q through W in Table 2.12.

Column Q is a ratio of elemental abundances found in unpaved roads. The potassium value is divided by the calcium value. This is an often repeated constant in the next two columns and was calculated in the interest of simplicity.

Column R is the calculated road mass sampled by the filter. Column S is the calculated soil mass sampled by the filter. As stated before in section 2.6, the only sources considered were soils and unpaved roads comprised of surface materials of crushed limestone. Therefore the total mass of calcium on the filter is expressed as:

$$\text{Ca}_{\text{MF}} = \% \text{Ca}_{\text{R}} (\text{RM}) + \% \text{Ca}_{\text{S}} (\text{SM}) \quad (2.13)$$

and the total mass of potassium on the filter is:

$$\text{K}_{\text{MF}} = \% \text{K}_{\text{R}} (\text{RM}) + \% \text{K}_{\text{S}} (\text{SM}) \quad (2.14)$$

The symbols used in equations (2.13) and (2.14) are the same with the exception of the elements calcium (Ca) and potassium (K). Subscript MF is the indicated element's total filter mass (μg). The percentage of the element with subscript R is the mean elemental abundance for unpaved roads. The

Chapter 2: Methodology

percentage of the element with subscript S is the mean elemental abundance for soils. RM is the total amount of road mass on the filters (ug) and SM is the total amount of soil mass on the filters (ug).

The two unknowns are the road mass and soil mass. Therefore, with two unknowns and two equations one can solve for road mass using equation (2.13) and substitute it into equation (2.14) to get:

$$K_{MF} = \frac{\%K_R}{\%Ca_R} [Ca_{MF} - \%Ca_S(SM)] + \%K_S(SM) \tag{2.15}$$

Equation (2.15) is solved for SM which is the soil mass on the filter (ug):

$$SM = \frac{Ca_{MF} \left(\frac{\%K_R}{\%Ca_R} \right) - K_{MF}}{\%Ca_S \left(\frac{\%K_R}{\%Ca_R} \right) - \%K_S} \tag{2.16}$$

In order to calculate the road mass on the filter, substitute equation (2.16) back into equation (2.13) (where (2.13) has been solved for road mass) and the road mass on the filter (ug) is:

$$RM = \frac{Ca_{MF} - \%Ca_S \left[\frac{Ca_{MF} \left(\frac{\%K_R}{\%Ca_R} \right) - K_{MF}}{\%Ca_S \left(\frac{\%K_R}{\%Ca_R} \right) - \%K_S} \right]}{\%Ca_R} \tag{2.17}$$

The model has now calculated the mass on the filter from unpaved roads and soils, the two sources being considered.

2.6.4 Output from the Model

The next columns on Table 2.12 are the desired model outputs. Here, the two sources' (unpaved roads and soils) contribution percentages are calculated for the two elements considered, calcium and potassium. Column T is the percentage of total calcium on the filter that originates from the road source. The calculation of this value comes from using the calculated values of the road mass and soil mass and the elemental abundance in those sources. Equation (2.18) shows this calculation.

$$Ca_{\text{from road source}} = \left[\frac{\%Ca_R(RM)}{\%Ca_R(RM) + \%Ca_S(SM)} \right] 100 \quad (2.18)$$

Since this is a two source model, the percentage of calcium from the soil source is just 100 minus the value obtained by equation (2.18). This value appears in column U.

Column V is the percentage of total potassium on the filter originating from the road source. Again, the calculation of this value comes from using the calculated values of the road mass and soil mass and the elemental abundance in those sources. Equation (2.19) shows this calculation.

$$K_{\text{from road source}} = \left[\frac{\%K_R(RM)}{\%K_R(RM) + \%K_S(SM)} \right] 100 \quad (2.19)$$

The percentage of potassium from the soil source is just 100 minus the value obtained by equation (2.19). This value appears in column W. The analysis of the output from the model is discussed in Chapter 3.

2.7 References

- Bajpai, A. C., I. M. Calus and J. A. Fairley, 1978: Statistical methods for engineers and scientists, John Wiley and Sons, Chichester, England, p 141-148.
- Barnard, William R., Gary J. Stensland and Donald F. Gatz, 1986: Alkaline materials flue from unpaved roads: source strength, chemistry and potential for acid rain neutralization, *Water, Air and Soil Pollution*, vol. 30, p. 285-293.
- Bartlett, Janyce D. and Gary J. Stensland, 1980: Ambient air filter extraction procedures, *In Study of Atmospheric Pollution Scavenging by R. G. Semonin et al.*, COO-1199-60, 18th Progress Report to the U. S. Department of Energy, Pollutant Characterization and Safety Research Division, Contract EY-76-S-02-1199, p. 76-81.
- Bryan, Audrey A. and Wayne Wendland, 1993: Local climatological data summary Champaign, Illinois 1888-1992, *SWS Miscellaneous Publication 98-11*, Department of Energy and Natural Resources, State of Illinois, p. 3.

Chapter 2: Methodology

Buck, Inc., 1985: mini-Buck Calibrator™ instruction manual, A.P. Buck, Inc., Orlando, Florida.

Dossett, S.R., 1987: An annotated description of the atmospheric chemistry sampling station at Bondville, Illinois, *In Study of Atmospheric Pollution Scavenging by R. G. Semonin et al.*, COO-1199-65, 21th Progress Report to the U. S. Department of Energy, Office of Health and Environmental Research, Contract DE-AC02-76EV01199, p. 330.

Gatz, Donald F., 1981: Comparison of two sampling methods for medium-volume aerosol sampling, *In Study of Atmospheric Pollution Scavenging by R. G. Semonin et al.*, COO-1199-63, 19th Progress Report to the U. S. Department of Energy, Pollutant Characterization and Safety Research Division, Contract DE-AC02-76EV01199, p. 15-23.

Gatz, Donald F., Gary J. Stensland, Michael V. Miller and Alistair C. D. Leslie, 1981: Sources of airborne calcium in rural central Illinois, *American Chemical Society, Society Symposium Series, No. 167*, Report No. 17, p. 303-308.

Gatz, Donald F., William R. Barnard and Gary J. Stensland, 1985: Dust from unpaved roads as a source of cations in precipitation, *78th Annual Meeting of the Air Pollution Control Association*, Report No. 85-6B.6, Detroit, Michigan, June 16-21.

Gatz, Donald F. and Gary J. Stensland, 1985: Comparison of total versus soluble data for ambient filter samples, *In Study of Atmospheric Pollution Scavenging by R. G. Semonin et al.*, COO-1199-33, 19th Progress Report to the U. S. Department of Energy, Office of Health and Environmental Research, Contract DE-AC02-76EV01199, p. 24-27.

Gelman™, 1970: Gelman air sampling kit instruction manual, Gelman Instrument Company, Ann Arbor, Michigan.

Haltiner, George J. and Frank L. Martin, 1957: *Dynamic and physical meteorology*, McGraw-Hill Book Company, New York, NY, p. 52-53.

Hinds, William C, 1982: *Aerosol technology, properties, behavior, and measurement of airborne particles*, John Wiley and Sons, New York, NY, p. 14.

Chapter 2: Methodology

Lapin, Lawrence L, 1990: Probability and statistics for modern engineering, PWS-Kent Publishing Company, Boston, MA, p. 266.

Microsoft® EXCEL Analysis ToolPak 1992: Function reference manual, Microsoft® Corporation, pp. 536.

Pattenden, N. J. and R. D. Wiffen, 1977: The particle size dependence of the collection efficiency of an environmental aerosol sampler, *Atmospheric Environment*, vol. 11, pp. 677-678.

Staggs, L., 1982: Aerosol data screening instructions, unpublished *In Aerosol data instructions for screening and filing notebook*.

Stensland, Gary J., 1993: Personal communications, determining ion standard deviations.

Stensland, Gary J. and Janyce D. Bartlett, 1979: Measurement of atmospheric nitrate, sulfate, ammonium and calcium using various filter setups, *In Study of Atmospheric Pollution Scavenging by R. G. Semonin et al.*, COO-1199-58, 17th Progress Report to the U. S. Department of Energy, Pollutant Characterization and Safety Research Division, Contract EY-76-S-02-1199, p. 48-50.

Stensland, Gary J. and Janyce D. Bartlett, 1980: Ambient aerosol measurements at Champaign, Illinois, *In Study of Atmospheric Pollution Scavenging by R. G. Semonin et al.*, COO-1199-60, 18th Progress Report to the U. S. Department of Energy, Pollutant Characterization and Safety Research Division, Contract EY-76-S-02-1199, p. 76-81.

Wilson, M. L., D. F. Elias and R. C. Jordan, 1983: Student manual second edition, *APTI Course 435 Atmospheric Sampling*, EPA 450/2-80-004, United States Environmental Protection Agency, Office of Air Quality Planning and Standards, Contract 68-02-3573, p. 3.33-3.40.

Chapter 3

Results and Discussion

3.1 Introduction

Analysis of the Bondville June 1, 1983, to May 31, 1988, screened data set involved the use of two approaches. One of these approaches, section 2.6's chemical mass balance (CMB) model, examines the data quantitatively. This CMB model demonstrates the influence of the two major dust sources identified in the literature, unpaved roads and soils, on the calcium and potassium mass collected on the sampled filters. The second approach is qualitative in nature. It consists of plotting the data and noting the patterns of the three ion's concentrations relative to each other and their change as a function of time.

3.2 Modeling Results

This quantitative approach uses the CMB model discussed in section 2.6. The model considers only two sources, unpaved road dust and soils, to account for the aerosol filter extracted ion concentrations of calcium and potassium. Figures 3.1 to 3.4 depict the calculated source apportionment from unpaved roads and soils for calcium and then potassium, respectively. Empirical factors in the model convert extractable (soluble) concentrations to total elemental concentrations. The percentage of total elemental mass on the filters, attributed to the particular source, is the ordinate on the Figures and time, as the month of the year, is the abscissa. The model was run for each daily filter that simultaneously had calcium and potassium airborne concentrations whose percent error was less than 50% (for screening methodology see section 2.6.1). The five year data set was grouped by months in this chapter because the primary temporal issue being considered is intra-annual aerosol variability which should be related to hypothesized emission sources' monthly or seasonal variations. Daily or year to year variability of the Bondville crustal aerosol concentrations are also of interest but are beyond the scope of this report.

Table 3.1 lists the number of daily filters by month that passed the 50% screening criterion and were used to calculate the monthly mean percentages and associated standard errors shown in Figures 3.1 to 3.4. The figures' filled circular points indicate these mean percentages by month for the five year

data set. The bold lines (termed precision bars) radiating from the mean points (filled circles) illustrate plus or minus (± 2) times the standard error of the mean. Lapin, 1990 defines the standard error of the mean ($\sigma_{\bar{x}}$) when the population is large as:

$$\sigma_{\bar{x}} = \frac{\sigma}{\sqrt{n}} \tag{3.1}$$

where σ is the population standard deviation and n is the sample size. As stated previously, Microsoft® EXCEL software calculated all statistics presented in this chapter.

Table 3.1. Number of screened daily filters used to calculate the source apportionment means and standard errors by month.

month	number of filters
June	125
July	136
August	127
September	117
October	122
November	97
December	94
January	117
February	98
March	111
April	108
May	127

The ± 2 times the standard error depiction is useful because one can conservatively state without a quantitative statistical test that two different months whose precision bars do not overlap are statistically different. Thus from looking at Figure 3.1, it can be said with confidence that July's value is different than December's and January's values, but not different than April's and May's values.

The model's results shown in Figures 3.1 to 3.4 agreed with the initial expectations that calcium's high elemental abundance in crushed limestone roads as compared to soils should cause unpaved road sources to be the major contributor of calcium. Similarly in turn, potassium's high elemental abundance in soils should have caused soils to be potassium's major source. Figure 3.1 shows that unpaved road sources account for greater than 70 % of total calcium. June's to August's values rise up to the 86%

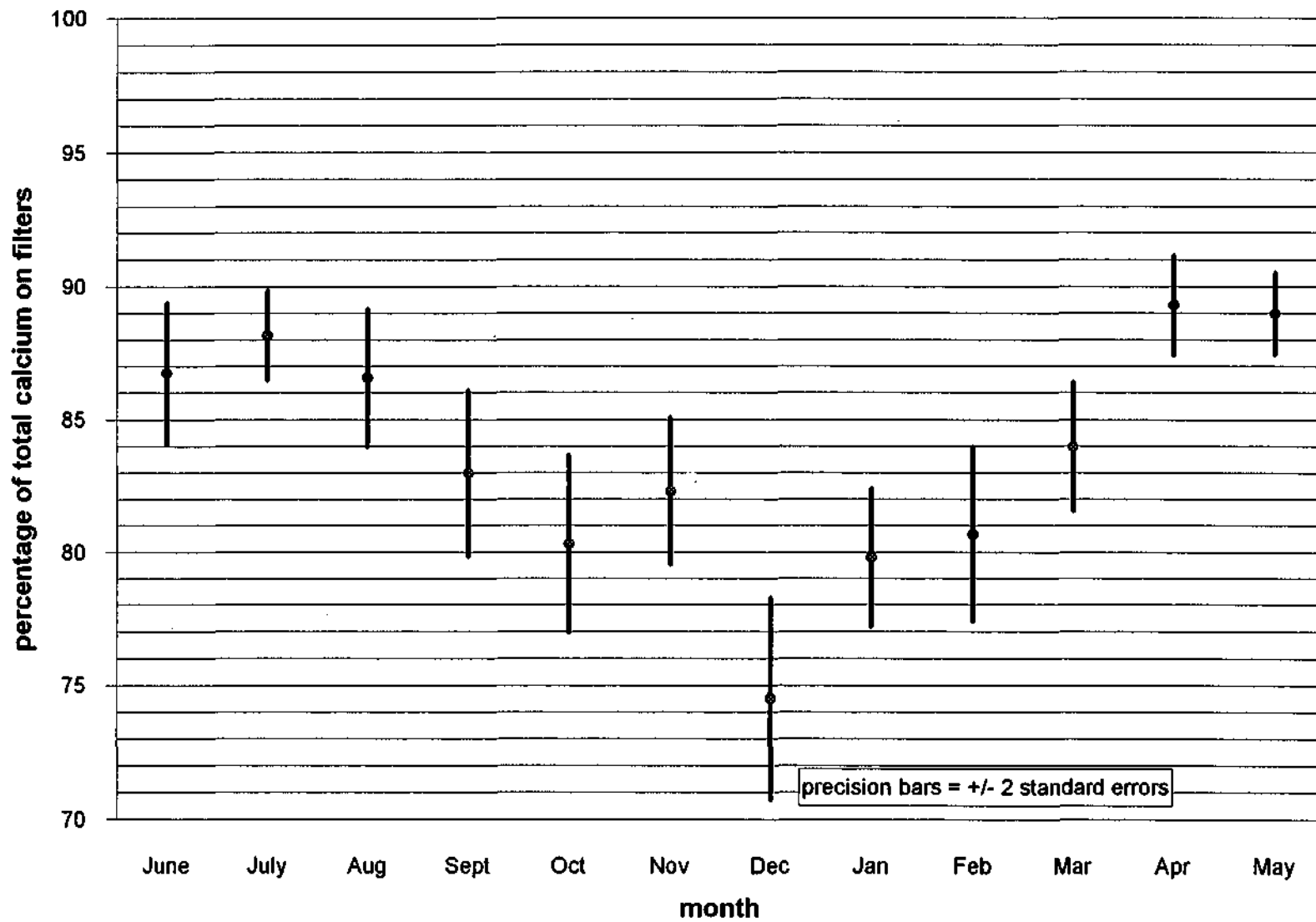


Figure 3.1. Source apportionment of calcium on Bondville aerosol filters from unpaved road source.

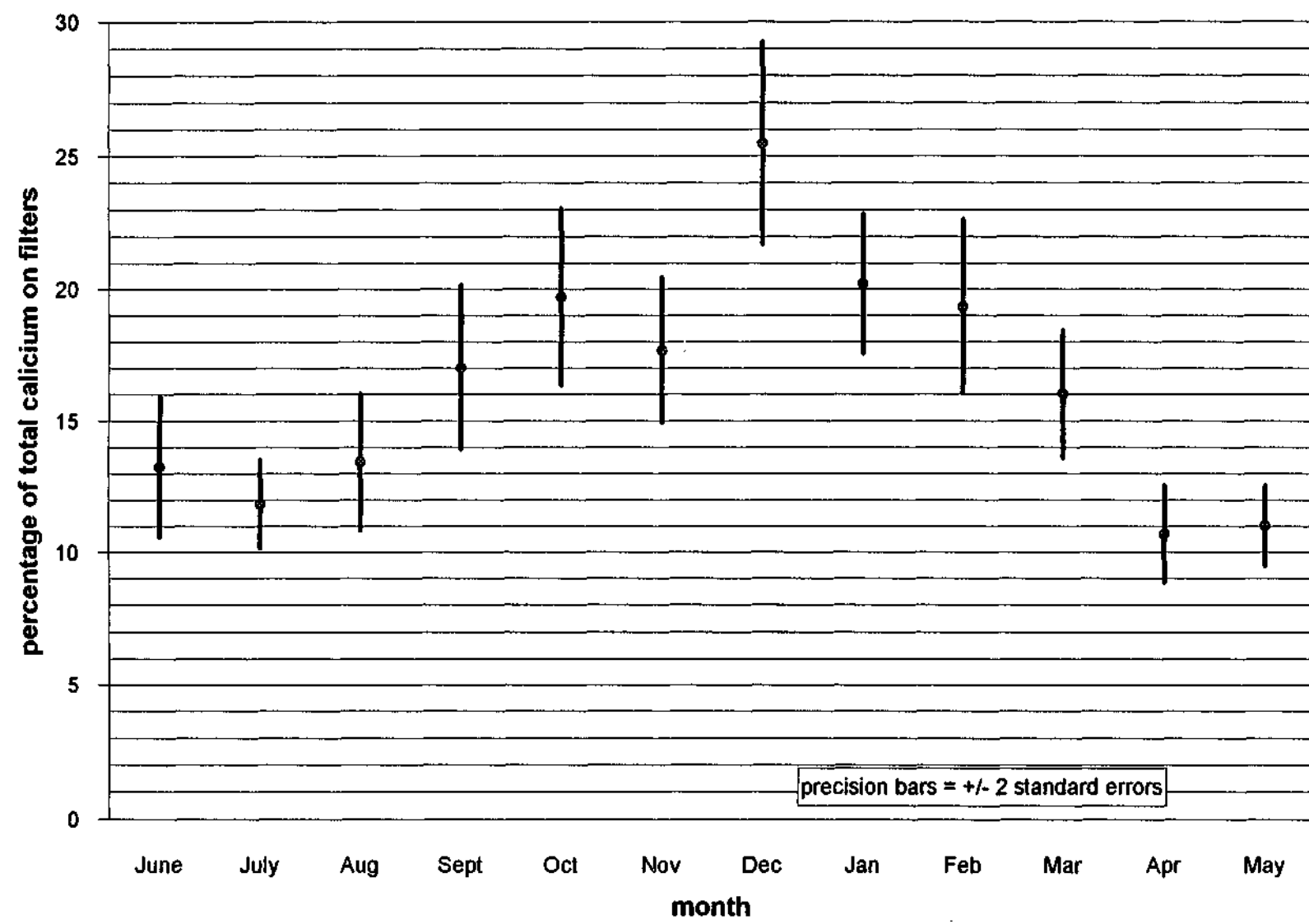


Figure 3.2. Source apportionment of calcium on Bondville aerosol filters from soil source.

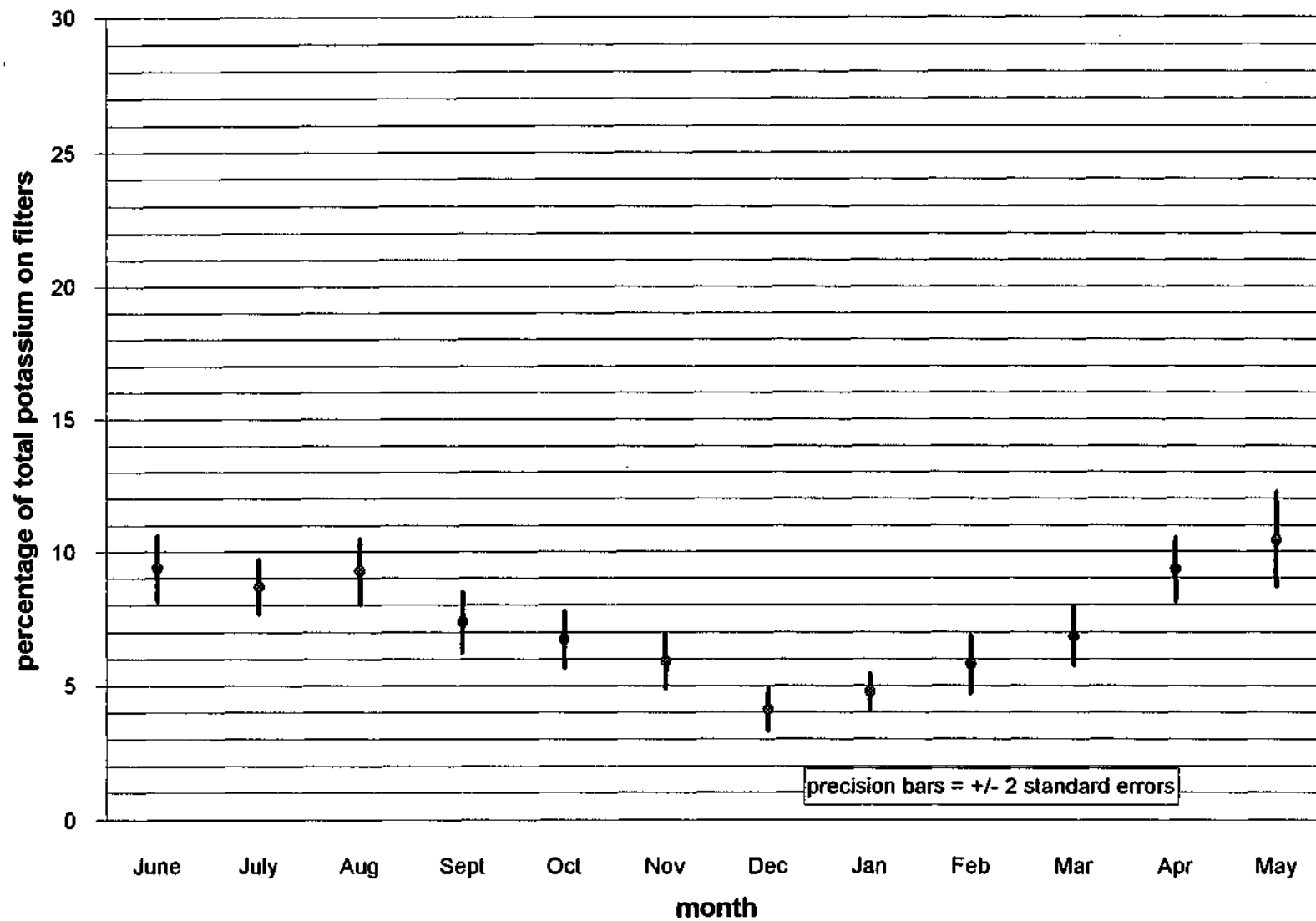


Figure 3.3. Source apportionment of potassium on Bondville aerosol filters from unpaved road source.

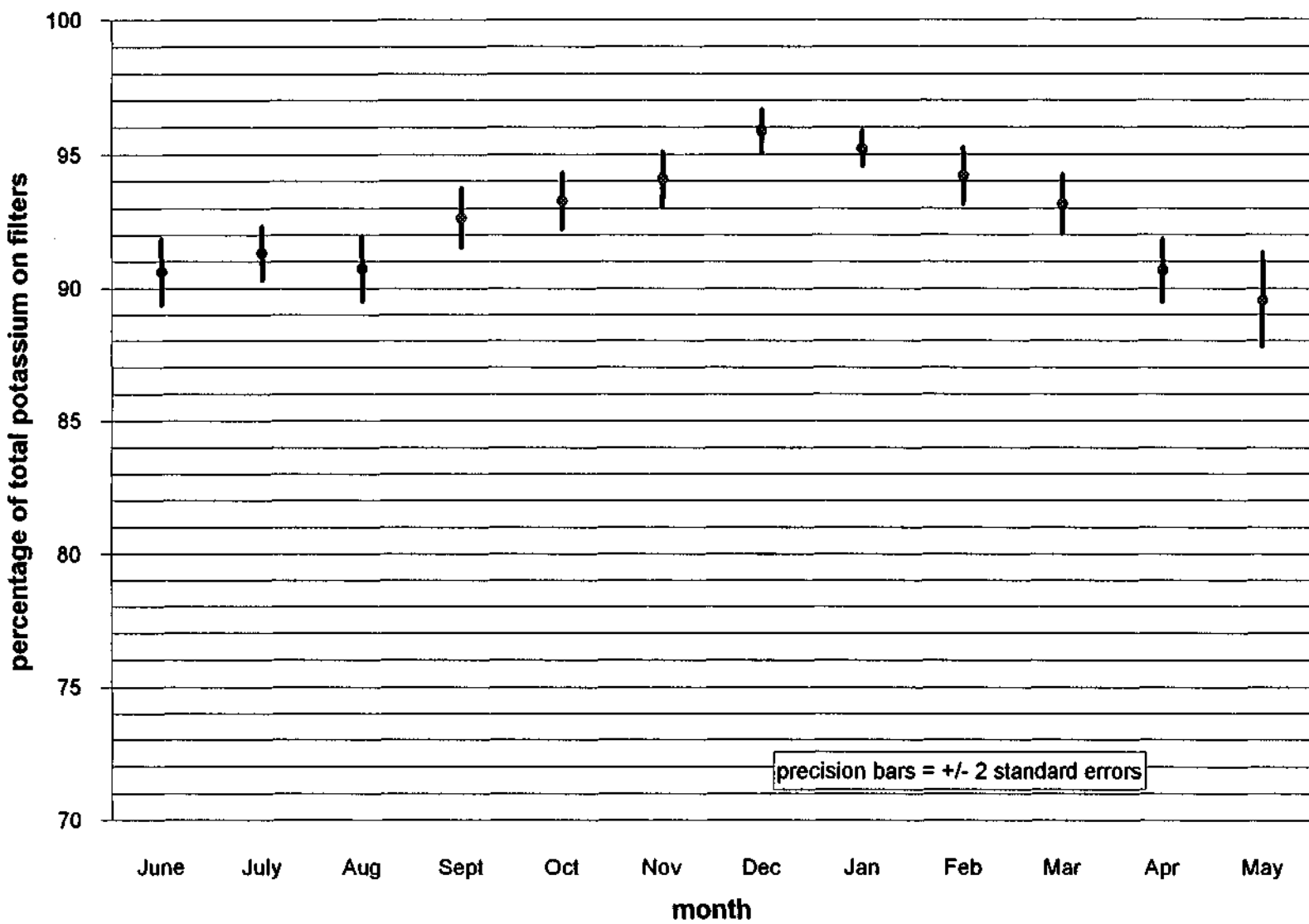


Figure 3.4. Source apportionment of potassium on Bondville aerosol filters from soil source.

value range. The 12 month unpaved road source average is 84% with a ± 2 times the standard error of 2.5%. These results agree well with Gatz et al., 1981 findings. Gatz et al.'s CMB model indicated that for the summer and early fall seasons unpaved roads contributed 86% of the airborne calcium with the remaining 14% attributed to soil sources. It follows that since Gatz et al.'s model is also a two source model that Figure 3.2's 14% value range supports their soil percentage value. It is interesting to note the agreement between the Bondville model with its large model data input spanning a five year sampling period and Gatz' et al.'s effort carried out for a short period in 1978.

Figure 3.4 shows that for all months greater than 89% of total potassium is due to soil sources and the 12 month average value is 93% with a ± 2 times the standard error of 1.2%. The highest values are for the winter months with a December through February average value of 95%.

One argument in support of the previous expressed expectations and actual model results relies on the comparison of total elemental abundance from each source. The high percentage of calcium in the limestone that covers unpaved roads (26.2%) versus Illinois soils (0.61%) could account for the importance of unpaved roads on airborne calcium levels. The NAPAP report (Irving, 1991) supports this argument. This report states that unpaved road source materials' enriched calcium composition (over 80% surfaced with crushed limestone, dolomite or gravel) relative to soils, cause the unpaved roads to account for much of the airborne calcium levels .

Figures 3.5 and 3.6 provide a comparison of the total aerosol mass modeled concentrations originating from the unpaved road source and soil source, respectively. These figures show the ambient aerosol mass concentration means with precision bars versus time by month. The model generated these values using the same procedures as in Figures 3.1 to 3.4. The model is effected by ignored aerosol masses when calculating the source contributions and aerosol masses, but since the model's results are derived using the elemental abundances of considered aerosols (calcium and potassium), the unconsidered element masses are irrelevant. Also noted is the model's exclusion of filter mass from sources other than unpaved roads and soil sources, e.g., sulfate on the Bondville filters from photochemical conversion of sulfur dioxide emitted from power plant point sources. This approach is supported by the literature research based assumption that for the Bondville site these sources are negligible compared to unpaved roads and soils.

The CMB model predicts that a greater amount of ambient aerosol mass is contributed by soil than unpaved road sources, e.g., in June 12.9 ug/m^3 for soils (of Figure 3.5) versus 3.2 ug/m^3 for unpaved roads (of Figure 3.6). Note the predicted soil mass concentrations are approximately 3.5 to 5.5 times greater than the road mass concentrations for the different months. In comparison, Gatz et al.'s

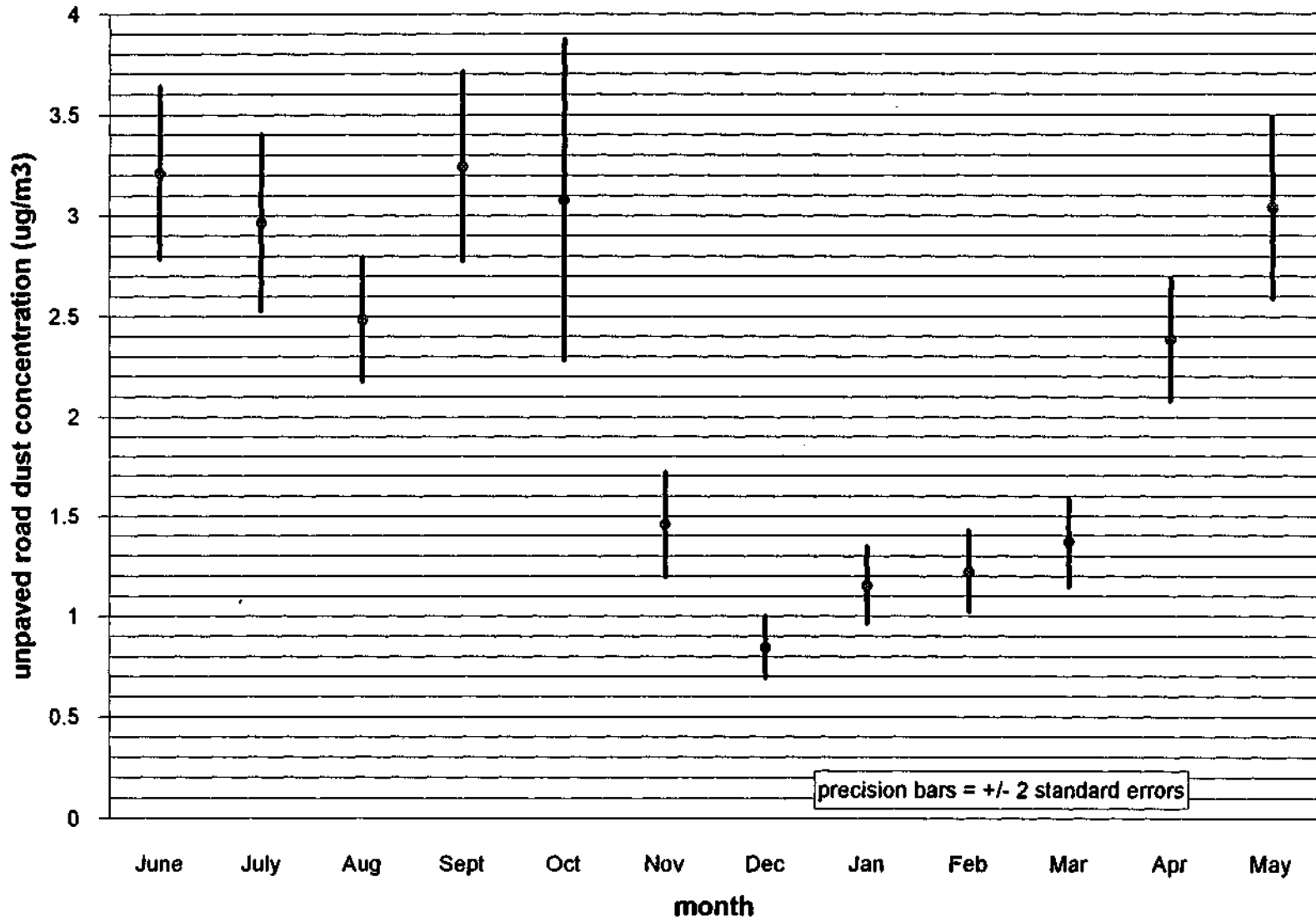


Figure 3.5. Modeled dust concentrations by month from the unpaved road source.

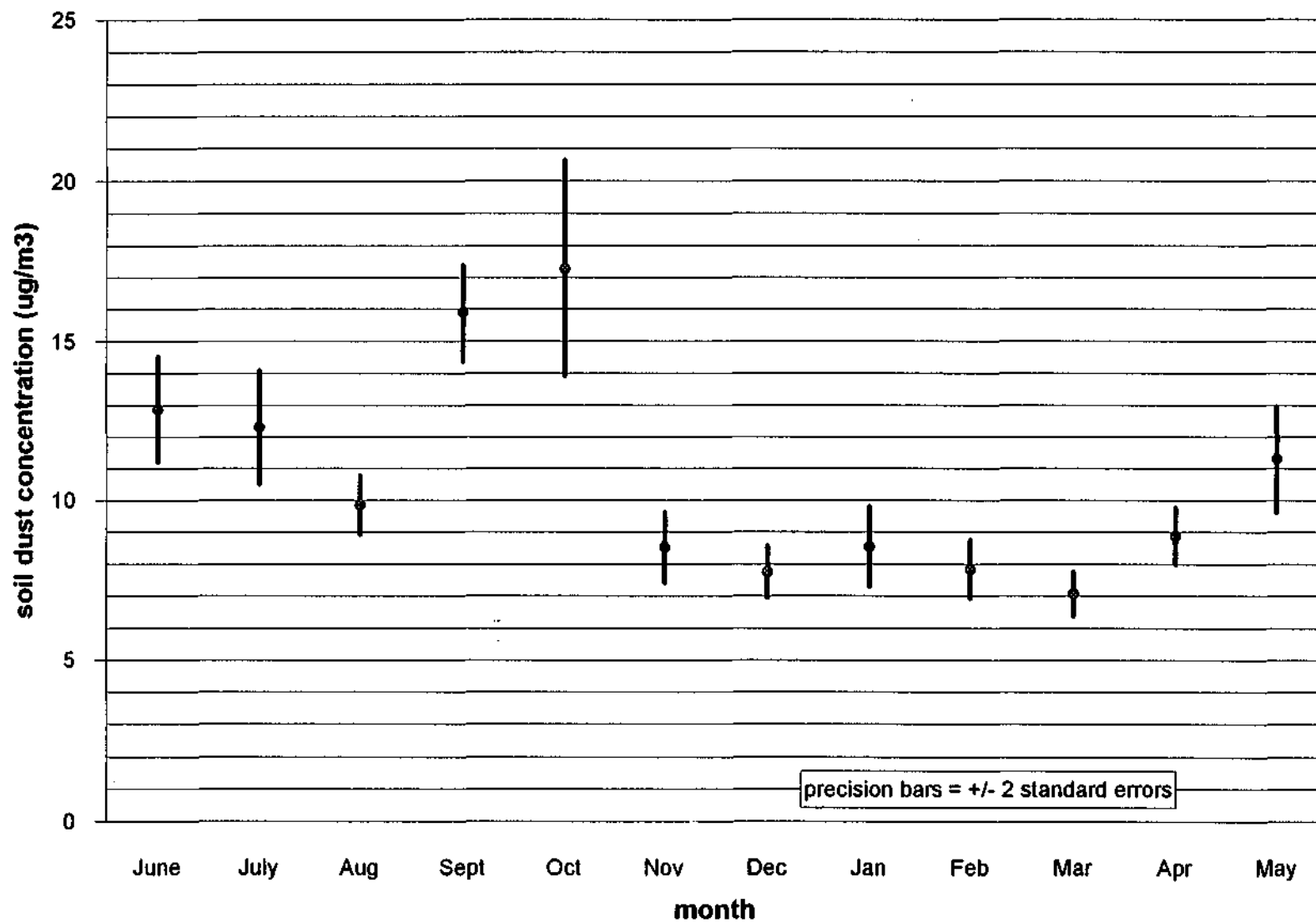


Figure 3.6. Modeled dust concentrations by month from the soil source.

model indicated that a mean value of 12% of the local total suspended particulate were from unpaved roads and 39% from soils. Therefore, Gatz et al.'s model calculates soil mass contributions as being almost 3.5 times greater than unpaved roads to aerosol mass which agrees well with Figures 3.5 and 3.6 (Gatz et al., 1981). In addition, note the yearly trends the sources exhibit. Unpaved road aerosol mass varies from approximately 3 ug/m^3 to 1 ug/m^3 or a factor of 3 while the soil aerosol mass varies from 16 ug/m^3 to 8 ug/m^3 or a factor of 2.

Intuitive field observations seem to substantiate Figure 3.6's results that depict a large aerosol mass contribution from the soil source. The amount of ground area covered by rural soil landscapes vastly exceeds unpaved roadbed areas, so aerosol flux from wind erosion of the road surfaces would be small compared to the soil surfaces. Gillette et al., 1992 source emission inventory supports this observation. They stated that, "the largest dust mass source is wind action (wind erosion and dust devils)" (Gillette et al., 1992). Field observations are not so conclusive when trying to predict the influence of anthropogenic activities on levels of airborne alkaline material. Examples of these activities are dust generated by traffic on unpaved roads and farm equipment usage in the fields. Therefore, an increase or decrease in the occurrence of these activities might result in observed changes in source contribution. Section 3.3 discusses its figures while looking to see if these observed changes occur.

Figure 3.4's results indicate that soils contribute greater than 87% of total potassium. This follows because the literature states that soils are the largest source of dust and potassium's elemental abundance in soils at 1.66% is greater than the 0.56% abundance characteristic of crushed limestone roads.

The aforementioned Gatz's CMB model results agreed well with this study's CMB model. The two models shared common methodology and sampling locations. Another comparison can be made of the Bondville model results to recent results from Gillette et al., 1992. Gillette et al. predicted the annual aerosol fluxes of alkaline elements and total mass for each of the 48 states from the following sources: unpaved roads, wind erosion from cultivated lands and dust devils over soil surfaces. Table 3.2 compares the results of the Bondville model and those of Gillette et al., 1992's emission flux calculations. Note the Bondville results are in parentheses. The calculation of Bondville's total mass values in Table 3.2 is obtained by computing the mean of the 12 monthly values for both unpaved road and soil source concentrations (depicted in Figures 3.5 and 3.6). Summing the two averages gave the total concentration from the sources. Each average was then divided by this sum to obtain a fraction. Multiplying the fraction by 100 gives the listed percentage.

Table 3.2. Percentage comparison of alkaline aerosol particle fluxes from Gillette et al., 1992's modeling effort and this study's Bondville CMB model results (in parentheses).

aerosol dust source	calcium (%)	potassium (%)	total mass (%)
unpaved roads	68.8 (74 to 89)	29.0 (4 to 10)	40.3 (11 to 41)
soils	31.1 (11 to 25)	71.1 (90 to 96)	59.7 (34 to 84)

There are several differences in the Bondville model's methodology and Gillette et al's. Gillette et al., 1992's model included wind erosion effects throughout the 48 contiguous United States including the West with its enriched alkaline element soils. In addition, most of the West's unpaved roads were assumed to be soil surfaced as opposed to crushed limestone or gravel surfaced. Gillette et al., 1992's modeling effort also used elemental abundances derived from soil and unpaved road samples collected from throughout the 48 states. These approaches could account for the observed models' differences. Considering the very different approaches in the Gillette nationally oriented model versus the Bondville locally oriented CMB model, we feel Table 3.2's differences are reasonable. Unpaved roads are more dominate for calcium in the Bondville CMB model than for the Gillette model. In addition, the Bondville CMB model is more dominate for potassium from the soils (Gillette et al., 1992).

3.3 Patterns in Monthly Ion's Ambient Concentrations

This section will qualitatively discuss the features in the five year monthly mean ion's ambient concentrations of the aerosol filter samples from the rural Bondville site. Total ambient concentrations were discussed in the previous section. In comparison, this section presents the soluble (or extractable) data where soluble is operationally defined as soaking the filters in a pH 3 hydrochloric acid solution while being agitated for 48 hours in a horizontal shaker. The intra-annual ion's ambient concentration patterns will be discussed in terms of assumed temporal patterns in the emission sources. It was thus important to first establish the relative importance of the primary sources of the crustal aerosols as was done in the previous section. For purpose of the qualitative discussion in this section it is important to remember that the CMB model suggests unpaved roads are the dominant source of calcium in Bondville aerosols (Figure 3.1) while soils are the dominant source for potassium in Bondville aerosols (Figure 3.4).

Before discussing the actual aerosol data, several issues will be explored because they are expected to be useful in explaining temporal trends in aerosols measured at Bondville. One of these issues is the climatological conditions effecting dust production on a seasonal basis. The expectation is

that warm temperatures and scattered rainfall with associated dry surfaces during the late spring, summer and early fall times would generally provide dry soil and road surfaces which in turn lead to enhanced dust production from the unpaved road and the bare soil source. The remaining months with colder temperatures and rainfalls more continuous in nature would produce poorer surface drying conditions. Also snows and frozen ground which undergo frequent freeze/thaw cycles would also provide frequent damp soils and road surfaces. Thus the colder months are generally associated with damp crustal surfaces and low dust emissions.

The sources' physical makeup should also factor into dust production. Progressive vegetative growth (surrounding midwest area being corn and soybean) during the growing season should diminish, over time, the ability of wind forces to erode soils, with the months of July and August being periods when soils are completely protected from wind erosion. Early plant growth present in the dry spring could increase dust production by further drying out soils and not yet providing adequate shielding from wind forces (Stensland, 1993).

Figures 3.7 to 3.11 show the mean ambient ion concentrations at the Bondville site by month for calcium, magnesium, potassium, sodium and sulfate, respectively. Table 3.3 presents the values used to generate these figures as well as median values and count (n), the number of filters passing the screening criteria. The column labeled count (N) on the sulfate portion of Table 3.3 gives the number of samples before applying the 50% screening criterion but after screening out samples that violated the sampling protocol. The percentages of daily filter samples in the data set that passed section 2.5.3's screening and make up Table 3.3 are 88.1% of the calcium data, 83.6% of the magnesium data, 91.4% of the potassium data, 41.4% of the sodium data and 99.2% of the sulfate data. Sodium and sulfate levels are not the focus of this study so these data will be discussed only briefly. Presenting the sodium and sulfate data completes the reporting of the Bondville aerosol project.

Figures 3.7 to 3.9 show that the lowest ambient ion concentrations occurred during the winter months (December to March). This may indicate that climate conditions (e.g., frequent damp soil and road surfaces) are controlling ambient ion concentrations. These months are usually cold and wet with mean temperatures below -1°C (except March which is below 4°C , see section 2.5.2). Since the landscape, corn and soybean fields, are often tilled in the fall, much bare soil is available to undergo wind erosion unless dampness prevents it. In recent years, minimum tillage procedures have been leaving more corn and soybean stalks on the surface which also decreases wind erosion of the soil (Stensland, 1993).

Table 3.3. Descriptive statistics for Bondville ambient aerosol concentrations extractable levels.

calcium ($\mu\text{g}/\text{m}^3$)				
	mean	2(S.E.)	median	count (n)
June	0.783	0.096	0.651	132
July	0.738	0.105	0.588	140
Aug	0.636	0.072	0.544	132
Sept	0.816	0.108	0.675	121
Oct	0.793	0.182	0.513	125
Nov	0.376	0.820	0.288	103
Dec	0.224	0.022	0.175	106
Jan	0.309	0.043	0.232	125
Feb	0.314	0.046	0.251	109
Mar	0.348	0.048	0.267	123
April	0.573	0.070	0.5	115
May	0.745	0.102	0.601	133

magnesium ($\mu\text{g}/\text{m}^3$)				
	mean	2(S.E.)	median	count (n)
June	0.128	0.014	0.105	129
July	0.116	0.016	0.091	138
Aug	0.102	0.010	0.086	130
Sept	0.147	0.018	0.108	118
Oct	0.131	0.022	0.085	121
Nov	0.063	0.010	0.047	94
Dec	0.038	0.004	0.031	87
Jan	0.054	0.008	0.043	105
Feb	0.053	0.006	0.043	105
Mar	0.063	0.008	0.048	118
April	0.107	0.014	0.077	115
May	0.136	0.018	0.106	132

potassium $\mu\text{g}/\text{m}^3$)				
	mean	2(S.E.)	median	count (n)
June	0.098	0.012	0.076	124
July	0.092	0.012	0.066	138
Aug	0.080	0.014	0.066	135
Sept	0.116	0.010	0.112	127
Oct	0.124	0.022	0.093	135
Nov	0.059	0.007	0.048	118
Dec	0.054	0.004	0.05	123
Jan	0.060	0.008	0.053	127
Feb	0.057	0.006	0.049	118
Mar	0.052	0.004	0.047	125
April	0.066	0.006	0.061	119
May	0.084	0.012	0.069	131

sodium ($\mu\text{g}/\text{m}^3$)				
	mean	2(S.E.)	median	count (n)
June	0.145	0.027	0.133	53
July	0.197	0.043	0.135	55
Aug	0.114	0.023	0.081	40
Sept	0.219	0.047	0.168	46
Oct	0.126	0.024	0.08	54
Nov	0.107	0.025	0.077	39
Dec	0.128	0.030	0.094	68
Jan	0.136	0.020	0.107	89
Feb	0.116	0.014	0.102	87
Mar	0.099	0.012	0.088	74
April	0.103	0.020	0.072	45
May	0.116	0.035	0.072	43

sulfate ($\mu\text{g}/\text{m}^3$)					
	mean	2(S.E.)	median	count (n)	count (N)
June	6.21	0.91	4.58	136	138
July	8.08	1.38	5.78	142	146
Aug	8.08	1.12	5.70	138	149
Sept	6.04	1.002	4.691	129	140
Oct	4.15	0.786	2.754	139	145
Nov	2.64	0.272	2.367	134	147
Dec	2.61	0.269	2.288	142	148
Jan	2.74	0.280	2.343	137	150
Feb	3.42	0.354	2.927	132	140
Mar	3.20	0.326	2.736	142	149
April	3.12	0.382	2.638	130	141
May	4.50	0.433	3.903	141	147

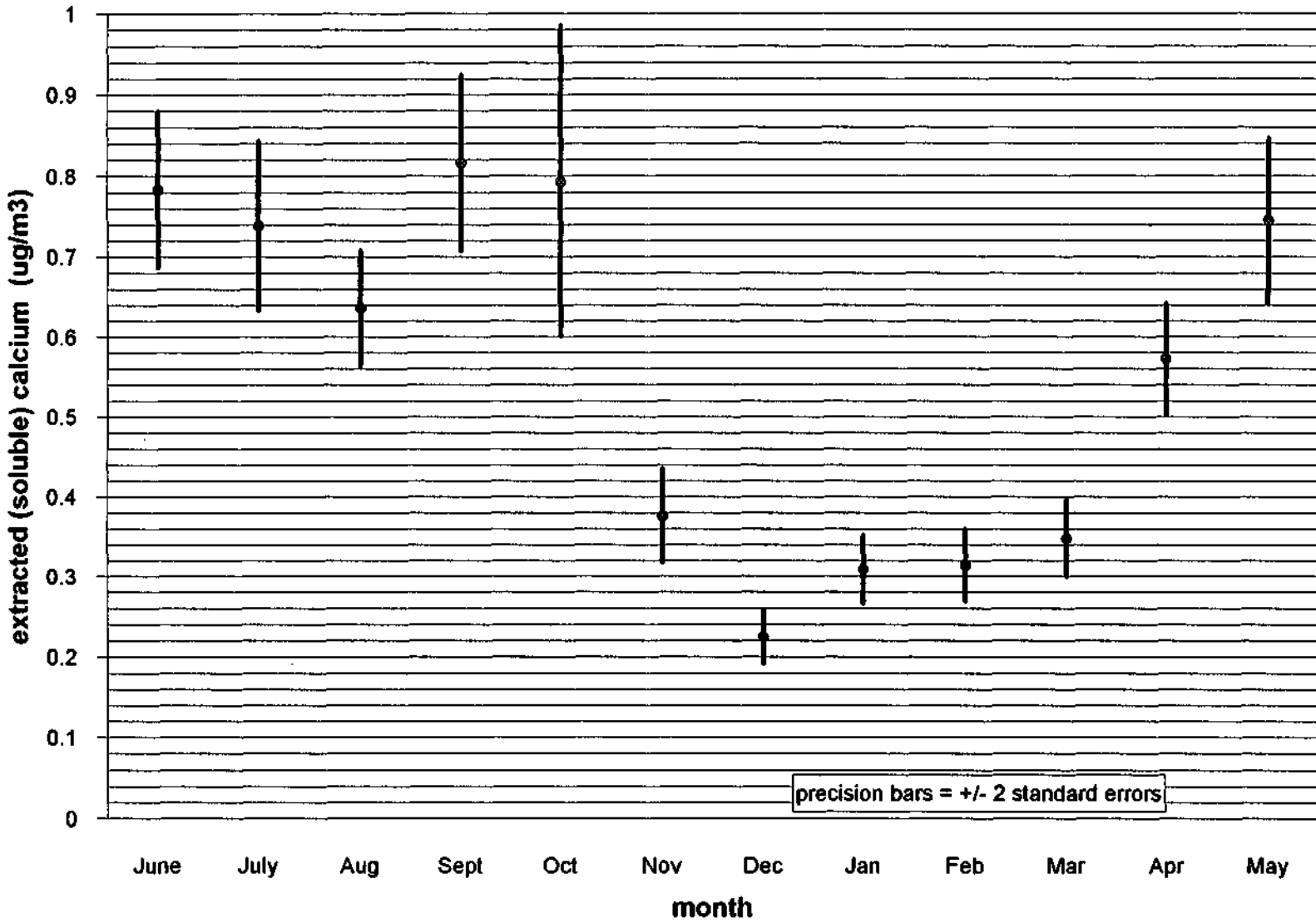


Figure 3.7. Mean ambient aerosol concentrations by month for calcium for the Bondville site, June 1983 through June 1988.

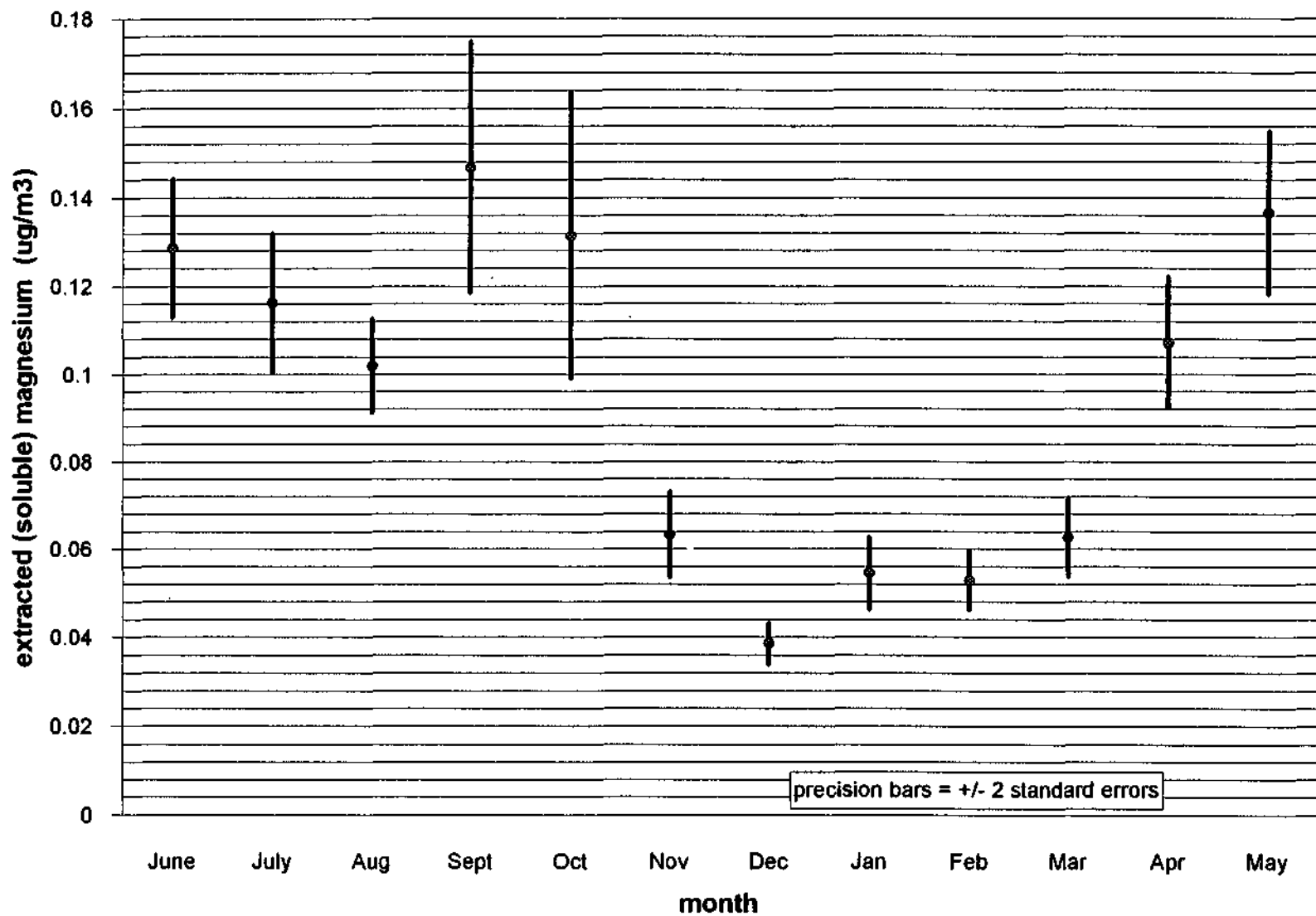


Figure 3.8. Mean ambient aerosol concentrations by month for magnesium for the Bondville site, June 1983 through June 1988.

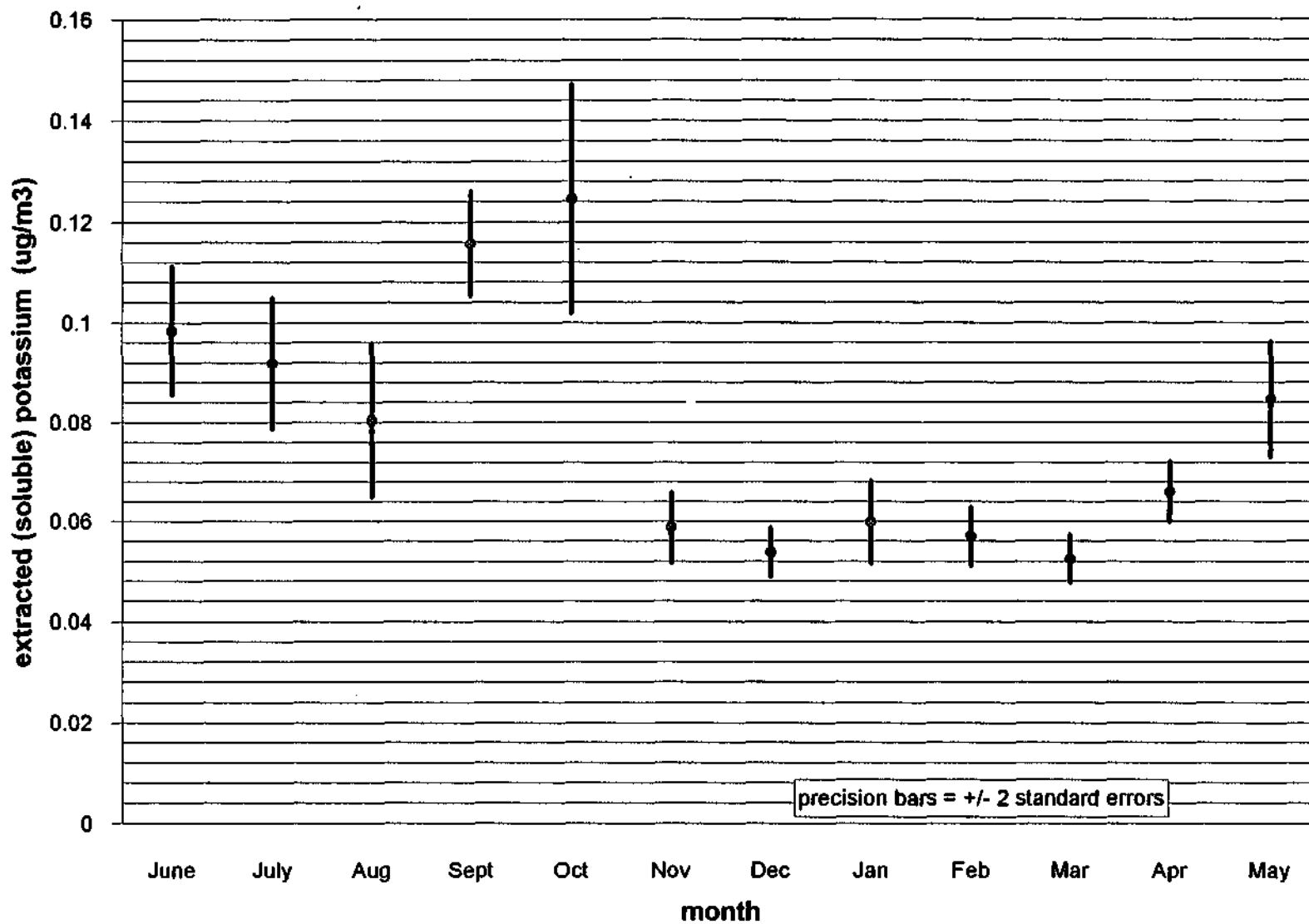


Figure 3.9. Mean ion's ambient concentrations by month for potassium for the Bondville site, June 1983 through June 1988.

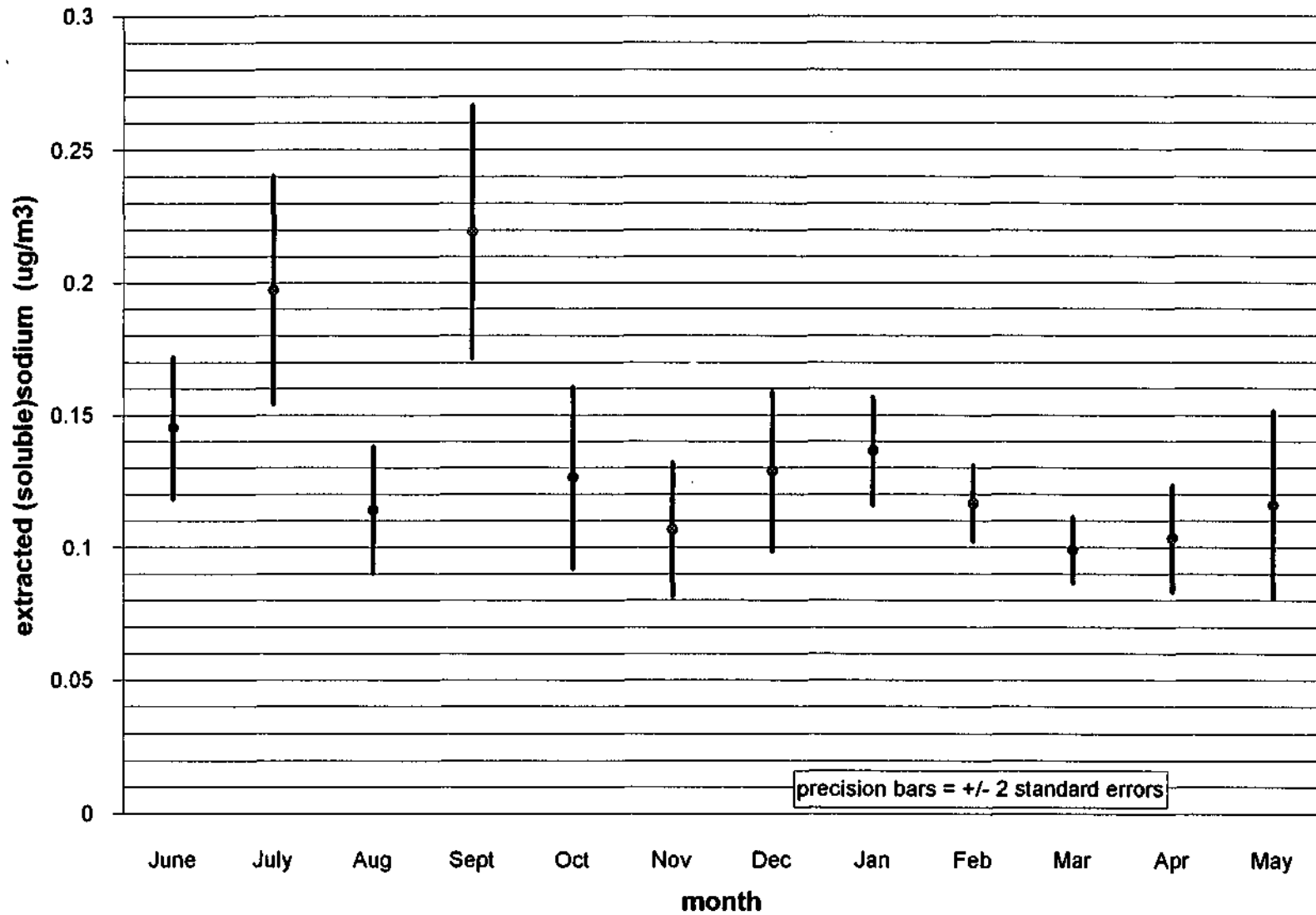


Figure 3.10 Mean ion's ambient concentrations by month for sodium for the Bondville site, June 1983 through June 1988.

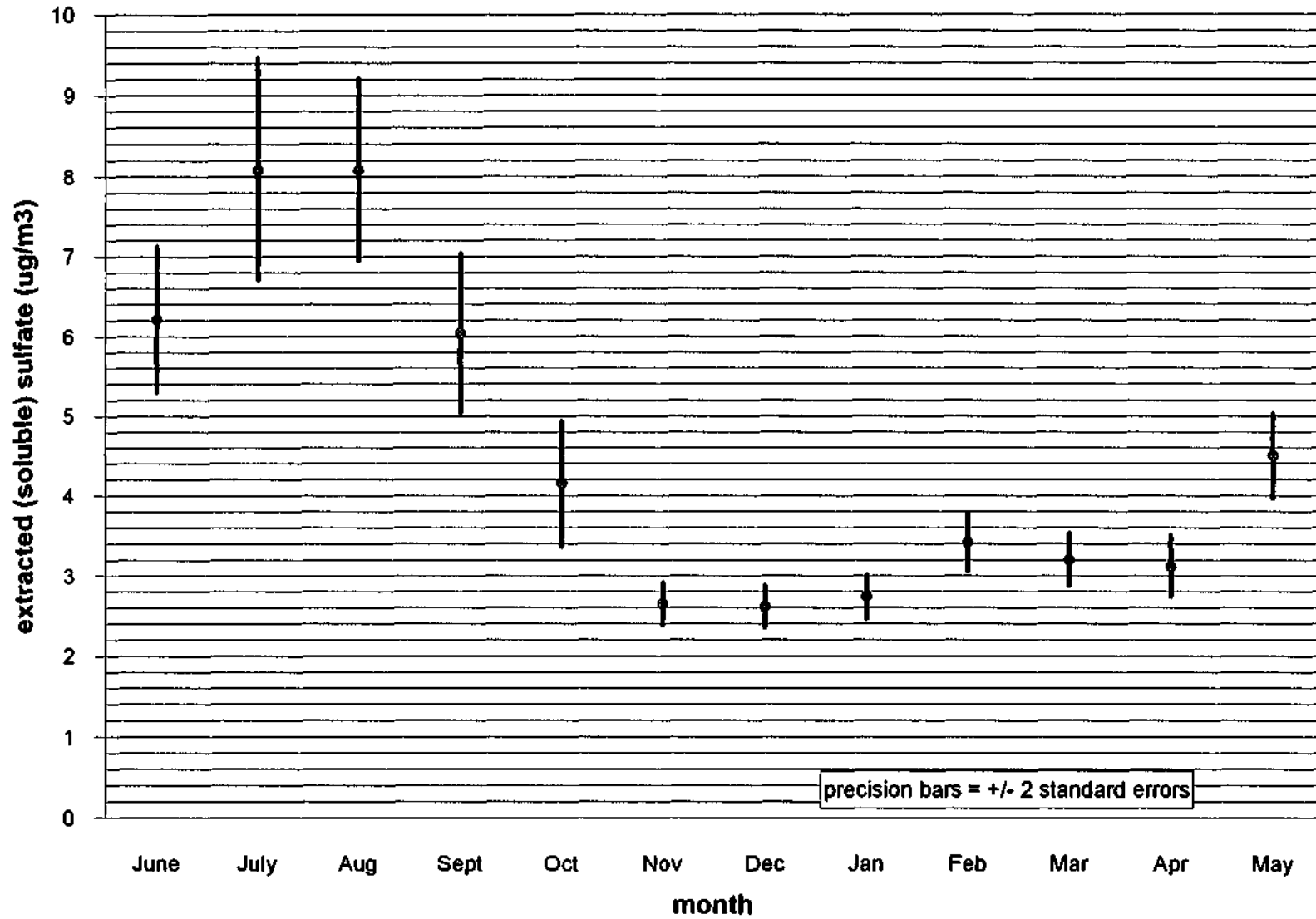


Figure 3.11 Mean ion's ambient concentrations by month for sulfate for the Bondville site, June 1983 through June 1988.

The calcium (Figure 3.7) and the magnesium (Figure 3.8) figures differ in concentration values with calcium levels larger by about a factor of four. Note, Figures 3.7 and 3.8 possess temporal patterns that track each other in a similar fashion. The most likely explanation is that these two ions are from the same source. Figure 2.3 in section 2.6.1 supports this belief by demonstrating a high correlation between magnesium versus calcium (correlation coefficient of 0.814). In addition, it is interesting to note Table 1.1 which presents elemental abundance values for unpaved roads, the calcium source according to the results generated by the CMB model. Calcium's elemental abundance for crushed limestone surfaces have greater values than magnesium's by about a factor of 8.

The temporal patterns seen for calcium and magnesium agree with initial expectations that these levels would reflect unpaved road source conditions. Thus, it was expected and observed that the warm and dry summer months of June through August would produce high mean values. It is assumed that this is due to dry roadbed conditions that support unpaved road dust emissions generated from vehicular traffic.

It was unexpected that September and October would have the highest mean concentrations for calcium and magnesium. However, the precision bars might indicate that the summer and early fall months' means are not statistically different (except August and September magnesium values). Nevertheless, it appears that September and October are the highest road dust production months. This coincides with the harvest season and could suggest that the higher than normal use of unpaved roads by heavy trucks hauling grain from fields to town may be an important dust emission source for the region.

A relative rise in calcium and magnesium concentrations occurs after spring thaw in April and May. This period coincides with the corn and soybean planting season which has associated heavier than normal unpaved road activity as the farmers move equipment from one field to another.

The mean potassium values of Figure 3.9 present some interesting results. It was expected and observed that the planting and harvesting activities would cause an increase in potassium concentrations relative to other months. These activities introduce soil dust into the atmosphere. This follows because section 3.2's CMB model concludes that soil is the significant source for potassium.

In addition, it was expected that potassium would steadily decrease during the summer months to the levels seen during the winter months. This would be due in part to the end of planting, tilling and spraying operations by mid June and the progressing plant growth providing ground cover, shielding bare soil from wind forces. A decrease in Figure 3.9 from June to August occurs, but the mean values are

actually higher than the levels seen during the April-May planting season. A possible explanation could be that this is not due to local potassium sources, but instead it is the long range transport of potassium from areas south to southwest of the sampling site. The Bondville site's dominant wind patterns in the warm months are from these directions (Dossett, 1987). These upwind areas might be finishing the first growing season crop (harvesting) and beginning the second growing season crop (planting) in June.

Gillette et al., 1992, points to dust devils as an important source of airborne dust in the western part of the United States, particularly in the southwestern parts of the United States. Dust devils occur for the most part during the summer time. Soil is an important source of potassium and the prevailing Bondville winds during the summer are from the south to southwest. Keeping this in mind we expected to see an increase in airborne potassium levels during this period. Noting Figure 3.9, the Bondville data does show high values for this period.

Noting Figures 3.7 to 3.9, observe that all three ions follow very similar temporal patterns. One conclusion could be that the ions are originating from the same source. However, the model clearly indicates that the primary source for calcium (and as indicated magnesium) is unpaved roads and for potassium is soils. In addition, Figures 2.8 and 2.9 demonstrate low correlation values for potassium versus calcium ($r = 0.423$) and potassium versus magnesium ($r = 0.406$), respectively, indicating a low probability that potassium is from the same source as calcium or magnesium. Therefore, the observations suggest that the emissions from the discussed sources (soil and unpaved road) are tracking each other in this rural environment.

Possible explanations for the emission sources tracking each other, follow. Field activities require the farmer to use the unpaved roads to transport farming equipment between different fields only accessible by unpaved roads. Also, the storage and shipment of farming products use the unpaved roads. Planting and harvesting are times of intensive field activity. Therefore, heightened field activities could cause an increase in potassium levels and associated unpaved road use could increase calcium and magnesium levels. In addition, normal traffic not intended for the fields will use a travel route favoring paved roads over unpaved road surfaces. Therefore, during times of limited field activities, unpaved road use will be limited due to user preference, thus serving to minimize important sources of airborne calcium and magnesium.

As stated before, this study's analysis focuses on the elements, calcium, magnesium and potassium, but discussion of the sodium and sulfate graphs are warranted. The sodium data was of the lowest quality amongst the data set (many of the calculated concentrations' percent error values were greater than 50%). Table 3.2 demonstrates this by a comparing sodium's n values (the number of filter

Chapter 3: Results and Discussion

values with a percent error less than 50%) to the other ions' n values. The sodium filters have the lowest number of filter samples that pass the screening criteria. The screening resulted in only 41.4% of the daily filters being used to generate the monthly means. Future efforts addressing high and variable blank problems in the sodium data should assist in upgrading the quality of the sodium data.

Observation of Figure 3.10, shows that the shape of the sodium graph is different than the similar shapes of Figures 3.7 to 3.9. High values are present for the summer months except for a low August value. Expectations were that the highest values would appear in the winter months. It was felt that the crustal and sea salt source contributions would be augmented by the airborne injection of sodium rich droplets by traffic traveling over salt deiced roadways.. The aforementioned future efforts to improve the quality of the sodium data set could alter the sodium graph.

Screening the sulfate filter samples resulted in the highest quality data set (most precise and fewest samples screened out). Calculation of the means by month used 99.2% of the filter values. The sulfate graph pattern has similarities to the calcium, magnesium and potassium patterns. One exception is that sulfate is highest during July, August and September and the others are highest during September and October. The high summertime sulfate values are not necessarily due to an increase in source contribution, but are consistent with the increase in photochemical reactions during this period. Increased gas phase production rates of hydroxyl and hydroperoxyl radicals contribute greatly to the gas phase oxidation of sulfur dioxide to sulfates. In addition, the low concentrations seen in December through April reflect the decrease of photochemical driven reactions in the winter (Irving, 1991).

As discussed in section 3.2, observations using our two source model indicate that the majority of calcium is from the unpaved road source. Figure 3.1 shows an approximate contribution of 85% of the total calcium is from unpaved roads from April to October. Using Figure 3.7, we see that approximately 0.7 ug/m^3 is the value for soluble airborne calcium during this period. Noting November through March's period the unpaved road contribution drops to 80%. Observe that for this period the calcium value decreases to 0.3 ug/m^3 . Therefore, this decrease in airborne calcium concentrations occurs along with an increase of the minor source's (soil) contribution to 20%.

Observations of potassium patterns produce different results. Figure 3.4 indicates that the percentage of potassium from soil sources is about 90% during April through October. The airborne soluble potassium's concentrations during this period are the highest values, around 1.0 ug/m^3 . The months of November through March see the soil source percentage increase to approximately 95% and the concentrations decrease to 0.06 ug/m^3 . Therefore, for potassium a decrease in airborne

Chapter 3: Results and Discussion

concentrations results in a stronger signal from its major source, soils. So during the winter time, the soil source's contribution increases for both airborne calcium and potassium concentrations.

3.4 References

Dossett, S.R., 1987: An annotated description of the atmospheric chemistry sampling station at Bondville, Illinois, *In Study of Atmospheric Pollution Scavenging by R. G. Semonin et al.*, COO-1199-65, 21th Progress Report to the U. S. Department of Energy, Office of Health and Environmental Research, Contract DE-AC02-76EV01199, p. 329-340.

Gatz, Donald F., Gary J. Stensland, Michael V. Miller and Alistair C. D. Leslie, 1981: Sources of airborne calcium in rural central Illinois, *American Chemical Society, Society Symposium Series, No. 167*, Report No. 17, p. 303-308.

Gillette, Dale A., Gary J. Stensland, Allen L Williams, William R. Barnard, Donald F. Gatz, Peter C. Sinclair and Tezz C. Johnson, 1992: Emissions of alkaline elements calcium, magnesium, potassium and sodium from open sources in the contiguous United States, *Global Biochemical Cycles*, vol. 6, no. 4, p. 437-457.

Irving, Patricia M. Ed., 1991: Acidic deposition: state of science and technology, *In The U. S. National Acid Assessment Program*, Government Printing Office, Washington, D.C., vol. 1, p. 1:102-1:109, p. 2:76.

Lapin, Lawrence L., 1990: Probability and statistics for modern engineering, PWS-Kent Publishing Company, Boston, MA, p. 266.

Stensland, Gary J., 1993: Personal communications, regional climate patterns and crop production.

Chapter 4: Summary, Conclusions and Recommendations

4.1 Summary

The efforts at the rural Bondville field site produced a large data set quantifying some of the soluble aerosol constituents sampled at that site. The filter extraction method used in the Bondville project was instituted to establish a data base of soluble ion concentrations. This data can then be compared to precipitation chemistry data. Trend analysis of the Bondville data set might assist in explaining the reason for the observed decrease in the nation's precipitation calcium levels over time (Irving, 1991).

The percent error calculation gave a quantified precision for each calculated ambient ion concentration. This precision approach makes the data set unique. Individual ion concentrations whose percent error exceeded 50% were considered poor quality (one or more of the measurements taken in order to calculate the ambient concentrations was questionable) and screened from the data set. This data quality screening method resulted in little data loss among the ion data set, except for sodium.

Prior to the calculation of the data set this study spent considerable effort to establish credible rotameter calibrations for the air volume samplers used at Bondville. The calibration efforts produced very tight reproducible rotameter calibration curves. This decreased the uncertainty in the sampled air volume values. Establishment of these precise calibrations should allow the use of this data set for future trend evaluations.

Analysis of the Bondville June 1, 1983, to May 31, 1988 screened data set was conducted using quantitative and a qualitative approach. The quantitative approach involved a CMB model that evaluated the influence of the two major dust sources considered (soils and unpaved roads) on the calcium and potassium filter masses. The qualitative analysis used the month to month averages of the soluble airborne calcium, magnesium and potassium concentrations. Observations of the patterns these averages formed were compared to expected emission source trends over time.

4.2 Conclusions

(1) The CMB model used daily filter samples for input with calcium and potassium concentrations that passed the aforementioned screening criteria. The model indicated that the soil source contributed 11% to 25% of total calcium and 89% to 96% of total potassium on the filter. The unpaved road source contributed 75% to 89% of total calcium and 4% to 11% of total potassium on the daily filters. Therefore, the model established for the rural Bondville site, unpaved road sources as the dominant contributor to airborne calcium and soil sources as the dominant contributor to airborne potassium.

(2) The Bondville CMB model results compared well with other modeling efforts. The 1981 Gatz et al. model predicted that for the summer and early fall of 1978, soil mass contributions were almost 3.5 times greater than unpaved road mass contributions to the total aerosol mass. The Bondville model exhibited a range of approximately 3.5 to 5.5 times greater soil mass contributions to unpaved road mass contributions over the five year sampling period. Surprisingly, Gillette et al., 1992 source percentages compared well to Bondville's model despite the differences between Bondville's regional approach and Gillette's national approach. The Bondville model results indicated greater influence on calcium levels from unpaved roads and potassium levels from soils than the Gillette model.

(3) The qualitative examination of the monthly averaged aerosol concentration data yielded many interesting observations. The concentrations of calcium, magnesium and potassium were lowest during the winter season. Possible explanations are the lack of agricultural activity stirring up soil dust and the region's climatic conditions (cold, cloudy, frequent freezing/thawing which all produce damp soil and road surfaces) serving to decrease dust production from the major sources.

It was expected that crop cover in June through August would decrease the soil source's contribution to airborne potassium and thus produce much lower potassium concentrations than in the spring and fall. However, the data showed that the summertime levels were higher than the winter levels. In addition, the summertime levels were also higher than the springtime concentrations, which are influenced by the planting season's tilling activities and only modestly lower than the fall concentrations, which are influenced by harvesting activities.

Calcium and magnesium concentration levels tracked each other throughout the year (a high correlation value of 0.814 as shown in Figure 2.7). This is likely due to their common major source, unpaved roads. Likewise, calcium and potassium probably have different sources due to their low correlation of daily concentrations (correlation value of 0.423 as shown in Figure 2.8). However, the correlation of monthly average values of calcium to both magnesium and potassium (compare Figures

3.7 to 3.8 and 3.9) is high. This strongly indicates some linkage in the rural environment between the two major sources, unpaved roads and soils. In support of this statement, it is noted that increased anthropogenic activities that impact the fields (i.e., tilling, planting and harvesting) also requires associated heavy use of unpaved road to access the fields. Access to many of these fields is by unpaved roads surfaced with crushed limestone.

(4) Finally, the Gillette et al., 1992, article points to the importance of wind action, which includes wind erosion and dust devils, as a source of atmospheric alkalinity. The region west of the Missouri-Mississippi rivers is the primary domain for wind action. The soils there are enriched in calcium and other alkaline elements relative to eastern states' soils. In the United States maximum dust production due to wind action occurs in the spring and for dust devils in the summer. Note on Figures 3.7 to 3.9 there is a slight increase in the calcium, magnesium and potassium concentrations as the spring period progresses and then high values from June to October. These western soil dust sources could be affecting the Bondville aerosol levels but the data does not lend strong support for this long range transport.

4.3 Recommendations

This data set is unique. The specially designed filter extraction procedure and sample analysis allows data comparison of the results to precipitation chemistry studies. In addition, the long term data record could assist in the analysis of trends in the measured ion levels. One area of interest might be the airborne calcium concentrations. Several aerosol studies have shown a decline in calcium concentrations over time. The entire Bondville data set might support these observations. This analysis would require processing the entire data set since the beginning of the project. The potential opportunity to apply this data set to these concerns and others, validates the continuation of the current weekly collection regime.

The project's sampling regime used the faced down funnel filter setup discussed in section 2.2. Two dichotomous samplers began weekly sampling in May 1993 at Bondville. They possess a coarse and fine cut fraction sizing head (10 μm and 2 μm , respectively). The samplers will collect data on aerosol size distribution and will ultimately be the sampling technique used in the Bondville project. Immediate future efforts will compare the dichotomous sampler filters against each other and the simultaneous collected funnel filters. This will provide information about the reproducibility of sampling results using the dichotomous samplers and the comparison of measured ion's ambient concentrations using the funnel filter setup to the dichotomous samplers. This comparison will quantify any difference

between the current funnel filter setup and the dichotomous samplers thus ensuring the integrity of the long term Bondville record.

This study's June 1983 to May 1988 calcium, sodium and sulfate outside hung blank means are statistically different from the Bondville sampling period, June 1978 to May 1983. The test used to prove this statistical difference was the student t test difference of the means method. Expectations are that the outside hung field blanks values for the entire daily sampling regime period should remain relatively constant over time. Future efforts addressing some instances where high and variable blank values appear might correct the ion blank means and bring the two periods' blank means into agreement.

The model uses soluble fraction constants (the mass of the extracted ion divided by the total elemental mass) to convert the calculated calcium's and potassium's soluble ion mass to a total elemental mass. The extraction method to determine these fraction constants differed from the extraction method used in the Bondville project. A more acidic solution (pH of 3) was used to extract the Bondville filters then the extract solution (pH of 5.6) used in this total versus soluble experiment. This comparison study of total versus extracted (soluble) mass needs to be repeated in order to account for the use of the pH 3 extraction solution in the Bondville project. The soluble fraction constants should increase in value by some undetermined amount due to the use of the more acidic extraction solution.

Total filter mass loading measurements were made throughout most of the Bondville project. These measurements require a quality assurance/quality control evaluation prior to their use. The CMB model generated Figures 3.5 and 3.6 which are graphs of aerosol mass at Bondville due to soils and unpaved roads, respectively. The patterns created by the filter loading monthly mean values might agree with these Figures' patterns. An agreement would further verify the model's results.

Finally, Figure's 3.9 potassium ambient concentrations for June to August are higher than several other months. Initial expectations were for decreasing potassium concentration as the growing season progresses because increased plant growth would shield bare soils from wind forces. The reason given for this phenomenon might be long range transport of potassium. However, further research is needed to understand the unexpected mean concentrations seen at the Bondville site.

Table A.1. Central tendency and variability of blank values measured in the Bondville aerosol project.

sulfate (mg/L)									
	hung field blanks Oct '79 to May '83 [BG37B]	hung field blanks Jun '83 to May '88 [BG37B]	not hung field blanks Sep '78 to Sep '80 [BG37B]	filtration column w/o filter: Mar '80 to Apr '81 [APBK]	new boxed filters: extracted then analyzed Dec '81 to Nov '83 [EXBK]	HA filter in filtration column Mar '80 to Apr '81 [HABK]	filters weighed, stored and reweighed Mar '80 to present [NUBK] [TFBK]	extract solution from repipettor Dec '83 to present [RPBK]	stored extraction solution Dec '83 to present [SLBK]
mean	0.31	0.10	0.12	0.06	0.30	0.12	0.13	0.06	0.07
std devia	0.40	0.12	0.02	0.04	0.35	0.05	0.07	0.07	0.08
median	0.05	0.05	0.10	0.10	0.05	0.10	0.05	0.05	0.05
count	88	241	27	36	33	38	292	68	69
phosphate (mg/L)									
	hung field blanks Oct '79 to May '83 [BG37B]	hung field blanks Jun '83 to May '88 [BG37B]	not hung field blanks Sep '78 to Sep '80 [BG37B]	filtration column w/o filter: Mar '80 to Apr '81 [APBK]	new boxed filters: extracted then analyzed Dec '81 to Nov '83 [EXBK]	HA filter in filtration column Mar '80 to Apr '81 [HABK]	filters weighed, stored and reweighed Mar '80 to present [NUBK] [TFBK]	extract solution from repipettor Dec '83 to present [RPBK]	stored extraction solution Dec '83 to present [SLBK]
mean	0.002	x	0.004	0.002	0.002	0.003	0.002	x	x
std devia	0.001	x-	0.004	0.002	0.0004	0.003	0.002	x-	x-
median	0.002	x	0.002	0.0015	0.0015	0.0015	0.0015	x	x
count	86	x	27	37	33	38	286	x	x

Table A.1 (continued). Central tendency and variability of blank values measured in the Bondville aerosol project.

calcium (mg/L)									
	hung field blanks Oct 79 to May '83 [BG37B]	hung field blanks Jun '83 to May '88 [BG37B]	not hung field blanks Sep 78 to Sep '80 [BG37B]	filtration column w/o filter: Mar '80 to Apr '81 [APBK]	new boxed filters: extracted then analyzed Dec '81 to Nov '83 [EXBK]	HA filter in filtration column Mar '80 to Apr '81 [HABK]	filters weighed, stored and reweighed Mar '80 to present [NUBK] [TFBK]	extract solution from repipettor Dec '83 to present [RPBK]	stored extraction solution Dec '83 to present [SLBK]
mean	0.033	0.022	0.026	0.016	0.020	0.024	0.014	0.007	0.005
std devia	0.025	0.016	0.026	0.005	0.013	0.019	0.013	0.005	0.001
median	0.02	0.02	0.02	0.015	0.015	0.02	0.0015	0.005	0.005
count	85	237	26	36	32	39	294	69	71
magnesium (mg/L)									
	hung field blanks Oct 79 to May '83 [BG37B]	hung field blanks Jun '83 to May '88 [BG37B]	not hung field blanks Sep 78 to Sep '80 [BG37B]	filtration column w/o filter: Mar '80 to Apr '81 [APBK]	new boxed filters: extracted then analyzed Dec '81 to Nov '83 [EXBK]	HA filter in filtration column Mar '80 to Apr '81 [HABK]	filters weighed, stored and reweighed Mar '80 to present [NUBK] [TFBK]	extract solution from repipettor Dec '83 to present [RPBK]	stored extraction solution Dec '83 to present [SLBK]
mean	0.003	0.003	0.004	0.002	0.0015	0.003	0.002	0.0015	0.0015
std devia	0.004	0.004	0.003	0.001	0	0.003	0.001	0	0
median	0.002	0.0015	0.002	0.0015	0.0015	0.0015	0.0015	0.0015	0.0015
count	87	240	27	37	33	38	291	70	71

Table A.1 (continued). Central tendency and variability of blank values measured in the Bondville aerosol project.

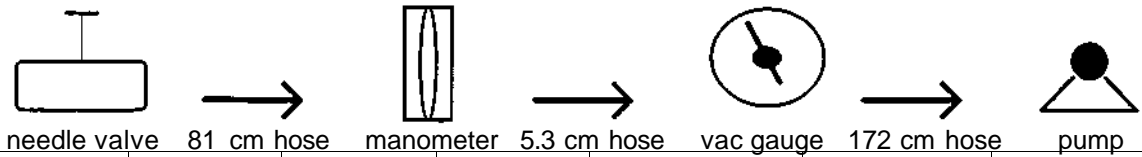
sodium (mg/L)									
	hung field blanks Oct 79 to May '83 [BG37B]	hung field blanks Jun '83 to May '88 [BG37B]	not hung field blanks Sep 78 to Sep '80 [BG37B]	filtration column w/o filter: Mar '80 to Apr '81 [APBK]	new boxed filters: extracted then analyzed Dec '81 to Nov '83 [EXBK]	HA filter in filtration column Mar '80 to Apr '81 [HABK]	filters weighed, stored and reweighed Mar '80 to present [NUBK] [TFBK]	extract solution from repipettor Dec '83 to present [RPBK]	stored extraction solution Dec '83 to present [SLBK]
mean	0.041	0.022	0.061	0.008	0.036	0.026	0.026	0.017	0.005
std devia	0.025	0.016	0.084	0.013	0.042	0.014	0.024	0.020	0.005
median	0.04	0.018	0.03	0.0015	0.023	0.025	0.020	0.0095	0.0015
count	84	242	27	36	33	36	296	70	70
potassium (mg/L)									
	hung field blanks Oct 79 to May '83 [BG37B]	hung field blanks Jun '83 to May '88 [BG37B]	not hung field blanks Sep 78 to Sep '80 [BG37B]	filtration column w/o filter: Mar '80 to Apr '81 [APBK]	new boxed filters: extracted then analyzed Dec '81 to Nov '83 [EXBK]	HA filter in filtration column Mar '80 to Apr '81 [HABK]	filters weighed, stored and reweighed Mar '80 to present [NUBK] [TFBK]	extract solution from repipettor Dec '83 to present [RPBK]	stored extraction solution Dec '83 to present [SLBK]
mean	0.006	0.006	0.007	0.005	0.004	0.007	0.004	0.005	0.003
std devia	0.004	0.005	0.003	0.005	0.003	0.004	0.005	0.005	0.005
median	0.006	0.005	0.006	0.0015	0.004	0.006	0.004	0.0015	0.0015
count	87	237	26	37	33	38	297	71	70

Table A.1 (continued). Central tendency and variability of blank values measured in the Bondville aerosol project.

zinc (mg/L)									
	hung field blanks Oct 79 to May '83 [BG37B]	hung field blanks Jun '83 to May '88 [BG37B]	not hung field blanks Sep 78 to Sep '80 [BG37B]	filtration column w/o filter: Mar '80 to Apr '81 [APBK]	new boxed filters: extracted then analyzed Dec '81 to Nov '83 [EXBK]	HA filter in filtration column Mar '80 to Apr '81 [HABK]	filters weighed, stored and reweighed Mar '80 to present [NUBK] [TFBK]	extract solution from repipettor Dec '83 to present [RPBK]	stored extraction solution Dec '83 to present [SLBK]
mean	0.005	x	0.004	0.005	0.005	0.007	0.004	x	x
std devia	0.005	x-	0.001	0.002	0.0015	0.005	0.001	x-	x-
median	0.003	x	0.005	0.0045	0.0045	0.0045	0.003	x	x
count	84	x	26	36	33	38	297	x	x

Table A.2. Calibration of the Gelman pump's vacuum gauges using a manometer.

Schematic:



EXPERIMENT							Ambient conditions	
Comparison: Gelman Pump's Vacuum Gauge and Blue Manometer.							pressure	29.075 in
WO/Tuesday March 09,1992 11:00 am.							temp	25.2 C
Gelman pump number	rotameter flow (L/min)	manometer reading (in Hg)	vac gauge reading (in Hg)	corrected vac gauge (in Hg)	vac gauge dif from mano $((V - M)/M)*100$ (%)	mean of vac gauge dif (%)		
0013	35	16.7	16.7	16.57	-0.78			
	40	15.4	15.4	15.27	-0.84	-0.857		
	45	13.7	13.7	13.57	-0.95			
0017	35	22.1	22.2	22.07	-0.14			
	40	20.4	20.3	20.17	-1.13	-0.659		
	45	18.2	18.2	18.07	-0.71			
0030	35	21.05	20.5	20.37	-3.23			
	40	18.65	18.2	18.07	-3.11	-2.695		
	45	16.05	15.9	15.77	-1.74			
0062	35	17.2	16.4	16.27	-5.41			
	40	18.75	17.9	17.77	-5.23	-5.552		
	45	17.1	16.2	16.07	-6.02			
0110	35	21.1	21.4	21.27	0.81			
	40	18.95	19.2	19.07	0.63	0.322		
	45	16.95	17	16.87	-0.47			
0111	35	20.8	20.2	20.07	-3.51			
	40	19.2	18.8	18.67	-2.76	-4.772		
	45	17.15	15.9	15.77	-8.05			
0457	35	21.8	20.7	20.57	-5.64			
	40	20.8	20.1	19.97	-3.99	-4.578		
	45	17.8	17.2	17.07	-4.10			
0591	35	20.35	18.6	18.47	-9.24			
	40	18.3	17.8	17.67	-3.44	-5.345		
	45	15.8	15.4	15.27	-3.35			